REPORT DOCUMENTATION PAGE

Form Approved
OMB No. 0704-0188

1. AGENCY USE ONLY *(Leave blank)*	2. REPORT DATE	3. REPORT TYPE AND DATES COVERED
	26.Apr.04	THESIS

4. TITLE AND SUBTITLE
CLOSED FORM GUIDANCE LAWS FOR INTERCEPTING MOVING TARGETS

5. FUNDING NUMBERS

6. AUTHOR(S)
2D LT BARTLEY CHRISTOPHER S

7. PERFORMING ORGANIZATION NAME(S) AND ADDRESS(ES)
RICE UNIVERSITY

8. PERFORMING ORGANIZATION REPORT NUMBER
CI04-149

9. SPONSORING/MONITORING AGENCY NAME(S) AND ADDRESS(ES)
THE DEPARTMENT OF THE AIR FORCE
AFIT/CIA, BLDG 125
2950 P STREET
WPAFB OH 45433

10. SPONSORING/MONITORING AGENCY REPORT NUMBER

11. SUPPLEMENTARY NOTES

12a. DISTRIBUTION AVAILABILITY STATEMENT
Unlimited distribution
In Accordance With AFI 35-205/AFIT Sup 1

12b. DISTRIBUTION CODE

13. ABSTRACT *(Maximum 200 words)*

DISTRIBUTION STATEMENT A
Approved for Public Release
Distribution Unlimited

20040503 086

14. SUBJECT TERMS

15. NUMBER OF PAGES
125

16. PRICE CODE

17. SECURITY CLASSIFICATION OF REPORT	18. SECURITY CLASSIFICATION OF THIS PAGE	19. SECURITY CLASSIFICATION OF ABSTRACT	20. LIMITATION OF ABSTRACT

RICE UNIVERSITY

Closed Form Guidance Laws for Intercepting Moving Targets

by

Christopher S. Bartley

A Thesis Submitted
in Partial Fulfillment of the
Requirements for the Degree

Master of Science

Approved, Thesis Committee:

Marcia K. O'Malley, Chairman
Assistant Professor of Mechanical Engineering

Fathi H. Ghorbel
Associate Professor of Mechanical Engineering

Angelo Miele
Foyt Professor Emeritus and Research Engineering Professor

Christopher S. D'Souza
Senior Member of Technical Staff, Charles Stark Draper Laboratory, Inc.

Houston, Texas

April, 2004

ABSTRACT

Closed Form Guidance Laws for Intercepting Moving Targets

by

Christopher S. Bartley

A family of air-to-surface guidance laws designed to intercept moving targets has been developed. They include the effect of gravity, as well as constraints on the terminal flight path and heading angle, and are designed for tracking moving targets. These guidance laws yield equations for the commanded accelerations. They are based firmly on optimal control theory and meet the first and second variation necessary conditions that originate from Pontryagin's Minimum Principle. In addition, these solutions also meet the second variation sufficient conditions for a minimum. They have been evaluated in six degree of freedom simulations. The results show that they perform as designed, even for airframes which are rather sluggish.

Acknowledgments

The author wishes to thank his advisor with Draper Labs, Dr. Christopher D'Souza, whose guidance and support were invaluable to the success of this research effort.

The author thanks his advisor at Rice University, Dr. Marcia O'Malley, for her time and effort throughout this process.

The author also wishes to thank Dr. Nazareth Bedrossian of Draper and Dr. Angelo Miele of Rice for their advice and encouragement.

Finally, the author wishes to thank Dr. Fathi Ghorbel for his continued support of the Draper/Rice graduate program.

The views expressed in this thesis are those of the author and do not reflect the official policy or position of the United States Air Force, Department of Defense, or the United States Government.

ASSIGNMENT

Draper Laboratory Report Number T-1475.

In consideration for the research opportunity and permission to prepare my thesis by and at The Charles Stark Draper Laboratory, Inc., I hereby assign my copyright of the thesis to The Charles Stark Draper Laboratory, Inc., Cambridge, Massachusetts.

(author's signature) April 23, 2004

Table of Contents

List of Figures

List of Tables

Chapter 1

Introduction

This thesis presents a family of optimal guidance laws for air-to-surface missiles. This work is motivated by a need for increased missile strike capability and the desire to minimize the commanded accelerations of a missile on an air-to-surface mission. This need arises from increased target maneuver capability, the need to constrain the missile to meet certain parameters on impact, and the desire to minimize the commanded accelerations that the missile must obtain thus maximizing the terminal velocity. The following paragraphs discuss prior work in air-to-surface missile guidance and introduce the optimal solution for the guidance of air-to-surface missiles.

Currently there exist many forms of guidance laws that engineers use to solve the missile-target intercept problem. The options include proportional navigation, augmented proportional navigation, proportional navigation command guidance, beam rider guidance, and command to line-of-sight guidance. These options can be more easily understood realizing that they all originate from one of three categories. The first category is proportional navigation. In proportional navigation the rate of change of the missile heading is proportional to the rate of rotation of the line-of-sight from the missile to the target [11]. Naturally all of these types of guidance assume complete knowledge of the target. The other category is that of line-of-sight guidance. In line-of-sight guidance the line-of-sight originates from an observer not on the missile. The observer faces directly toward the target forming the line-of-sight. The missile is ordinarily fired from the observer position and the missile steering commands are proportional to the angle of the missile off the line-of-sight [11]. In line-of-sight guidance there is no consideration for the velocity of the target and therefore the missile

will not orient itself to lead the target by a certain distance in order to anticipate its movement. The missile simply follows the line-of-sight exactly and thus will need to have greater maneuvering capability in order to intercept a maneuvering target than is needed in proportional navigation. Line-of-sight guidance is typically used for short-range intercepts. The third category of guidance is called pursuit guidance. In pursuit guidance typically a missileborne tracker is assumed which will be used to lock on to the target. The only difference in pursuit guidance and line-of-sight guidance is that in line-of-sight guidance the observer who supplies the missile with target information is not attached to the missile. In pursuit guidance this observer is attached to the missile itself and therefore there is no third-party observer. Also, pursuit guidance doesn't anticipate the targets movement and simply orients itself directly at the target at all times [11].

The first missile to use proportional navigation was the Lark missile, which successfully intercepted its first target in December of 1950. Since that time proportional navigation guidance has been used in virtually all of the world's tactical radar, infrared (IR), and television (TV) guided missiles [16]. The proportional navigation law yields commanded accelerations that are perpendicular to a line of sight vector between the missile and the target. The commands are proportional to the rotational rate of the line-of-sight and the closing velocity [21]. The guidance law can be expressed as

$$n_c = N' V_c \dot{\lambda} \tag{1.1}$$

where n_c is the commanded acceleration, N' is the effective navigation ratio (usually 3-5), V_c is the closing velocity, and $\dot{\lambda}$ is the rotational rate of the line of sight vector. In order to understand proportional navigation consider Figure 1.1. This figure represents an inertial coordinate system fixed to the surface of a flat-Earth model (i.e., the x axis is downrange and the y axis can either be altitude or crossrange). Using this coordinate frame it is possible to integrate components of the accelerations and velocities in terms of x and y directions without having to consider the extra terms

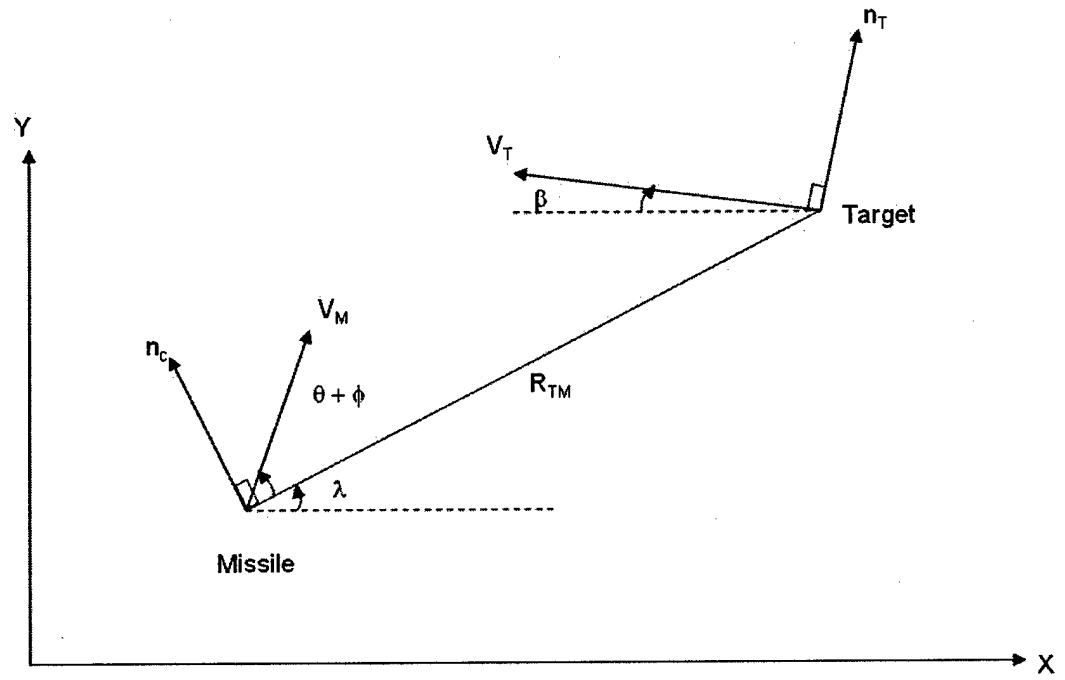

Figure 1.1: Two-dimensional missile-target engagement geometry [21]

due to the Coriolis effect. The missile and target travel at constant velocity and the effects of drag and gravity are neglected. In the figure the velocity of the missile is denoted by the vector V_M as the target velocity is characterized by the vector V_T. The range R_{TM} is the distance down the line of sight separating the missile and the target. The commanded acceleration of the missile n_c is perpendicular to the instantaneous line of sight and the target acceleration n_T is perpendicular to the target velocity V_T. The angle λ represents the angle between the horizontal and the line of sight vector and β represents the flight path angle of the target. Now it is possible to see from the figure that the missile is moving with a velocity magnitude V_M at an angle $\theta + \phi$. θ is known as the missile lead angle which is theoretically the correct angle for the missile to be on a collision triangle with the target. In other words, if the missile is on a collision triangle, no further acceleration commands are required for the missile to hit the target [21]. The angle ϕ is known as the heading error and denotes the

initial deviation of the missile from the collision triangle. It is desired to make the magnitude of the line of sight vector R_{TM} approach zero where target interception would occur. The closing velocity V_c is defined as follows

$$V_c = -\dot{R}_{TM}. \tag{1.2}$$

It is possible to see that the closing velocity V_c will be zero when the magnitude of the line of sight vector R_{TM} is at a minimum. The rate of rotation of the line of sight vector can be obtained as follows

$$\dot{\lambda} = \frac{R_{TM1}V_{TM1} - R_{TM2}V_{TM1}}{R_{TM}^2}. \tag{1.3}$$

Now by using the equation for the closing velocity V_c and the rotational rate of the line of sight vector $\dot{\lambda}$ it is possible to determine the commanded acceleration n_c. Depending on the capabilities of the missile being used, the effective navigation ratio will range from a minimum of three to a maximum of five [21]. Keep in mind that the effective navigation ratio is an indication of the overall capability of the missile that is being used to track the target and relates directly to the acceleration and sensor capabilities of the missile. If the effective navigation ratio is three, it means that the missile must be able to accelerate at three times the magnitude of the target. Proportional navigation does not take the effects of gravity into account, the time to target is merely an estimation, and it is not an optimal guidance law that minimizes either the total flight time or the commanded acceleration.

Augmented proportional navigation is another guidance law used in today's missile technology. Augmented proportional navigation is proportional navigation with an extra term to account for a maneuvering target [16]. The equation to calculate the commanded accelerations for the missile using augmented proportional navigation is as follows

$$n_c = N'V_c\dot{\lambda} + \frac{N'n_T}{2} \tag{1.4}$$

where n_T is the acceleration of the target. From the analysis performed in [21] it is possible to see that the required missile acceleration decreases monotonically with

time, regardless of the effective navigation ratio, rather than increasing monotonically with time as was the case with proportional navigation. Also, it is possible to see that the augmented proportional navigation approach requires less overall acceleration of the missile than the traditional proportional navigation approach. However, for an effective navigation ratio of five the maximum required acceleration for augmented proportional navigation is higher than the maximum required acceleration for proportional navigation. Experience has demonstrated that if the effective navigation ratio is five the augmented proportonal navigation technique requires less acceleration about seventy-five percent of the time compared to proportional navigation. Although augmented proportional navigation has many benefits over proportional navigation it still does not take into account gravity, the time to target is still merely an estimate, and although it for the most part requires less acceleration than proportional navigation it is still not an optimal solution. Additionally proportional navigation in general was developed for high velocity targets and has been applied to stationary surface targets. Proportional navigation is not well suited for the air-to-surface guidance problem.

Many other guidance laws such as proportional navigation command guidance, beam rider guidance, and command to line-of-sight guidance fall under the category of line-of-sight guidance systems. Proportional navigation command guidance, also known as a manual guided weapon system, implies that the human operator has the task of tracking both the target and the missile [9]. Traditionally proportional navigation is implemented in a homing loop. In the homing loop all the necessary information that the missile needs to intercept the target is obtained by a seeker. A seeker is a device that is fixed to the front of the missile that provides target position and velocity information. When using a seeker with proportional navigation the range to the target is not usually needed to calculate the commanded accelerations. In the case when command proportional navigation is being used the range from the missile to the target is a necessary component. Since the range from the missile

to target tends toward zero as the flight progresses, the effective noise on the line-of-sight angle will get very large toward the end of the flight. This means that command guidance systems generally have to contend with more noise than homing systems near the end of the flight [21]. Beam rider guidance systems use a target tracker whose purpose is to maintain the antenna boresight pointing at the center of the reflecting area of the target. The missile usually carries a sophisticated receiver which can detect the missile's angular deviation from the center of the beam [9]. If the beam is always on the target and the missile is always on the beam, an intercept will result. The beam originates from someone on the ground sighting the target as displayed in Figure 1.2. The beam riding guidance principle is probably one of the first methods used because of its simplicity and ease of implementation [21]. Also beam riding performance can be significantly improved by taking the beam motion into account. This is similar to improving proportional navigation by taking into account the target motion (augmented proportional navigation). By taking into account the beam motion the acceleration required decreases and the accuracy of the intercept increases [21]. Beam riding guidance is achieved using semi-automatic systems where the human operator only tracks the target [9]. Figure 1.2 indicates some of the well known features of the surface-to-air guided weapon system Rapier [8] and should give some insight into beam riding guidance. It is important to note that none of the guidance systems mentioned consider the effects of gravity, are merely able to estimate the overall flight time, and are not able to minimize commanded accelerations or final flight times.

Therefore, a need exists for an optimal air-to-surface guidance law that will take the effects of gravity into account, will allow the total time to target to be solved analytically, and will minimize the commanded accelerations or the total flight path time depending on what is desired. The problem is posed using Figure 1.3 where the frame x, y, and z is a reference frame fixed on the Earth's surface. Both the missile

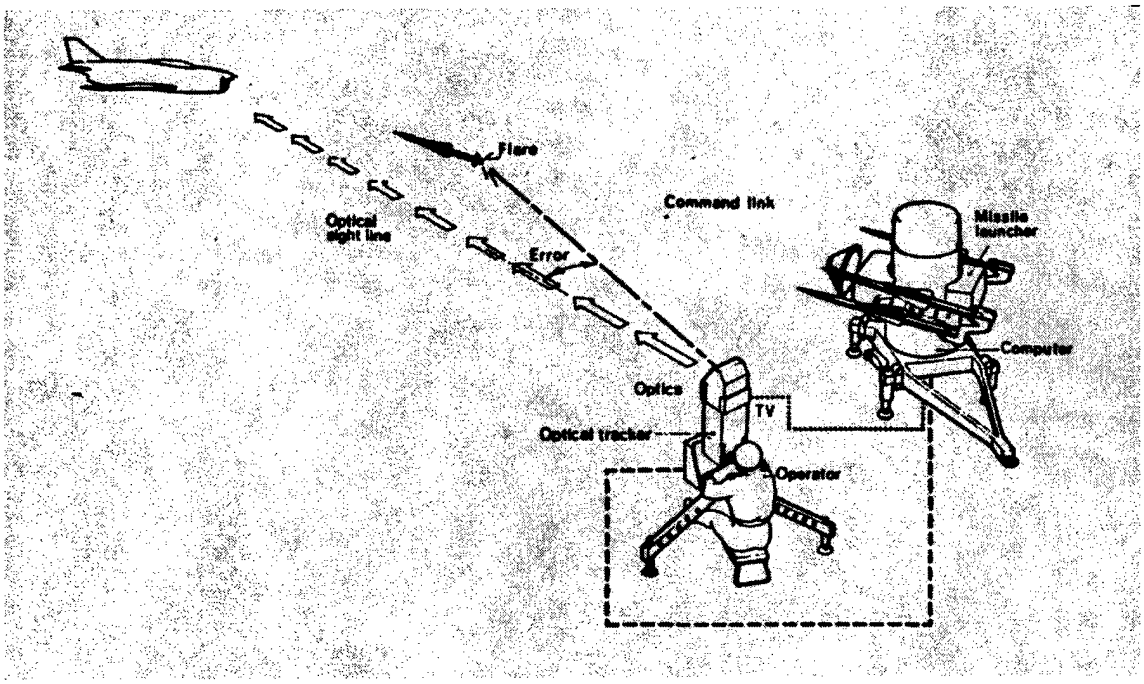

Figure 1.2: Rapier - a semiautomatic system [9]

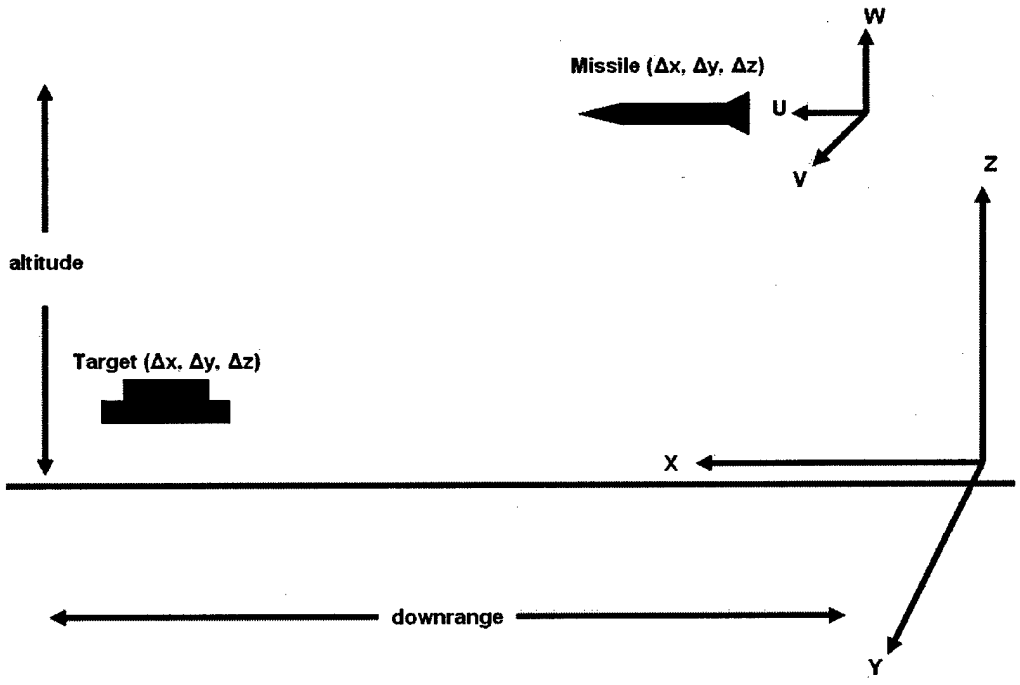

Figure 1.3: Proposed reference frame and physical problem setup

and the target velocities are denoted where u is a velocity in the x direction, v is a velocity in the y direction, and w represents a velocity in the z direction.

A family of guidance laws has been developed that takes gravity into account, allows the time to target to be solved analytically, and is designed for air-to-surface missiles tracking moving targets. Additionally the analytic guidance laws allow options to simply intercept the target without terminal angle constraints, to enforce a terminal flight path angle constraint, to enforce a terminal heading angle constraint, or to constrain both as displayed in Figure 1.4. In addition each guidance law has the capability, if desired, to minimize the total flight path time. These new guidance laws commanded accelerations are in the x, y, and z directions. They have been obtained using the first variation necessary conditions and the transversality conditions from Pontryagin's Minimum Principle [10]. In order to ensure that they are indeed optimal it is necessary to ensure that they not only meet the first variation necessary conditions for a minimum but also the second variation sufficient conditions for a minimum. In optimal control theory the first variation necessary conditions confirm that the solution is indeed capable of being a minimum, but is not necessarily a minimum. All minimizing solutions will satisfy the first and second variation necessary conditions. The second variation sufficient conditions, if met, will confirm that the solution is indeed a minimum. Although the necessary conditions were used to derive the guidance laws, and the necessary conditions were satisfied, it is possible that the guidance laws are still not minima (they could be a saddle point). The second variation sufficient conditions unambiguously verify the minimality of the solutions. All of the guidance laws in this thesis satisfy the first and second variation necessary conditions and the second variation sufficient conditions for a minimum. A consequence of these guidance laws is reduced actuator usage, while achieving maximum terminal velocity by minimizing commanded acceleration which reduces drag. Also, these laws can minimize the total flight time which gives maximum capability to the missile

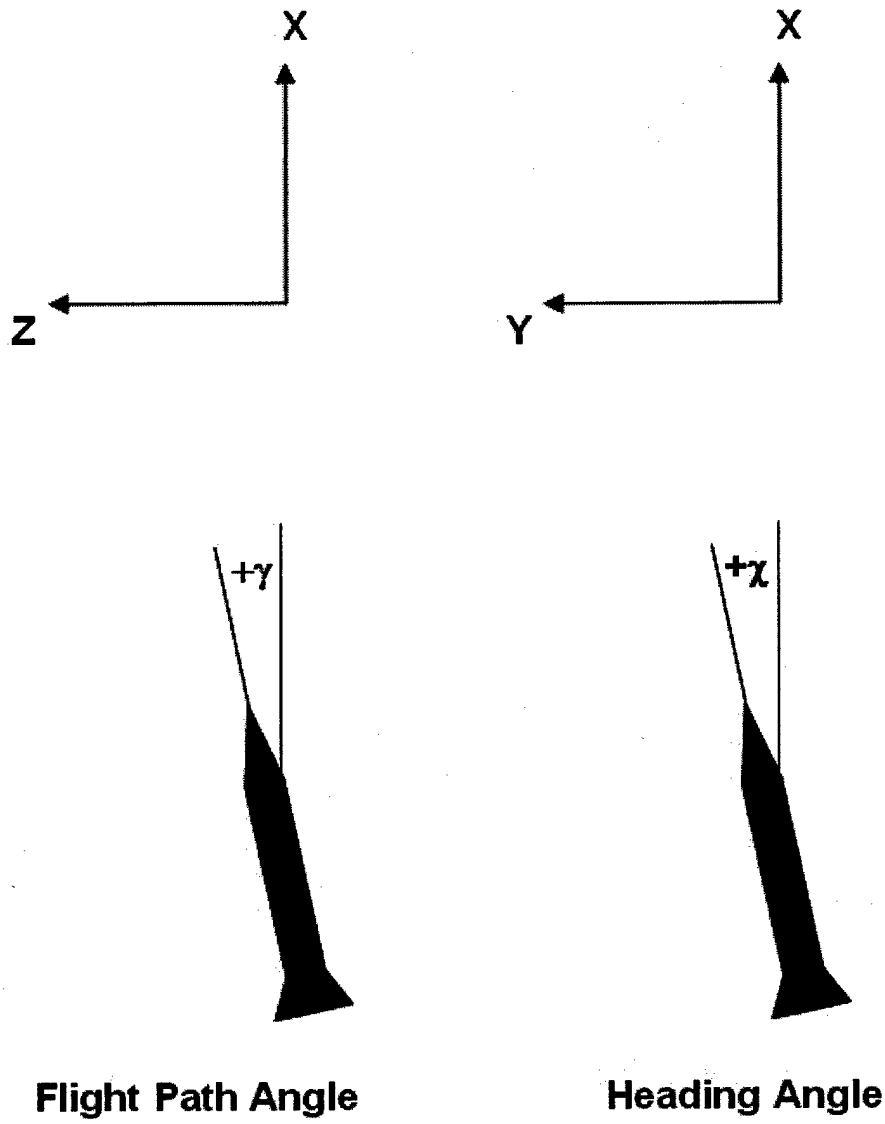

Figure 1.4: Defined flight path angle and heading angle

when intercept time is an important factor. These new solutions provide numerous options and capabilities that were not previously available.

In Chapter 2 the guidance laws are developed using the first variation conditions that arise out of Pontryagin's Minimum Principle. These conditions state that the solution is a minimum, maximum, or a saddle point. Later these conditions are used

to also verify the optimality of the solution in Chapter 5. Chapter 3 considers the second variation necessary conditions and demonstrates that the guidance laws do indeed meet these conditions. The second variation necessary conditions rule out the possibility that the candidate solution is a maximum, but do not ensure that it is a minimum. Chapter 4 considers the second variation sufficient conditions. The second variation sufficient conditions prove that the solution being considered is indeed a minimum. In Chapter 5 the first variation conditions are used to verify that the family of guidance laws that were derived are indeed correct. Next it is shown that the analytic guidance laws meet the second variation sufficient conditions. Also, an optimization tool known as DIDO is used to determine the numerically optimal trajectories given certain conditions and can be compared with the analytic guidance laws. Also, the guidance laws are incorporated into and tested in an existing 6-DOF missile simulation. The guidance laws performed extremely well when implemented into this missile simulation. Chapter 6 reviews the derivations and analysis performed and then draws conclusions about the family of guidance laws based on these findings.

Chapter 2

First Variation Necessary Conditions

In order to derive optimal control guidance laws there must first exist a foundation upon which they are to be built. Therefore it is necessary to derive a set of first order necessary conditions that must be satisfied in order to obtain an optimal solution [10]. Given the performance index, which is to be minimized, of the form

$$J = E(x_f, t_f) + \int_{t_o}^{t_f} F(x, y, \tau)\, d\tau \tag{2.1}$$

subject to the following dynamics

$$\dot{x} = f(x, u, t) \quad x(t_o) = x_o \tag{2.2}$$

with the terminal conditions

$$e(x_f, t_f) = 0 \tag{2.3}$$

the constraints are adjoined to the performance index with Lagrange multipliers

$$J' = G(x_f, t_f, \nu) + \int_{t_o}^{t_f} H(x, u, \lambda, \tau) - \lambda^T \dot{x}\, d\tau \tag{2.4}$$

where the Hamiltonian and Bolza function are

$$H(x, u, \lambda, t) = F(x, u, t) + \lambda^T f(x, u, t) \tag{2.5}$$

$$G(x_f, t_f, \nu) = E(x_f, t_f) + \nu^T e(x_f, t_f). \tag{2.6}$$

Taking variations, the adjoined performance index becomes

$$\begin{aligned} \delta J' = {} & G_{x_f}\delta x_f + G_{t_f}\delta t_f + G_\nu \delta\nu + \{[H(x, u, \lambda, t) - \lambda^T \dot{x}]\delta t\}_{t=t_o}^{t=t_f} \\ & + \int_{t_o}^{t_f} H_x\tilde{\delta}x + H_u\tilde{\delta}u + H_\lambda\tilde{\delta}\lambda - \tilde{\delta}\lambda^T\dot{x} - \lambda^T\tilde{\delta}\dot{x}\, d\tau. \end{aligned} \tag{2.7}$$

The above variation references Leibnitz's rule with regard to taking variations of an integral I, if

$$I = \int_{t_o}^{t_f} F(z(\tau), \tau)\, d\tau \tag{2.8}$$

the variation of I is

$$\delta I = [F\delta t]_{t=t_o}^{t=t_f} + \int_{t_o}^{t_f} \tilde{\delta} F \delta\tau. \tag{2.9}$$

In addition, the relation between the time fixed variation $\tilde{\delta}(\,)$ and the time free variation $\delta(\,)$ is

$$\delta(\,) = \tilde{\delta}(\,) + \dot{(\,)}\tilde{t}. \tag{2.10}$$

Recalling that $G_\nu = e = 0$ and $H_\lambda = f(x,u,t)$ and $[f(x,u,\tau) - \dot{x}]\tilde{\delta}\lambda = 0$, it follows that

$$\begin{aligned} \delta J' &= G_{x_f}\delta x_f + G_{t_f}\delta t_f + \{[H(x,u,\lambda,t) - \lambda^T\dot{x}]\delta t\}_{t=t_o}^{t=t_f} \\ &\quad + \int_{t_o}^{t_f} H_x\tilde{\delta}x + H_u\tilde{\delta}u - \lambda^T\tilde{\delta}\dot{x}\, d\tau. \end{aligned} \tag{2.11}$$

Since t_o is specified, $\delta t_o = 0$. Also, $\tilde{\delta}x_f$ is

$$\tilde{\delta}x_f = \delta x_f - \dot{x}_f\delta t_f. \tag{2.12}$$

Now using integration by parts the third term in the integral simplifies to

$$\int_{t_o}^{t_f} \lambda^T\tilde{\delta}\dot{x}\, d\tau = [\lambda^T\tilde{\delta}x]_{t=t_o}^{t=t_f} - \int_{t_o}^{t_f} \dot{\lambda}^T\tilde{\delta}x\, d\tau \tag{2.13}$$

$$= \dot{\lambda}_f^T\tilde{\delta}x_f - \int_{t_o}^{t_f} \dot{\lambda}^T\tilde{\delta}x\, d\tau. \tag{2.14}$$

Now the first variation of the adjoined performance index becomes

$$\begin{aligned} \delta J' &= (G_{x_f} - \lambda_f^T)\delta x_f + (G_{t_f} + H_f)\delta t_f \\ &\quad + \int_{t_o}^{t_f} (H_x\tilde{\delta}x + \dot{\lambda}^T)\tilde{\delta}x + H_u\tilde{\delta}u\, d\tau. \end{aligned} \tag{2.15}$$

Up to this point nothing has been said about the Lagrange multipliers or costates, λ. They are now *chosen* such that the coefficients of the dependent variations, δx,

vanish. Therefore eliminating all but the independent variations, the first variation is

$$\delta J' = (G_{x_f} + H_f)\delta t_f + \int_{t_o}^{t_f} H_u \tilde{\delta} u \, d\tau \tag{2.16}$$

with

$$\dot{\lambda} = -H_x^T \quad \text{and} \quad \lambda_f = G_{x_f}^T. \tag{2.17}$$

Finally, the coefficients of $\tilde{\delta} u$ and δt_f, the independent variations, must vanish for the first variation to vanish, thus

$$H_u = 0 \quad \text{and} \quad H_f = -G_{t_f}. \tag{2.18}$$

Therefore the **first variation necessary conditions** (the Euler-Lagrange equations) are

$$\dot{\lambda} = -H_x(x, u, \lambda, t) \tag{2.19}$$

$$\dot{x} = f(x, u, t) \qquad x_o = x(t_o) \tag{2.20}$$

$$H_u = 0 \tag{2.21}$$

with the transversality conditions

$$\lambda_f = G_{x_f}^T \tag{2.22}$$

$$H_f = -G_{t_f} \tag{2.23}$$

$$e(x_f, t_f) = 0. \tag{2.24}$$

These necessary conditions fall out of Pontryagin's Minimum Principle.

By taking the total derivative with respect to time of the Hamiltonian a useful result appears

$$H = H(x, u, t, \lambda) \tag{2.25}$$

$$\frac{dH}{dt} = \frac{\partial H}{\partial t} + \frac{\partial H}{\partial x}\frac{dx}{dt} + \frac{\partial H}{\partial u}\frac{du}{dt} + \frac{\partial H}{\partial \lambda}\frac{d\lambda}{dt}. \tag{2.26}$$

If the Hamiltonian is not explicitly a function of time, $\frac{\partial H}{\partial t} = 0$. Also, based on the first variation necessary conditions $H_u = 0$. Notice that $\frac{\partial H}{\partial x} = -\dot{\lambda}$ and $\frac{\partial H}{\partial \lambda} = \dot{x}$. Therefore

$$\frac{dH}{dt} = \frac{\partial H}{\partial x}\frac{dx}{dt} + \frac{\partial H}{\partial \lambda}\frac{d\lambda}{dt} \tag{2.27}$$

$$= -\dot{\lambda}^T\dot{x} + \dot{x}^T\dot{\lambda} = 0. \tag{2.28}$$

From the transversality conditions

$$H = \text{constant} = -G_{t_f}. \tag{2.29}$$

Now not only is H_f equal to $-G_{t_f}$ but the Hamiltonian at every point in time is equal to $-G_{t_f}$. This result gives an excellent condition that can be used to determine if the necessary conditions for a minimum are met at every instance in time, if the Hamiltonian is not an explicit function of time.

2.1 Dynamics of the System

The equations of motion in Cartesian coordinates are:

$$\dot{x} = u \tag{2.30}$$

$$\dot{y} = v \tag{2.31}$$

$$\dot{z} = w \tag{2.32}$$

$$\dot{u} = a_x \tag{2.33}$$

$$\dot{v} = a_y \tag{2.34}$$

$$\dot{w} = a_z + g \tag{2.35}$$

x refers to the downrange position of the vehicle, y refers to the crossrange position of the vehicle, z is the altitude of the vehicle, u is the downrange velocity, v is the crossrange velocity, w is the vertical velocity, a_x is the downrange acceleration, a_y is the crossrange acceleration, and a_z is the vertical acceleration. In addition the

constraints are as follows

$$x_f = x_T - u_T(t_f - t) \tag{2.36}$$

$$y_f = y_T - v_T(t_f - t) \tag{2.37}$$

$$z_f = z_T - w_T(t_f - t) \tag{2.38}$$

where the subscript T refers to the target.

2.2 Three Dimensional Moving Target with no Additional Constraints

2.2.1 The Performance Index and Problem Set-up

This performance index is posed as

$$\min J = \Gamma\, t_f + \frac{1}{2}\int_{t_o}^{t_f} a_x^2 + a_y^2 + a_z^2\, d\tau \tag{2.39}$$

subject to the aforementioned dynamics Eqns. 2.30-2.35, with a specified initial state x_o, y_o, z_o, u_o, v_o, and w_o. The following enforced terminal constraints are

$$e_x = x_f - x_T + u_T(t_f - t) = 0 \tag{2.40}$$

$$e_y = y_f - y_T + v_T(t_f - t) = 0 \tag{2.41}$$

$$e_z = z_f - z_T + w_T(t_f - t) = 0. \tag{2.42}$$

where the subscript T annotates the state of the target. Γ is a weighting parameter on the final time (if it is unspecified). This is a trade-off between the minimum time problem and the minimum control effort problem. Normally Γ is set to zero in order to minimize the commanded acceleration. Increasing Γ to a large number has the effect of finding a minimum time trajectory. The Hamiltonian and the Bolza function are

$$H = \frac{1}{2}(a_x^2 + a_y^2 + a_z^2) + \lambda_x u + \lambda_y v + \lambda_z w + \lambda_u a_x + \lambda_v a_y + \lambda_w(a_z + g) \tag{2.43}$$

$$G = \Gamma t_f + \nu_x e_x + \nu_y e_y + \nu_z e_z. \tag{2.44}$$

2.2.2 The First Variation Conditions

The Pontryagin Minimum Principle, along with the transversality condition on the final state, yield the following equations

$$\dot{\lambda_x} = 0 \tag{2.45}$$

$$\dot{\lambda_y} = 0 \tag{2.46}$$

$$\dot{\lambda_z} = 0 \tag{2.47}$$

$$\dot{\lambda_u} = -\lambda_x \tag{2.48}$$

$$\dot{\lambda_v} = -\lambda_y \tag{2.49}$$

$$\dot{\lambda_w} = -\lambda_z \tag{2.50}$$

with the terminal conditions

$$\lambda_{x_f} = \nu_x \tag{2.51}$$

$$\lambda_{y_f} = \nu_y \tag{2.52}$$

$$\lambda_{z_f} = \nu_z \tag{2.53}$$

$$\lambda_{u_f} = 0 \tag{2.54}$$

$$\lambda_{v_f} = 0 \tag{2.55}$$

$$\lambda_{w_f} = 0 \tag{2.56}$$

If we define

$$t_{go} \triangleq t_f - t \tag{2.57}$$

the Lagrange multipliers are found to be

$$\lambda_x = \nu_x \tag{2.58}$$

$$\lambda_y = \nu_y \tag{2.59}$$

$$\lambda_z = \nu_z \tag{2.60}$$

$$\lambda_u = \nu_x t_{go} \tag{2.61}$$

$$\lambda_v = \nu_y t_{go} \tag{2.62}$$

$$\lambda_w = \nu_z t_{go} \tag{2.63}$$

and the controls a_x, a_y, a_z, obtained from the Euler Lagrange equations, are

$$a_x = -\lambda_u = -\nu_x t_{go} \tag{2.64}$$

$$a_y = -\lambda_v = -\nu_y t_{go} \tag{2.65}$$

$$a_z = -\lambda_w = -\nu_z t_{go}. \tag{2.66}$$

The states can now be written as

$$x = -\frac{\nu_x t_{go}^3}{6} - u_f t_{go} + x_T + u_T t_{go} \tag{2.67}$$

$$y = -\frac{\nu_y t_{go}^3}{6} - v_f t_{go} + y_T + v_T t_{go} \tag{2.68}$$

$$z = -\frac{\nu_z t_{go}^3}{6} + \frac{g t_{go}^2}{2} - w_f t_{go} + z_T + w_T t_{go} \tag{2.69}$$

$$u = \frac{\nu_x t_{go}^2}{2} + u_f \tag{2.70}$$

$$v = \frac{\nu_y t_{go}^2}{2} + v_f \tag{2.71}$$

$$w = \frac{\nu_z t_{go}^2}{2} + w_f - g t_{go}. \tag{2.72}$$

The states in the x, y, and z directions are all independent of each other as well as their associated controls a_x, a_y, and a_z. Solving for the Lagrange multipliers in terms

of the states yields

$$\nu_x = \frac{3(u-u_T)}{a^2} + \frac{3(x-x_T)}{a^3} \tag{2.73}$$

$$\nu_y = \frac{3(v-v_T)}{a^2} + \frac{3(y-y_T)}{a^3} \tag{2.74}$$

$$\nu_z = \frac{3(w-w_T)}{a^2} + \frac{3(z-z_T)}{a^3} \tag{2.75}$$

and the controls can be expressed as

$$a_x = -\frac{3}{t_{go}^2}(x - x_T + t_{go}(u-u_T)) \tag{2.76}$$

$$a_y = -\frac{3}{t_{go}^2}(y - y_T + t_{go}(v-v_T)) \tag{2.77}$$

$$a_z = -\frac{3}{t_{go}^2}(z - z_T + t_{go}(w-w_T)) - \frac{3g}{2} \tag{2.78}$$

The acceleration can compactly be written as

$$\mathbf{a} = -\frac{3}{t_{go}^2}(\mathbf{v}t_{go} + \mathbf{r}) - \frac{3\mathbf{g}}{2} \tag{2.79}$$

where

$$\mathbf{r} \triangleq \begin{bmatrix} x_V - x_T \\ y_V - y_T \\ z_V - z_T \end{bmatrix} \tag{2.80}$$

$$\mathbf{v} \triangleq \begin{bmatrix} u_V - u_T \\ v_V - v_T \\ w_V - w_T \end{bmatrix} \tag{2.81}$$

$$\mathbf{g} \triangleq [0 \quad 0 \quad g]^T. \tag{2.82}$$

Thus, a closed-loop feedback guidance law which is dependent only on the current state, the terminal state, and the time to target has been obtained. The variational method was used because it allows for a solution of the final time.

2.2.3 Solving for the Final Time

The transversality condition from the Pontryagin Minimum Principle associated with the free final time condition ($H_f = -G_{t_F}$) results in the following equation

$$\frac{1}{2}(a_x^2 + a_y^2 + a_z^2) + \lambda_x u + \lambda_y v + \lambda_z w + \lambda_u a_x + \lambda_v a_y + \lambda_z(a_z + g) = -G_{t_f} \quad (2.83)$$

where

$$-G_{t_f} = -\Gamma + \nu_x u_T + \nu_y v_T + \nu_z w_T. \quad (2.84)$$

A useful condition is obtained from the first integral (being a constant), since the Hamiltonian is independent of time, which can be expressed as

$$H = -\frac{1}{2}(a_x^2 + a_y^2 + a_z^2) + \nu_x u + \nu_y v + \nu_z w + \lambda_w g \quad (2.85)$$

and after combining the Hamiltonian and the Bolza function the following result can be expressed.

$$0 = (2\Gamma + \frac{3}{4}\mathbf{g}\cdot\mathbf{g})t_{go}^4 - 3(\mathbf{v}\cdot\mathbf{v} + \mathbf{r}\cdot\mathbf{g})t_{go}^2 - 12(\mathbf{v}\cdot\mathbf{r})t_{go} - 9(\mathbf{r}\cdot\mathbf{r}) \quad (2.86)$$

In most cases it is desired to minimize the commanded acceleration and thus Γ should be set to zero. However if it is desired to minimize the flight time, then Γ would be set to a large positive number.

2.2.4 The Analytic Solution for t_{go}

The equation for t_{go} can be solved analytically [7]. First the equation begins in the form noted in the previous section.

$$At_{go}^4 + Bt_{go}^3 + Ct_{go}^2 + Dt_{go} + E = 0 \quad (2.87)$$

After dividing through by A the equation becomes

$$t_{go}^4 + B't_{go}^3 + C't_{go}^2 + D't_{go} + E' = 0. \quad (2.88)$$

Translate the equation such that the cubic term is eliminated therefore

$$y^4 + Py^2 + Qy + R = 0 \tag{2.89}$$

where

$$P = 6h^2 + 3B'h + C' \tag{2.90}$$

$$Q = 4h^3 + 3B'h^2 + 2C'h + D' \tag{2.91}$$

$$R = h^4 + B'h^3 + C'h^2 + D'h + E' \tag{2.92}$$

with

$$x = y + h \tag{2.93}$$

and

$$h = -\frac{B'}{4}. \tag{2.94}$$

Next obtain the cubic resolvent

$$t^3 + 2Pt^2 + (P^2 - 4R)t - Q^2 = 0 \tag{2.95}$$

or

$$Z^3 + aZ + b = 0 \tag{2.96}$$

where

$$a = \frac{1}{3}[3(P^2 - 4R) - 4P^2] \tag{2.97}$$

$$b = \frac{1}{27}[16P^3 - 18P(P^2 - 4R) - 27Q^2] \tag{2.98}$$

with

$$Z = t - s \tag{2.99}$$

$$s = -\frac{2}{3}P. \tag{2.100}$$

Next calculate (Δ) as

$$\Delta = \frac{a^3}{27} + \frac{b^2}{4}. \tag{2.101}$$

If $\Delta > 0$, solve the resolvent by the Cardan formula so that the roots are

$$Z_1 = \sqrt[3]{-\frac{b}{2}+\sqrt{\Delta}}+\sqrt[3]{-\frac{b}{2}-\sqrt{\Delta}} \tag{2.102}$$

$$Z_2 = \text{complex} \tag{2.103}$$

$$Z_3 = \text{complex.} \tag{2.104}$$

If $\Delta = 0$, the roots of the resolvent are

$$Z_1 = 2\sqrt[3]{-\frac{b}{2}} \tag{2.105}$$

$$Z_2 = \sqrt[3]{\frac{b}{2}} \tag{2.106}$$

$$Z_3 = \sqrt[3]{\frac{b}{2}}. \tag{2.107}$$

If $\Delta < 0$, the resolvant is solved using the trigonometric technique. Therefore

$$Z_1 = E_o \cos(\frac{\phi}{3}) \tag{2.108}$$

$$Z_2 = E_o \cos(\frac{\phi}{3}+120°) \tag{2.109}$$

$$Z_3 = E_o \cos(\frac{\phi}{3}+240°) \tag{2.110}$$

where

$$E_o \equiv 2\sqrt{-\frac{a}{3}} \tag{2.111}$$

and the angle ϕ is defined by

$$\cos(\phi) = -\frac{b}{2\sqrt{-\frac{a^3}{27}}} \tag{2.112}$$

$$\sin(\phi) = +\sqrt{1-\cos^2(\phi)} \tag{2.113}$$

According to the sign of Δ, the critical root of the cubic resolvent is

$$R' \equiv \max\left[\text{realroots}(Z_1+s, Z_2+s, Z_3+s)\right]. \tag{2.114}$$

A positive real root will always be found. Now that R' is obtained, the parameters ξ and β can be obtained from

$$\xi = \frac{1}{2}(P + R' - \frac{Q}{\sqrt{R'}}) \tag{2.115}$$

$$\beta = \frac{1}{2}(P + R' + \frac{Q}{\sqrt{R'}}) \tag{2.116}$$

Knowing ξ and β, the factorization of Eq. 4.58 is

$$(y^2 + \sqrt{R'}\, y + \xi)(y^2 - \sqrt{R'}\, y + \beta) = 0. \tag{2.117}$$

The solution of the two quadratics yields the $y_i (i = 1, 4)$ of Eq. 4.58. Therefore the roots of Eq. 4.56 are

$$x_i = y_i + h, \quad i = 1, \ldots, 4. \tag{2.118}$$

2.3 Three Dimensional Moving Target with a Constraint on Final Flight Path Angle

2.3.1 The Performance Index and Problem Set-up

This minimum control effort (acceleration) problem can be posed as

$$\min J = \Gamma\, t_f + \frac{1}{2}\int_{t_o}^{t_f} a_x^2 + a_y^2 + a_z^2\, d\tau \tag{2.119}$$

subject to the aforementioned dynamics Eqns. 2.30-2.35, with a specified initial state x_o, y_o, z_o, u_o, v_o, and w_o. The following terminal constraints will also be enforced

$$e_x = x_f - x_T + u_T(t_f - t) \tag{2.120}$$

$$e_y = y_f - y_T + v_T(t_f - t) \tag{2.121}$$

$$e_z = z_f - z_T + w_T(t_f - t) \tag{2.122}$$

$$e_4 = w_f - u_f \tan\gamma_f. \tag{2.123}$$

Again, Γ is a weighting parameter on the final time (if it is unspecified), and can be used for a minimum time problem. The Hamiltonian and the Bolza function for the

case of a three dimensional moving target with a constraint on the final flight path angle are

$$\begin{aligned} H &= \frac{1}{2}(a_x^2 + a_y^2 + a_z^2) + \lambda_x u + \lambda_y v + \lambda_z w + \lambda_u a_x + \lambda_v a_y \\ &\quad + \lambda_w(a_z + g) \qquad (2.124) \\ G &= \Gamma t_f + \nu_x e_x + \nu_y e_y + \nu_z e_z + \nu_4 e_4. \qquad (2.125) \end{aligned}$$

2.3.2 The First Variation Conditions

The Pontryagin Minimum Principle, along with the transversality condition on the final state, yield the following equations

$$\dot{\lambda_x} = 0 \qquad (2.126)$$

$$\dot{\lambda_y} = 0 \qquad (2.127)$$

$$\dot{\lambda_z} = 0 \qquad (2.128)$$

$$\dot{\lambda_u} = -\lambda_x \qquad (2.129)$$

$$\dot{\lambda_v} = -\lambda_y \qquad (2.130)$$

$$\dot{\lambda_w} = -\lambda_z \qquad (2.131)$$

with the terminal conditions

$$\lambda_{x_f} = \nu_x \qquad (2.132)$$

$$\lambda_{y_f} = \nu_y \qquad (2.133)$$

$$\lambda_{z_f} = \nu_z \qquad (2.134)$$

$$\lambda_{u_f} = -\nu_4 \tan\gamma_f \qquad (2.135)$$

$$\lambda_{v_f} = 0 \qquad (2.136)$$

$$\lambda_{w_f} = \nu_4 \qquad (2.137)$$

If we define

$$t_{go} \triangleq t_f - t \qquad (2.138)$$

the Lagrange multipliers are found to be

$$\lambda_x = \nu_x \tag{2.139}$$

$$\lambda_y = \nu_y \tag{2.140}$$

$$\lambda_z = \nu_z \tag{2.141}$$

$$\lambda_u = \nu_x t_{go} - \nu_4 \tan\gamma_f \tag{2.142}$$

$$\lambda_v = \nu_y t_{go} \tag{2.143}$$

$$\lambda_w = \nu_z t_{go} + \nu_4 \tag{2.144}$$

and the controls a_x, a_y, and a_z, again derived from the Euler Lagrange equations, are

$$a_x = -\lambda_u = -\nu_x t_{go} + \nu_4 \tan\gamma_f \tag{2.145}$$

$$a_y = -\lambda_v = -\nu_y t_{go} \tag{2.146}$$

$$a_z = -\lambda_w = -\nu_z t_{go} - \nu_4. \tag{2.147}$$

The states can be written as

$$x = -\frac{\nu_x t_{go}^3}{6} + \frac{\nu_4 \tan\gamma_f t_{go}^2}{2} - u_f t_{go} + x_T + u_T t_{go} \tag{2.148}$$

$$y = -\frac{\nu_y t_{go}^3}{6} - v_f t_{go} + y_T + v_T t_{go} \tag{2.149}$$

$$z = -\frac{\nu_z t_{go}^3}{6} + \frac{\nu_4 t_{go}^2}{2} + \frac{g t_{go}^2}{2} - w_f t_{go} + z_T + w_T t_{go} \tag{2.150}$$

$$u = \frac{\nu_x t_{go}^2}{2} - \nu_4 \tan\gamma_f t_{go} + u_f \tag{2.151}$$

$$v = \frac{\nu_y t_{go}^2}{2} + v_f \tag{2.152}$$

$$w = \frac{\nu_z t_{go}^2}{2} + \nu_4 t_{go} + w_f - g t_{go} \tag{2.153}$$

The states in the x, y, and z directions are all independent of each other as well as their associated controls a_x, a_y, and a_z. Solving for the Lagrange multipliers in terms

of the states yields

$$\nu_x = -\frac{3\alpha_2}{t_{go}^2}w' + \frac{3\alpha_1 - 2}{t_{go}^2}u' + \frac{2u}{t_{go}^2} \tag{2.154}$$

$$\nu_y = \frac{1}{t_{go}^2}v' + \frac{2v}{t_{go}^2} \tag{2.155}$$

$$\nu_z = -\frac{3\alpha_2}{t_{go}^2}u' + \frac{3\alpha_3 - 2}{t_{go}^2}w' + \frac{2w}{t_{go}^2} + \frac{2g}{t_{go}} \tag{2.156}$$

where

$$\alpha_1 = 1 + \sin^2\gamma_f \tag{2.157}$$

$$\alpha_2 = \sin\gamma_f \cos\gamma_f \tag{2.158}$$

$$\alpha_3 = 1 + \cos^2\gamma_f \tag{2.159}$$

and the controls can be expressed as

$$a_x = -\frac{\alpha_1}{t_{go}}u' + \frac{\alpha_2}{t_{go}}w' - \frac{2u}{t_{go}} \tag{2.160}$$

$$a_y = -\frac{1}{t_{go}}(v' + 2v) \tag{2.161}$$

$$a_z = -\frac{\alpha_3}{t_{go}}w' + \frac{\alpha_2}{t_{go}}u' - \frac{2(w + gt_{go})}{t_{go}} \tag{2.162}$$

where

$$u' = u + \frac{3x}{t_{go}} - \frac{3x_T}{t_{go}} - 3u_T \tag{2.163}$$

$$v' = v + \frac{3y}{t_{go}} - \frac{3y_T}{t_{go}} - 3v_T \tag{2.164}$$

$$w' = w + \frac{3z}{t_{go}} - \frac{3z_T}{t_{go}} - 3w_T - \frac{gt_{go}}{2} \tag{2.165}$$

and finally

$$g \triangleq -32.174\frac{ft}{sec^2}. \tag{2.166}$$

2.3.3 Solving for the Final Time

The transversality condition from the Pontryagin Minimum Principle associated with the free final time condition ($H_f = -G_{t_F}$) results in the following equation

$$\frac{1}{2}(a_x^2 + a_y^2 + a_z^2) + \lambda_x u + \lambda_y v + \lambda_z w + \lambda_u a_x + \lambda_v a_y + \lambda_z(a_z + g) = -G_{t_f} \tag{2.167}$$

where

$$-G_{t_f} = -\Gamma + \nu_x u_T + \nu_y v_T + \nu_z w_T. \tag{2.168}$$

A more useful condition is obtained from the first integral (being a constant), since the Hamiltonian is independent of time, which can be expressed as

$$H = -\frac{1}{2}(a_x^2 + a_y^2 + a_z^2) + \nu_x u + \nu_y v + \nu_z w + \lambda_w g \tag{2.169}$$

and after combining the Hamiltonian and the Bolza function the following result can be expressed.

$$0 = C_4 t_{go}^4 + C_3 t_{go}^3 + C_2 t_{go}^2 + C_1 t_{go} + C_0 \tag{2.170}$$

where

$$C_4 = g^2(\frac{b_3}{4} - \frac{b_9}{2}) + \Gamma \tag{2.171}$$

$$C_3 = 0 \tag{2.172}$$

$$\begin{aligned} C_2 = {} & (b_1 - \cos^2\gamma_f)u^2 + (b_2 - 1)v^2 + (b_3 - \sin^2\gamma_f)w^2 + b_6uw \\ & +3g[-b_3(z - z_T) + b_6(x - x_T) + b_9(z - z_T) - \frac{3}{2}b_6(x - x_T)] \\ & +9[b_1u_T^2 + b_2v_T^2 + b_3w_T^2 + 3b_6u_Tw_T] \\ & -(6b_1 - 3\cos^2\gamma_f)u_Tu - (6b_2 - 3)v_Tv - (6b_3 - 3\sin^2\gamma_f)w_Tw \\ & -6b_6w_Tu - 6b_6wu_T + 3\alpha_2(w - 3w_T)u_T - 2uu_T \\ & -(3\alpha_1 - 2)(u - 3u_T)u_T - (v - 3v_T)v_T - 2vv_T \\ & +3\alpha_2(u - 3u_T)w_T - (3\alpha_3 - 2)(w - 3w_T)w_T - 2ww_T \end{aligned} \tag{2.173}$$

$$\begin{aligned} C_1 = {} & 9[b_1(-2xu_T + 2x_Tu_T) + b_2(-2yv_T + 2y_Tv_T) + b_3(-2zw_T + 2z_Tw_T) \\ & +3b_6(-xw_T + x_Tw_T - zu_T + z_Tu_T)] + (6b_1 - 3\cos^2\gamma_f)(x - x_T)u \\ & +(6b_2 - 3)(y - y_T)v + (6b_3 - 3\sin^2\gamma_f)(z - z_T)w \\ & +6b_6(z - z_T)u + 6b_6(x - x_T)w + 3\alpha_2(3z - 3z_T)u_T \\ & -(3\alpha_1 - 2)(3x - 3x_T)u_T - (3y - 3y_T)v_T + 3\alpha_2(3x - 3x_T)w_T \\ & -(3\alpha_3 - 2)(3z - 3z_T)w_T \end{aligned} \tag{2.174}$$

$$\begin{aligned} C_0 = {} & 9[b_1(x^2 - 2xx_T + x_T^2) + b_2(y^2 - 2yy_T + y_T^2) \\ & b_3(z^2 - 2zz_T + z_T^2) + 3b_6(xz - xz_T - zx_T + x_Tz_T)] \end{aligned} \tag{2.175}$$

and

$$b_1 = \frac{3\cos^2\gamma_f - 4}{2} \tag{2.176}$$

$$b_2 = -\frac{1}{2} \tag{2.177}$$

$$b_3 = \frac{3\sin^2\gamma_f - 4}{2} \tag{2.178}$$

$$b_6 = \sin\gamma_f\cos\gamma_f \tag{2.179}$$

$$b_9 = \sin^2\gamma_f - 2. \tag{2.180}$$

2.4 Three Dimensional Moving Target with a Constraint on Final Heading Angle

2.4.1 The Performance Index and Problem Set-up

This minimum control effort (acceleration) problem can be posed as

$$\min J = \Gamma\, t_f + \frac{1}{2}\int_{t_o}^{t_f} a_x^2 + a_y^2 + a_z^2\, d\tau \tag{2.181}$$

with a specified initial state x_o, y_o, z_o, u_o, v_o, and w_o. The following terminal constraints will also be enforced

$$e_x = x_f - x_T + u_T(t_f - t) \tag{2.182}$$

$$e_y = y_f - y_T + v_T(t_f - t) \tag{2.183}$$

$$e_z = z_f - z_T + w_T(t_f - t) \tag{2.184}$$

$$e_4 = v_f - u_f \tan\chi_f. \tag{2.185}$$

Γ is a weighting parameter on the final time (if it is unspecified). This is a trade-off between the minimum time problem and the minimum control effort problem. The Hamiltonian and the Bolza function for this derivation are

$$\begin{aligned} H &= \frac{1}{2}(a_x^2 + a_y^2 + a_z^2) + \lambda_x u + \lambda_y v + \lambda_z w + \lambda_u a_x + \lambda_v a_y \\ &\quad + \lambda_w(a_z + g) \end{aligned} \tag{2.186}$$

$$G = \Gamma t_f + \nu_x e_x + \nu_y e_y + \nu_z e_z + \nu_4 e_4 \tag{2.187}$$

2.4.2 The First Variation Conditions

The Pontryagin Minimum Principle, along with the transversality condition on the final state, yield the following equations

$$\dot{\lambda_x} = 0 \tag{2.188}$$

$$\dot{\lambda_y} = 0 \tag{2.189}$$

$$\dot{\lambda_z} = 0 \tag{2.190}$$

$$\dot{\lambda_u} = -\lambda_x \tag{2.191}$$

$$\dot{\lambda_v} = -\lambda_y \tag{2.192}$$

$$\dot{\lambda_w} = -\lambda_z \tag{2.193}$$

with the terminal conditions

$$\lambda_{x_f} = \nu_x \tag{2.194}$$

$$\lambda_{y_f} = \nu_y \tag{2.195}$$

$$\lambda_{z_f} = \nu_z \tag{2.196}$$

$$\lambda_{u_f} = -\nu_4 \tan \chi_f \tag{2.197}$$

$$\lambda_{v_f} = \nu_4 \tag{2.198}$$

$$\lambda_{w_f} = 0. \tag{2.199}$$

If we define

$$t_{go} \triangleq t_f - t \tag{2.200}$$

the Lagrange multipliers are found to be

$$\lambda_x = \nu_x \tag{2.201}$$

$$\lambda_y = \nu_y \tag{2.202}$$

$$\lambda_z = \nu_z \tag{2.203}$$

$$\lambda_u = \nu_x t_{go} - \nu_4 \tan\gamma_f \tag{2.204}$$

$$\lambda_v = \nu_y t_{go} + \nu_4 \tag{2.205}$$

$$\lambda_w = \nu_z t_{go} \tag{2.206}$$

and the controls, a_x, a_y, a_z are

$$a_x = -\lambda_u = -\nu_x t_{go} + \nu_4 \tan(\gamma_f) \tag{2.207}$$

$$a_y = -\lambda_v = -\nu_y t_{go} - \nu_4 \tag{2.208}$$

$$a_z = -\lambda_w = -\nu_z t_{go}. \tag{2.209}$$

The states can be written as

$$x = -\frac{\nu_x t_{go}^3}{6} + \frac{\nu_4 \tan\gamma_f t_{go}^2}{2} - u_f t_{go} + x_T + u_T t_{go} \tag{2.210}$$

$$y = -\frac{\nu_y t_{go}^3}{6} - \frac{\nu_4 t_{go}^2}{2} - v_f t_{go} + y_T + v_T t_{go} \tag{2.211}$$

$$z = -\frac{\nu_z t_{go}^3}{6} + \frac{g t_{go}^2}{2} - w_f t_{go} + z_T + w_T t_{go} \tag{2.212}$$

$$u = \frac{\nu_x t_{go}^2}{2} - \nu_4 \tan\gamma_f t_{go} + u_f \tag{2.213}$$

$$v = \frac{\nu_y t_{go}^2}{2} + \nu_4 t_{go} + v_f \tag{2.214}$$

$$w = \frac{\nu_z t_{go}^2}{2} + w_f - g t_{go}. \tag{2.215}$$

The states in the x, y, and z directions are all independent of each other as well as their associated controls a_x, a_y, and a_z. Solving for the Lagrange multipliers in terms

of the states yields

$$\nu_x = \frac{3}{t_{go}^2}\alpha_1 u - \frac{3}{t_{go}^2}\alpha_2 v + \frac{9}{t_{go}^3}\alpha_3 x - \frac{9}{t_{go}^3}\alpha_2 y - \frac{6}{t_{go}^3}x \tag{2.216}$$

$$\nu_y = -\frac{3}{t_{go}^2}\alpha_2 u + \frac{3}{t_{go}^2}\alpha_3 v - \frac{9}{t_{go}^3}\alpha_2 x + \frac{9}{t_{go}^3}\alpha_3 y - \frac{6}{t_{go}^3}y \tag{2.217}$$

$$\nu_z = \frac{3}{t_{go}^2}(w + \frac{z}{t_{go}} + \frac{1}{2}gt_{go}) \tag{2.218}$$

where

$$\alpha_1 = 1 + \sin^2\chi_f \tag{2.219}$$

$$\alpha_2 = \sin\chi_f \cos\chi_f \tag{2.220}$$

$$\alpha_3 = 1 + \cos^2\chi_f \tag{2.221}$$

and the controls can be expressed as

$$a_x = -\frac{\alpha_1}{t_{go}}u' + \frac{\alpha_2}{t_{go}}v' - \frac{2u}{t_{go}} \tag{2.222}$$

$$a_y = \frac{\alpha_2}{t_{go}}u' - \frac{\alpha_3}{t_{go}}v' - \frac{2v}{t_{go}} \tag{2.223}$$

$$a_z = -\frac{3}{t_{go}}(w + \frac{z}{t_{go}} + \frac{1}{2}gt_{go}) \tag{2.224}$$

where

$$u' = u + \frac{3x}{t_{go}} \tag{2.225}$$

$$v' = v + \frac{3y}{t_{go}} \tag{2.226}$$

$$w' = w + \frac{3z}{t_{go}} - \frac{gt_{go}}{2} \tag{2.227}$$

and

$$x = x - x_T - u_T t_{go} \tag{2.228}$$

$$y = y - y_T - v_T t_{go} \tag{2.229}$$

$$z = z - z_T - w_T t_{go}. \tag{2.230}$$

2.4.3 Solving for the Final Time

The transversality condition from the Pontryagin Minimum Principle associated with the free final time condition ($H_f = -G_{t_F}$) results in the following equation

$$\frac{1}{2}(a_x^2 + a_y^2 + a_z^2) + \lambda_x u + \lambda_y v + \lambda_z w + \lambda_u a_x + \lambda_v a_y + \lambda_z(a_z + g) = -G_{t_f} \quad (2.231)$$

where

$$-G_{t_f} = -\Gamma + \nu_x u_T + \nu_y v_T + \nu_z w_T. \quad (2.232)$$

A more useful condition is obtained from the first integral (being a constant), since the Hamiltonian is independent of time, which can be expressed as

$$H = -\frac{1}{2}(a_x^2 + a_y^2 + a_z^2) + \nu_x u + \nu_y v + \nu_z w + \lambda_w g \quad (2.233)$$

and after combining the Hamiltonian and the Bolza function the following result can be expressed.

$$0 = C_4 t_{go}^4 + C_3 t_{go}^3 + C_2 t_{go}^2 + C_1 t_{go} + C_0 \quad (2.234)$$

where

$$C_4 = \frac{3}{4}g^2 + 2\Gamma \tag{2.235}$$

$$C_3 = 0 \tag{2.236}$$

$$\begin{aligned} C_2 = {} & -(\alpha_1+2)u^2 - (\alpha_3+2)v^2 + 2\alpha_2 uv - 3w^2 - 3g(z-z_T) \\ & -9(3\sin^2\chi_f + 1)u_T^2 - 9(3\cos^2\chi_f + 1)v_T^2 - 9w_T^2 \\ & +54\alpha_2 u_T v_T + 12\alpha_1 u_T u - 12\alpha_2 v_T u - 12\alpha_2 u_T v \\ & +12\alpha_3 v_T v + 12 w_T w - 6\alpha_1 u u_T + 6\alpha_2 v u_T + 6\alpha_2 u v_T \\ & -6\alpha_3 v v_T - 6 w w_T + 6(3\sin^2\chi_f + 1)u_T^2 - 36\alpha_2 v_T u_T \\ & +6(3\cos^2\chi_f + 1)v_T^2 + 6w_T^2 \end{aligned} \tag{2.237}$$

$$\begin{aligned} C_1 = {} & -9(3\sin^2\chi_f + 1)(-2xu_T + 2x_T u_T) - 9(3\cos^2\chi_f + 1)(-2yv_T + 2y_T v_T) \\ & -9(-2zw_T + 2z_T w_T) + 54\alpha_2(-xv_T + x_T v_T - yu_T + y_T u_T) \\ & -12\alpha_1(x - x_T)u + 12\alpha_2(y - y_T)u + 12\alpha_2(x - x_T)v - 12\alpha_3(y - y_T)v \\ & -12(z - z_T)w - 6(3\sin^2\chi_f + 1)(x - x_T)u_T + 18\alpha_2(y - y_T)u_T \\ & +18\alpha_2(x - x_T)v_T - 6(3\cos^2\chi_f + 1)(y - y_T)v_T - 6(z - z_T)w_T \end{aligned} \tag{2.238}$$

$$\begin{aligned} C_0 = {} & -9(3\sin^2\chi_f + 1)(x^2 - 2xx_T + x_T^2) - 9(3\cos^2\chi_f + 1)(y^2 - 2yy_T + y_T^2) \\ & -9(z^2 - 2zz_T + z_T^2) + 54\alpha_2(xy - xy_T - yx_T + x_T y_T). \end{aligned} \tag{2.239}$$

2.5 Three Dimensional Moving Target with Constraints on Final Heading Angle and Final Flight Path Angle

2.5.1 The Performance Index and Problem Set-up

This minimum control effort (acceleration) problem can be posed as

$$\min J = \Gamma\, t_f + \frac{1}{2}\int_{t_o}^{t_f} a_x^2 + a_y^2 + a_z^2\, d\tau \tag{2.240}$$

subject to the aforementioned dynamics (Eqs. (3.1)-(3.6)), with a specified initial state x_o, y_o, z_o, u_o, v_o, and w_o. The following terminal constraints will also be enforced

$$e_x = x_f - x_T + u_T(t_f - t) \tag{2.241}$$

$$e_y = y_f - y_T + v_T(t_f - t) \tag{2.242}$$

$$e_z = z_f - z_T + w_T(t_f - t) \tag{2.243}$$

$$e_4 = w_f - u_f \tan\gamma_f \tag{2.244}$$

$$e_5 = w_f \tan\chi_f - v_f \sin\gamma_f. \tag{2.245}$$

Γ is a weighting parameter on the final time (if it is unspecified). This is a trade-off between the minimum time problem and the minimum control effort problem. The Hamiltonian and the Bolza function for this derivation are

$$\begin{aligned} H &= \frac{1}{2}(a_x^2 + a_y^2 + a_z^2) + \lambda_x u + \lambda_y v + \lambda_z w + \lambda_u a_x + \lambda_v a_y \\ &\quad + \lambda_w(a_z + g) \end{aligned} \tag{2.246}$$

$$G = \Gamma t_f + \nu_x e_x + \nu_y e_y + \nu_z e_z + \nu_4 e_4 + \nu_5 e_5. \tag{2.247}$$

2.5.2 The First Variation Conditions

The Pontryagin Minimum Principle, along with the transversality condition on the final state, yield the following equations

$$\dot{\lambda_x} = 0 \tag{2.248}$$

$$\dot{\lambda_y} = 0 \tag{2.249}$$

$$\dot{\lambda_z} = 0 \tag{2.250}$$

$$\dot{\lambda_u} = -\lambda_x \tag{2.251}$$

$$\dot{\lambda_v} = -\lambda_y \tag{2.252}$$

$$\dot{\lambda_w} = -\lambda_z \tag{2.253}$$

with the terminal conditions

$$\lambda_{x_f} = \nu_x \tag{2.254}$$

$$\lambda_{y_f} = \nu_y \tag{2.255}$$

$$\lambda_{z_f} = \nu_z \tag{2.256}$$

$$\lambda_{u_f} = -\nu_4 \tan\gamma_f \tag{2.257}$$

$$\lambda_{v_f} = -\nu_5 \sin\gamma_f \tag{2.258}$$

$$\lambda_{w_f} = \nu_4 + \nu_5 \tan\chi_f \tag{2.259}$$

If we define

$$t_{go} \triangleq t_f - t \tag{2.260}$$

the Lagrange multipliers are found to be

$$\lambda_x = \nu_x \tag{2.261}$$

$$\lambda_y = \nu_y \tag{2.262}$$

$$\lambda_z = \nu_z \tag{2.263}$$

$$\lambda_u = \nu_x t_{go} - \nu_4 \tan\gamma_f \tag{2.264}$$

$$\lambda_v = \nu_y t_{go} - \nu_5 \sin\gamma_f \tag{2.265}$$

$$\lambda_w = \nu_z t_{go} + \nu_4 + \nu_5 \tan\chi_f \tag{2.266}$$

and the controls, a_x, a_y, a_z are

$$a_x = -\lambda_u = -\nu_x t_{go} + \nu_4 \tan\gamma_f \tag{2.267}$$

$$a_y = -\lambda_v = -\nu_y t_{go} + \nu_5 \sin\gamma_f \tag{2.268}$$

$$a_z = -\lambda_w = -\nu_z t_{go} - \nu_4 - \nu_5 \tan\chi_f. \tag{2.269}$$

The states can be written as

$$x = -\frac{\nu_x t_{go}^3}{6} + \frac{\nu_4 \tan\gamma_f t_{go}^2}{2} - u_f t_{go} + x_T + u_T t_{go} \quad (2.270)$$

$$y = -\frac{\nu_y t_{go}^3}{6} + \frac{\nu_5 \sin\gamma_f t_{go}^2}{2} - v_f t_{go} + y_T + v_T t_{go} \quad (2.271)$$

$$z = -\frac{\nu_z t_{go}^3}{6} - \frac{\nu_4 t_{go}^2}{2} - \frac{\nu_5 \tan\chi_f t_{go}^2}{2} + \frac{g t_{go}^2}{2} - w_f t_{go} + z_T + w_T t_{go} \quad (2.272)$$

$$u = \frac{\nu_x t_{go}^2}{2} - \nu_4 \tan\gamma_f t_{go} + u_f \quad (2.273)$$

$$v = \frac{\nu_y t_{go}^2}{2} - \nu_5 \sin\gamma_f t_{go} + v_f \quad (2.274)$$

$$w = \frac{\nu_z t_{go}^2}{2} + \nu_4 t_{go} + \nu_5 \tan\chi_f t_{go} + w_f - g t_{go} \quad (2.275)$$

The states in the x, y, and z directions are all independent of each other as well as their associated controls a_x, a_y, and a_z. Solving for the Lagrange multipliers in terms of the states yields

$$\nu_x = \frac{3}{t_{go}^2}\alpha_1 u' - \frac{3}{t_{go}^2}\alpha_2 v' - \frac{3}{t_{go}^2}\alpha_3 w' - \frac{6x}{t_{go}^3} \quad (2.276)$$

$$\nu_y = -\frac{3}{t_{go}^2}\alpha_2 u' + \frac{3}{t_{go}^2}\alpha_5 v' - \frac{3}{t_{go}^2}\alpha_4 w' - \frac{6y}{t_{go}^3} \quad (2.277)$$

$$\nu_z = -\frac{3}{t_{go}^2}\alpha_3 u' - \frac{3}{t_{go}^2}\alpha_4 v' + \frac{3}{t_{go}^2}\alpha_6 w' + \frac{-6z + 3g t_{go}^2}{t_{go}^3} \quad (2.278)$$

where

$$\alpha_1 = 2 - \cos^2\gamma_f \cos^2\chi_f \quad (2.279)$$

$$\alpha_2 = \sin\chi_f \cos\chi_f \cos\gamma_f \quad (2.280)$$

$$\alpha_3 = \sin\gamma_f \cos\gamma_f \cos^2\chi_f \quad (2.281)$$

$$\alpha_4 = \sin\gamma_f \sin\chi_f \cos\chi_f \quad (2.282)$$

$$\alpha_5 = 1 + \cos^2\chi_f \quad (2.283)$$

$$\alpha_6 = 2 - \sin^2\gamma_f \cos^2\chi_f \quad (2.284)$$

$$\alpha_7 = 2 - \sin^2\chi_f \quad (2.285)$$

and the controls can be expressed as

$$a_x = -\frac{\alpha_1}{t_{go}}u' + \frac{\alpha_2}{t_{go}}v' + \frac{\alpha_3}{t_{go}}w' - \frac{2u}{t_{go}} \quad (2.286)$$

$$a_y = \frac{\alpha_2}{t_{go}}u' - \frac{\alpha_7}{t_{go}}v' + \frac{\alpha_4}{t_{go}}w' - \frac{2v}{t_{go}} \quad (2.287)$$

$$a_z = \frac{\alpha_3}{t_{go}}u' + \frac{\alpha 4}{t_{go}}v' - \frac{\alpha_6}{t_{go}}w' - \frac{2(w + gt_{go})}{t_{go}} \quad (2.288)$$

where

$$u' = u + \frac{3x}{t_{go}} \quad (2.289)$$

$$v' = v + \frac{3y}{t_{go}} \quad (2.290)$$

$$w' = w + \frac{3z}{t_{go}} - \frac{gt_{go}}{2} \quad (2.291)$$

and

$$x = x - x_T - u_T t_{go} \quad (2.292)$$

$$y = y - y_T - v_T t_{go} \quad (2.293)$$

$$z = z - z_T - w_T t_{go}. \quad (2.294)$$

2.5.3 Solving for the Final Time

The transversality condition from the Pontryagin Minimum Principle associated with the free final time condition ($H_f = -G_{t_F}$) results in the following equation

$$\frac{1}{2}(a_x^2 + a_y^2 + a_z^2) + \lambda_x u + \lambda_y v + \lambda_z w + \lambda_u a_x + \lambda_v a_y + \lambda_z(a_z + g) = -G_{t_f} \quad (2.295)$$

where

$$-G_{t_f} = -\Gamma + \nu_x u_T + \nu_y v_T + \nu_z w_T. \quad (2.296)$$

A more useful condition is obtained from the first integral (being a constant), since the Hamiltonian is independent of time, which can be expressed as

$$H = -\frac{1}{2}(a_x^2 + a_y^2 + a_z^2) + \nu_x u + \nu_y v + \nu_z w + \lambda_w g \quad (2.297)$$

and after combining the Hamiltonian and the Bolza function the following result can be expressed

$$0 = C_4 t_{go}^4 + C_3 t_{go}^3 + C_2 t_{go}^2 + C_1 t_{go} + C_0 \tag{2.298}$$

where

$$C_4 = g^2\frac{4-\sin^2\gamma_f\cos^2\chi_f}{8}+\Gamma \tag{2.299}$$

$$C_3 = 0 \tag{2.300}$$

$$\begin{aligned}C_2 = {} & \frac{\cos^2\chi_f\cos^2\gamma_f-4}{2}u^2+\frac{\sin^2\chi_f-4}{2}v^2+\frac{\sin^2\gamma_f\cos^2\chi_f-4}{2}w^2\\ & +b_4uv+b_6uw+b_5vw-\frac{3}{2}g[\sin^2\gamma_f\cos^2\chi_f(z-z_T)\\ & +\sin\gamma_f\sin\chi_f\cos\chi_f(y-y_T)+\sin\gamma_f\sin\gamma_f\cos^2\chi_f(x-x_T)]\\ & -6[b_7u_tu+b_8v_tv+b_9w_tw+(uv_T+vu_T)b_4+(vw_T+v_Tw)b_5\\ & +(uw_T+u_Tw)b_6]+9[b_1u_T^2+b_2v_T^2+b_3w_T^2+3b_4u_Tv_T\\ & +3b_5v_Tw_T+3b_6u_Tw_T]+3(b_7u+b_4v+b_6w)u_T+3(b_4u+b_5w+b_8v)v_T\\ & +3(b_6u+b_5v+b_9w)w_T-9(b_7u_T+b_4v_T+b_6w_T)u_T-6u_T^2\\ & -9(b_4u_T+b_8v_T+b_5w_T)v_T-6v_T^2\\ & -9(b_6u_T+b_5v_T+b_9w_T)w_T-6w_T^2\end{aligned} \tag{2.301}$$

$$\begin{aligned}C_1 = {} & 6[(b_7(x-x_T)u+b_8(y-y_T)v+b_9(z-z_T)w\\ & +((y-y_T)u+(x-x_T)v)b_4+((z-z_T)v+(y-y_T)w)b_5\\ & +((z-z_T)u+(x-x_T)w)b_6]+9[b_1(-2xu_T+2x_Tu_T)\\ & +b_2(-2yv_T+2y_Tv_T)+b_3(-2zw_T+2z_Tw_T)\\ & +3b_4(-xv_T+x_Tv_T-yu_T+y_Tu_T)+3b_5(-yw_T+y_Tw_T-zv_T+z_Tv_T)\\ & 3b_6(-xw_T+x_Tw_T-zu_T+z_Tu_T)]+9[b_7(x-x_T)+b_4(y-y_T)\\ & +b_6(z-z_T)]u_T+6(x-x_T)u_T+9[b_4(x-x_T)+b_8(y-y_T)\\ & +b_5(z-z_T)]v_T+6(y-y_T)v_T+9[b_6(x-x_T)+b_5(y-y_T)\\ & +b_9(z-z_T)]w_T+6(z-z_T)w_T\end{aligned} \tag{2.302}$$

$$\begin{aligned}C_0 = {} & 9[b_1(x^2-2xx_T+x_T^2)+b_2(y^2-2yy_T+y_T^2)\\ & +b_3(z^2-2zz_T+z_T^2)+3b_4(xy-xy_T-x_Ty+x_Ty_T)\\ & +3b_5(yz-yz_T-y_Tz+z_Ty_T)+3b_6(xz-xz_T-x_Tz+x_Tz_T)].\end{aligned} \tag{2.303}$$

Chapter 3

The Second Variation Necessary Conditions

In order establish whether the proposed guidance laws are optimal solutions the second variation necessary conditions must be satisfied. Once it is determined that the proposed guidance laws satisfy the second variation necessary conditions it will then be possible to examine the second variation sufficient conditions and definitely establish the optimality of the solution. The second variation necessary condition for a weak relative minimum, also known as Legendre-Clebsch condition, simply states

$$H_{uu} \geq 0. \tag{3.1}$$

The second variation necessary condition for a strong relative minimum is the Weierstrass condition which is

$$H(t, x, u_\star, \lambda) - H(t, x, u, \lambda) > 0 \tag{3.2}$$

where $u_\star$ is an admissible comparison control and u is the optimal control. Once these two conditions are met it is possible to conclude that the second variation necessary conditions have been satisfied. These conditions are not sufficient for a minimum, but it is known that the optimal path is not a maximum [10].

3.1 Applying the Second Variation Necessary Conditions

Given the Hamiltonian of the form

$$H = \frac{1}{2}(a_x^2 + a_y^2 + a_z^2) + \lambda_x u + \lambda_y v + \lambda_z w + \lambda_u a_x + \lambda_v a_y + \lambda_w (a_z + g) \tag{3.3}$$

where

$$u = \begin{bmatrix} a_x \\ a_y \\ a_z \end{bmatrix}. \tag{3.4}$$

In order to satisfy the Legendre-Clebsch condition the second partial derivative of the Hamiltonian with respect to the control must be greater than or equal to zero. Using the given Hamiltonian the second partial derivative of the Hamiltonian with respect to the control is as follows

$$H_{uu} = \begin{bmatrix} 1 & 0 & 0 \\ 0 & 1 & 0 \\ 0 & 0 & 1 \end{bmatrix}. \tag{3.5}$$

The identity matrix that results satisfies the Legendre-Clebsch condition for all four analytic guidance laws. The next condition that must be satisfied is the Weierstrass condition. The Weierstrass condition simply states that the Hamiltonian calculated using the optimal control subtracted from the Hamiltonian calculated using an admissible comparison control must be greater than zero. The Hamiltonian calculated using the admissible comparison control is as follows

$$H^\star = \frac{1}{2}(a_{x_\star}^2 + a_{y_\star}^2 + a_{z_\star}^2) + \lambda_x u + \lambda_y v + \lambda_z w + \lambda_u a_{x_\star} + \lambda_v a_{y_\star} + \lambda_w (a_{z_\star} + g). \tag{3.6}$$

Recall from Eqn. 2.64-2.66 that $\lambda_u = -a_x$, $\lambda_v = -a_y$, and $\lambda_w = -a_z$. Eqn. 2.64-2.66 came directly from the derivation for the guidance law considering a three dimensional moving target with no additional constraints, however, this condition is valid for all four guidance laws. Using this knowledge the Hamiltonian calculated using the optimal control and the Hamiltonian calculated using the admissible comparison control are as follows

$$H = \frac{1}{2}(a_x^2 + a_y^2 + a_z^2) + \lambda_x u + \lambda_y v + \lambda_z w + -a_x^2 - a_y^2 - a_z^2 - a_z g \tag{3.7}$$

$$\begin{aligned} H^\star = {} & \frac{1}{2}(a_{x_\star}^2 + a_{y_\star}^2 + a_{z_\star}^2) + \lambda_x u + \lambda_y v + \lambda_z w - a_x a_{x_\star} \\ & - a_y a_{y_\star} - a_z a_{z_\star} - a_z g. \end{aligned} \tag{3.8}$$

In order to check the Weierstrass condition the Hamiltonian with the optimal control must be subtracted from the Hamiltonian with the admissable comparison control. After performing the necessary algebra the results is as follows

$$H^{\star} - H = \frac{1}{2}(a_x - a_{x_\star})^2 + \frac{1}{2}(a_y - a_{y_\star})^2 + \frac{1}{2}(a_z - a_{z_\star})^2 \tag{3.9}$$

$$H^{\star} - H \geq 0. \tag{3.10}$$

Therefore the Weierstrass condition and the Legendre-Clebsch condition are both satisfied, thereby satisfying the second variation necessary conditions. Again, these conditions must be met in order for an optimal solution to exist, but these conditions do not mean that an optimal condition has been found. They do however rule out the possibility that the solution is a maximum [10]. This result applies to all four guidance laws.

Chapter 4

Establishing Optimality: The Second Variation Sufficient Conditions

Even with the guidance laws being derived using the first variation necessary conditions, the question must be raised as to the optimality of the solution. This can be verified using second order sufficient conditions [10]. If a solution meets the second order sufficient conditions then it is verified to be a minimum solution. Given the performance index of the form

$$J = E(x_f, t_f) + \int_{t_o}^{t_f} F(x, y, \tau)\, d\tau \tag{4.1}$$

with a solution satisfying the Pontryagin Minimum Principle, the solution is a minimum if the following conditions are satisfied

$$H_{uu} > 0 \tag{4.2}$$

$$\hat{S} \quad finite, \qquad t_o \leq t < t_f \tag{4.3}$$

where

$$\hat{S} = S - UV^{-1}U^T. \tag{4.4}$$

The matrices U and V are defined as

$$U = \begin{bmatrix} R & m \end{bmatrix} \tag{4.5}$$

$$V = \begin{bmatrix} Q & n \\ n^T & \alpha \end{bmatrix}. \tag{4.6}$$

The variables S, R, m, Q, n, and α are obtained as solutions to the following set of first order differential equations

$$\dot{S} = -C - A^T S - SA + SBS \tag{4.7}$$

$$\dot{R} = (SB - A^T)R \tag{4.8}$$

$$\dot{m} = (SB - A^T)m \tag{4.9}$$

$$\dot{Q} = R^T B R \tag{4.10}$$

$$\dot{n} = R^T B m \tag{4.11}$$

$$\dot{\alpha} = M^T B m \tag{4.12}$$

where

$$A = f_x - f_u H_{uu}^{-1} H_{ux} \tag{4.13}$$

$$B = f_u H_{uu}^{-1} H_{ux} \tag{4.14}$$

$$C = H_{xx} - H_{xu} H_{uu}^{-1} H_{ux} \tag{4.15}$$

and the final conditions are defined as

$$S_f = G_{x_f x_f} \tag{4.16}$$

$$R_f = e_{x_f}^T \tag{4.17}$$

$$m_f = \Omega_{x_f}^T \tag{4.18}$$

$$Q_f = 0 \tag{4.19}$$

$$n_f = \dot{e}_f \tag{4.20}$$

$$\alpha_f = \dot{\Omega}_f \tag{4.21}$$

where

$$\Omega = L_f + G_{x_f} f_f + G_{t_f} = 0 \tag{4.22}$$

$$L(t,x,u) = \frac{1}{2}\int_{t_o}^{t_f} a_x^2 + a_y^2 + a_z^2 \, d\tau \tag{4.23}$$

$$f(t,x,u) = \dot{x}. \tag{4.24}$$

If the conditions on $\hat{S}$ and H_{uu} are met then the guidance laws are indeed optimal solutions of the given performance index.

4.1 Three Dimensional Moving Target with no Additional Constraints

In order to evaluate the sufficient conditions Eqns. 4.2 and 4.3 recall the Hamil -tonian and Bolza functions are

$$\begin{aligned} H &= \frac{1}{2}(a_x^2 + a_y^2 + a_z^2) + \lambda_x u + \lambda_y v + \lambda_z w + \lambda_u a_x + \lambda_v a_y \\ &\quad +\lambda_w(a_z + g) \qquad (4.25) \\ G &= \Gamma t_f + \nu_x[x_f - x_T - u_T(t_f - t)] + \nu_y[y_f - y_T - v_T(t_f - t)] \\ &\quad +\nu_z[z_f - z_T - w_T(t_f - t)]. \qquad (4.26) \end{aligned}$$

The terminal constraints for this scenario are defined to be

$$\boldsymbol{e} = \begin{bmatrix} x_f - x_T - u_T(t_f - t) \\ y_f - y_T - v_T(t_f - t) \\ z_f - z_T - w_T(t_f - t) \end{bmatrix} \qquad (4.27)$$

and f is equal to $\dot{x}$ with the following form

$$f(x,u,t)^T = [\quad u \quad v \quad w \quad a_x \quad a_y \quad a_z + g \quad]^T. \qquad (4.28)$$

The first and second partial derivatives of the Hamiltonian with respect to the control are

$$H_u = \begin{bmatrix} a_x + \lambda_u \\ a_y + \lambda_v \\ a_z + \lambda_w \end{bmatrix} \qquad (4.29)$$

$$H_{uu} = \begin{bmatrix} 1 & 0 & 0 \\ 0 & 1 & 0 \\ 0 & 0 & 1 \end{bmatrix} \qquad (4.30)$$

and also the partial derivative of the Hamiltonian with respect to u and then x yields

$$H_{ux} = 0_{3\times 6}. \tag{4.31}$$

H_{uu} is a constant identity matrix, which is greater than zero, and fulfills one of the second variation conditions for a minimum. The second partial derivative of the Hamiltonian with respect to x is

$$H_{xx} = 0_{6\times 6}. \tag{4.32}$$

The partial derivatives of f with respect to u and x are respectively

$$f_x = \begin{bmatrix} 0 & 0 & 0 & 1 & 0 & 0 \\ 0 & 0 & 0 & 0 & 1 & 0 \\ 0 & 0 & 0 & 0 & 0 & 1 \\ 0 & 0 & 0 & 0 & 0 & 0 \\ 0 & 0 & 0 & 0 & 0 & 0 \\ 0 & 0 & 0 & 0 & 0 & 0 \end{bmatrix} \tag{4.33}$$

$$f_u = \begin{bmatrix} 0 & 0 & 0 \\ 0 & 0 & 0 \\ 0 & 0 & 0 \\ 1 & 0 & 0 \\ 0 & 1 & 0 \\ 0 & 0 & 1 \end{bmatrix}. \tag{4.34}$$

Evaluating Eqns. 4.13-4.15 using f_x, f_u, H_{uu}, H_{ux}, and H_{xx} we get

$$A = f_x - f_u H_{uu}^{-1} H_{ux} = f_x = \begin{bmatrix} 0_{3\times 3} & I_{3\times 3} \\ 0_{3\times 3} & 0_{3\times 3} \end{bmatrix} \tag{4.35}$$

$$B = f_u H_{uu}^{-1} f_u^T = f_u f_u^T = \begin{bmatrix} 0_{3\times 3} & 0_{3\times 1} \\ 0_{3\times 3} & I_{3\times 3} \end{bmatrix} \tag{4.36}$$

$$C = H_{xx} - H_{xu} H_{uu}^{-1} H_{ux} = 0_{6\times 6}. \tag{4.37}$$

Using the set of first order differential equations Eqns. 4.7-4.12 with the final conditions designated by Eqns. 4.16-4.21 the solutions S, R, Q, m, n, and α can be found. The solution S is obtained rather simply by integrating Eqn. 4.7 and enforcing the final condition

$$S_f = G_{x_f x_f} = 0_{6\times 6} \tag{4.38}$$

such that the solution S is

$$S = 0_{6\times 6} \tag{4.39}$$

The solution R is obtained by integrating Eqn. 4.8 and applying the final condition

$$R_f = e_{x_f}^T = \begin{bmatrix} 1 & 0 & 0 \\ 0 & 1 & 0 \\ 0 & 0 & 1 \\ 0 & 0 & 0 \\ 0 & 0 & 0 \\ 0 & 0 & 0 \end{bmatrix} \tag{4.40}$$

such that the solution R is

$$R = \begin{bmatrix} 1 & 0 & 0 \\ 0 & 1 & 0 \\ 0 & 0 & 1 \\ t_f - t & 0 & 0 \\ 0 & t_f - t & 0 \\ 0 & 0 & t_f - t \end{bmatrix}. \tag{4.41}$$

Integrating Eqn. 4.10 leads to the solution for Q by applying the final condition

$$Q_f = 0_{3\times 3}. \tag{4.42}$$

The solution Q is

$$Q = \begin{bmatrix} -\frac{1}{3}(t_f - t)^3 & 0 & 0 \\ 0 & -\frac{1}{3}(t_f - t)^3 & 0 \\ 0 & 0 & -\frac{1}{3}(t_f - t)^3 \end{bmatrix}. \tag{4.43}$$

The next solution to be obtained is m which requires the terminal condition m_f

$$m_f = \Omega_{x_f}^T = \begin{bmatrix} 0 \\ 0 \\ 0 \\ \nu_x \\ \nu_y \\ \nu_z \end{bmatrix}. \tag{4.44}$$

After integrating $\dot{m}$ subject to the final condition the following solution is obtained

$$\dot{m} = (SB - A^T)m = -A^T m \tag{4.45}$$

$$m = \begin{bmatrix} 0 \\ 0 \\ 0 \\ \nu_x \\ \nu_y \\ \nu_z \end{bmatrix}. \tag{4.46}$$

The next solution that must be obtained is n and the terminal conditions for n are

$$n_f = \dot{e}_f = e_{t_f} + e_{x_f} f_f = \begin{bmatrix} u_f - u_T \\ v_f - v_T \\ w_f - w_T \end{bmatrix}. \tag{4.47}$$

Now enforcing the final conditions on n and integrating $\dot{n}$ the solution is

$$\dot{n} = R^T B m \tag{4.48}$$

$$n = \begin{bmatrix} -\frac{1}{2}\nu_x(t_f - t)^2 + u_f - u_T \\ -\frac{1}{2}\nu_y(t_f - t)^2 + v_f - v_T \\ -\frac{1}{2}\nu_z(t_f - t)^2 + w_f - w_T \end{bmatrix}. \tag{4.49}$$

The final differential equation that must be solved is $\dot{\alpha}$ and the final condition for α is

$$\alpha_f = \dot{\Omega}_f = \Omega_{t_f} + \Omega_{x_f}\dot{x}_f = \nu_x a_{x_f} + \nu_y a_{y_f} + \nu_z(a_{z_f} + g). \tag{4.50}$$

Finally the resulting solution of α is

$$\alpha = -(\nu_x^2 + \nu_y^2 + \nu_z^2)(t_f - t) + \nu_x a_{x_f} + \nu_y a_{y_f} + \nu_z(a_{z_f} + g). \tag{4.51}$$

Using the solutions of S, R, m, Q, n, and α the matrices V and U can be formed

$$V = \begin{bmatrix} Q & n \\ n^T & \alpha \end{bmatrix} \tag{4.52}$$

$$U = \begin{bmatrix} R & m \end{bmatrix}. \tag{4.53}$$

In order to check the optimality of a solution the matrices U and V must be determined at every point of the solution. If U does not go to infinity and V has a nonzero determinant then the condition on $\hat{S}$ will be satisfied. Therefore, if these conditions are met, the guidance laws for a three dimensional moving target with no additional constraints would indeed be a minimum.

4.2 Three Dimensional Moving Target with a Terminal Flight Path Angle Constraint

In order to evaluate the sufficient conditions Eqns. 4.2 and 4.3 recall the Hamil -tonian and Bolza functions are

$$\begin{aligned} H &= \frac{1}{2}(a_x^2 + a_y^2 + a_z^2) + \lambda_x u + \lambda_y v + \lambda_z w + \lambda_u a_x \\ &\quad + \lambda_v a_y + \lambda_w(a_z + g) \end{aligned} \tag{4.54}$$

$$\begin{aligned} G &= \Gamma t_f + \nu_x[x_f - x_T - u_T(t_f - t)] + \nu_y[y_f - y_T - v_T(t_f - t)] \\ &\quad + \nu_z[z_f - z_T - w_T(t_f - t)] + \nu_4[w_f - u_f \tan\gamma_f]. \end{aligned} \tag{4.55}$$

The terminal constraints for this scenario are defined to be

$$\boldsymbol{e} = \begin{bmatrix} x_f - x_T - u_T(t_f - t) \\ y_f - y_T - v_T(t_f - t) \\ z_f - z_T - w_T(t_f - t) \\ w_f - u_f \tan(\gamma_f) \end{bmatrix} \tag{4.56}$$

and f is equal to $\dot{x}$ with the following form

$$f(x,u,t)^T = [\quad u \quad v \quad w \quad a_x \quad a_y \quad a_z + g \quad]^T. \tag{4.57}$$

The first and second partial derivatives of the Hamiltonian with respect to the control are

$$H_u = \begin{bmatrix} a_x + \lambda_u \\ a_y + \lambda_v \\ a_z + \lambda_w \end{bmatrix} \tag{4.58}$$

$$H_{uu} = \begin{bmatrix} 1 & 0 & 0 \\ 0 & 1 & 0 \\ 0 & 0 & 1 \end{bmatrix} \tag{4.59}$$

and also the partial derivative of the Hamiltonian with respect to u and then x yields

$$H_{ux} = 0_{3\times 6}. \tag{4.60}$$

H_{uu} is a constant identity matrix, which is greater than zero, and fulfills one of the second variation conditions for a minimum. The second partial derivative of the Hamiltonian with respect to x is

$$H_{xx} = 0_{6\times 6}. \tag{4.61}$$

The partial derivatives of f with respect to u and x are respectively

$$f_x = \begin{bmatrix} 0 & 0 & 0 & 1 & 0 & 0 \\ 0 & 0 & 0 & 0 & 1 & 0 \\ 0 & 0 & 0 & 0 & 0 & 1 \\ 0 & 0 & 0 & 0 & 0 & 0 \\ 0 & 0 & 0 & 0 & 0 & 0 \\ 0 & 0 & 0 & 0 & 0 & 0 \end{bmatrix} \tag{4.62}$$

$$f_u = \begin{bmatrix} 0 & 0 & 0 \\ 0 & 0 & 0 \\ 0 & 0 & 0 \\ 1 & 0 & 0 \\ 0 & 1 & 0 \\ 0 & 0 & 1 \end{bmatrix}. \tag{4.63}$$

Evaluating Eqns. 4.13-4.15 using f_x, f_u, H_{uu}, H_{ux}, and H_{xx} we get

$$A = f_x - f_u H_{uu}^{-1} H_{ux} = f_x = \begin{bmatrix} 0_{3\times3} & I_{3\times3} \\ 0_{3\times3} & 0_{3\times3} \end{bmatrix} \tag{4.64}$$

$$B = f_u H_{uu}^{-1} f_u^T = f_u f_u^T = \begin{bmatrix} 0_{3\times3} & 0_{3\times1} \\ 0_{3\times3} & I_{3\times3} \end{bmatrix} \tag{4.65}$$

$$C = H_{xx} - H_{xu} H_{uu}^{-1} H_{ux} = 0_{6\times6}. \tag{4.66}$$

Using the set of first order differential equations Eqns. 4.7-4.12 with the final conditions designated by Eqns. 4.16-4.21 the solutions S, R, Q, m, n, and α can be found. The solution S is obtained rather simply by integrating Eqn. 4.7 and enforcing the final condition

$$S_f = G_{x_f x_f} = 0_{6\times6} \tag{4.67}$$

such that the solution S is

$$S = 0_{6\times6}. \tag{4.68}$$

The solution R is obtained by integrating Eqn. 4.8 and applying the final condition

$$R_f = e_{x_f}^T = \begin{bmatrix} 1 & 0 & 0 & 0 \\ 0 & 1 & 0 & 0 \\ 0 & 0 & 1 & 0 \\ 0 & 0 & 0 & -\tan\gamma_f \\ 0 & 0 & 0 & 0 \\ 0 & 0 & 0 & 1 \end{bmatrix} \tag{4.69}$$

such that the solution R is

$$R = \begin{bmatrix} 1 & 0 & 0 & 0 \\ 0 & 1 & 0 & 0 \\ 0 & 0 & 1 & 0 \\ t_f - t & 0 & 0 & -\tan\gamma_f \\ 0 & t_f - t & 0 & 0 \\ 0 & 0 & t_f - t & 1 \end{bmatrix}. \tag{4.70}$$

Integrating Eqn. 4.10 leads to the solution for Q by applying the final condition

$$Q_f = 0_{4\times 4}. \tag{4.71}$$

The solution Q is

$$Q = \begin{bmatrix} -\frac{1}{3}t_{go}^3 & 0 & 0 & \frac{1}{2}t_{go}^2\tan\gamma_f \\ 0 & -\frac{1}{3}t_{go}^3 & 0 & 0 \\ 0 & 0 & -\frac{1}{3}t_{go}^3 & -\frac{1}{2}t_{go}^2 \\ \frac{1}{2}t_{go}^2\tan\gamma_f & 0 & -\frac{1}{2}t_{go}^2 & -(1+\tan^2\gamma_f)t_{go} \end{bmatrix} \tag{4.72}$$

where

$$t_{go} = t_f - t. \tag{4.73}$$

The next solution to be obtained is m which requires the terminal condition m_f

$$m_f = \Omega_{x_f}^T = \begin{bmatrix} 0 \\ 0 \\ 0 \\ \nu_x \\ \nu_y \\ \nu_z \end{bmatrix}. \tag{4.74}$$

After integrating $\dot{m}$ subject to the final condition the following solution is obtained

$$\dot{m} = (SB - A^T)m = -A^T m \tag{4.75}$$

$$m = \begin{bmatrix} 0 \\ 0 \\ 0 \\ \nu_x \\ \nu_y \\ \nu_z \end{bmatrix}. \tag{4.76}$$

The next solution that must be obtained is n and the terminal conditions for n are

$$n_f = \dot{e}_f = e_{t_f} + e_{x_f} f_f = \begin{bmatrix} u_f - u_T \\ v_f - v_T \\ w_f - w_T \\ -\tan\gamma_f a_{x_f} + a_{z_f} + g \end{bmatrix}. \tag{4.77}$$

Now enforcing the final conditions on n and integrating $\dot{n}$ the solution is

$$\dot{n} = R^T B m \tag{4.78}$$

$$n = \begin{bmatrix} -\frac{1}{2}\nu_x(t_f - t)^2 + u_f - u_T \\ -\frac{1}{2}\nu_y(t_f - t)^2 + v_f - v_T \\ -\frac{1}{2}\nu_z(t_f - t)^2 + w_f - w_T \\ (\nu_x \tan\gamma_f - \nu_z)t_{go} - \tan\gamma_f a_{x_f} + a_{z_f} + g \end{bmatrix}. \tag{4.79}$$

The final differential equation that must be solved is $\dot{\alpha}$ and final condition for α is

$$\alpha_f = \dot{\Omega}_f = \Omega_{t_f} + \Omega_{x_f}\dot{x}_f = \nu_x a_{x_f} + \nu_y a_{y_f} + \nu_z(a_{z_f} + g). \tag{4.80}$$

Finally the resulting solution of α is

$$\alpha = -(\nu_x^2 + \nu_y^2 + \nu_z^2)(t_f - t) + \nu_x a_{x_f} + \nu_y a_{y_f} + \nu_z(a_{z_f} + g). \tag{4.81}$$

Using the solutions of S, R, m, Q, n, and α the matrices V and U can be formed

$$V = \begin{bmatrix} Q & n \\ n^T & \alpha \end{bmatrix} \tag{4.82}$$

$$U = \begin{bmatrix} R & m \end{bmatrix}. \tag{4.83}$$

As before, in order to check the optimality of a solution the matrices U and V must be determined at every point of the solution. If U does not go to infinity and V has a nonzero determinant then the condition on $\hat{S}$ will be satisfied and the solution will indeed be a minimum.

4.3 Three Dimensional Moving Target with a Terminal Heading Angle Constraint

In order to evaluate the sufficient conditions Eqns. 4.2 and 4.3 recall the Hamil -tonian and Bolza functions are

$$\begin{aligned} H &= \frac{1}{2}(a_x^2 + a_y^2 + a_z^2) + \lambda_x u + \lambda_y v + \lambda_z w + \lambda_u a_x + \lambda_v a_y \\ &\quad + \lambda_w(a_z + g) \end{aligned} \tag{4.84}$$

$$\begin{aligned} G &= \Gamma t_f + \nu_x[x_f - x_T - u_T(t_f - t)] + \nu_y[y_f - y_T - v_T(t_f - t)] \\ &\quad + \nu_z[z_f - z_T - w_T(t_f - t)] + \nu_4[v_f - u_f \tan\chi_f]. \end{aligned} \tag{4.85}$$

The terminal constraints for this scenario are defined to be

$$\boldsymbol{e} = \begin{bmatrix} x_f - x_T - u_T(t_f - t) \\ y_f - y_T - v_T(t_f - t) \\ z_f - z_T - w_T(t_f - t) \\ v_f - u_f \tan \chi_f \end{bmatrix} \tag{4.86}$$

and f is equal to $\dot{x}$ with the following form

$$f(x,u,t)^T = [\quad u \quad v \quad w \quad a_x \quad a_y \quad a_z + g \quad]^T. \tag{4.87}$$

The first and second partial derivatives of the Hamiltonian with respect to the control are

$$H_u = \begin{bmatrix} a_x + \lambda_u \\ a_y + \lambda_v \\ a_z + \lambda_w \end{bmatrix} \tag{4.88}$$

$$H_{uu} = \begin{bmatrix} 1 & 0 & 0 \\ 0 & 1 & 0 \\ 0 & 0 & 1 \end{bmatrix} \tag{4.89}$$

and also the partial derivative of the Hamiltonian with respect to u and then x yields

$$H_{ux} = 0_{3\times 6}. \tag{4.90}$$

H_{uu} is a constant identity matrix, which is greater than zero, and fulfills one of the second variation conditions for a minimum. The second partial derivative of the Hamiltonian with respect to x is

$$H_{xx} = 0_{6\times 6}. \tag{4.91}$$

The partial derivatives of f with respect to u and x are respectively

$$f_x = \begin{bmatrix} 0 & 0 & 0 & 1 & 0 & 0 \\ 0 & 0 & 0 & 0 & 1 & 0 \\ 0 & 0 & 0 & 0 & 0 & 1 \\ 0 & 0 & 0 & 0 & 0 & 0 \\ 0 & 0 & 0 & 0 & 0 & 0 \\ 0 & 0 & 0 & 0 & 0 & 0 \end{bmatrix} \tag{4.92}$$

$$f_u = \begin{bmatrix} 0 & 0 & 0 \\ 0 & 0 & 0 \\ 0 & 0 & 0 \\ 1 & 0 & 0 \\ 0 & 1 & 0 \\ 0 & 0 & 1 \end{bmatrix}. \tag{4.93}$$

Evaluating Eqns. 4.13-4.15 using f_x, f_u, H_{uu}, H_{ux}, and H_{xx} we get

$$A = f_x - f_u H_{uu}^{-1} H_{ux} = f_x = \begin{bmatrix} 0_{3\times3} & I_{3\times3} \\ 0_{3\times3} & 0_{3\times3} \end{bmatrix} \tag{4.94}$$

$$B = f_u H_{uu}^{-1} f_u^T = f_u f_u^T = \begin{bmatrix} 0_{3\times3} & 0_{3\times1} \\ 0_{3\times3} & I_{3\times3} \end{bmatrix} \tag{4.95}$$

$$C = H_{xx} - H_{xu} H_{uu}^{-1} H_{ux} = 0_{6\times6}. \tag{4.96}$$

Using the set of first order differential equations Eqns. 4.7-4.12 with the final conditions designated by Eqns. 4.16-4.21 the solutions S, R, Q, m, n, and α can be found. The solution S is obtained rather simply by integrating Eqn. 4.7 and enforcing the final condition

$$S_f = G_{x_f x_f} = 0_{6\times6} \tag{4.97}$$

such that the solution S is

$$S = 0_{6\times6} \tag{4.98}$$

The solution R is obtained by integrating Eqn. 4.8 and applying the final condition

$$R_f = e_{x_f}^T = \begin{bmatrix} 1 & 0 & 0 & 0 \\ 0 & 1 & 0 & 0 \\ 0 & 0 & 1 & 0 \\ 0 & 0 & 0 & -\tan\chi_f \\ 0 & 0 & 0 & 1 \\ 0 & 0 & 0 & 0 \end{bmatrix} \tag{4.99}$$

such that the solution R is

$$R = \begin{bmatrix} 1 & 0 & 0 & 0 \\ 0 & 1 & 0 & 0 \\ 0 & 0 & 1 & 0 \\ t_f - t & 0 & 0 & -\tan\chi_f \\ 0 & t_f - t & 0 & 1 \\ 0 & 0 & t_f - t & 0 \end{bmatrix}. \tag{4.100}$$

Integrating Eqn. 4.10 leads to the solution for Q by applying the final condition

$$Q_f = 0_{4\times 4}. \tag{4.101}$$

The solution Q is

$$Q = \begin{bmatrix} -\frac{1}{3}t_{go}^3 & 0 & 0 & \frac{1}{2}t_{go}^2\tan\chi_f \\ 0 & -\frac{1}{3}t_{go}^3 & 0 & -\frac{1}{2}t_{go}^2 \\ 0 & 0 & -\frac{1}{3}t_{go}^3 & 0 \\ \frac{1}{2}t_{go}^2\tan\chi_f & -\frac{1}{2}t_{go}^2 & 0 & -(1+\tan^2\chi_f)t_{go} \end{bmatrix} \tag{4.102}$$

where

$$t_{go} = t_f - t. \tag{4.103}$$

The next solution to be obtained is m which requires the terminal condition m_f

$$m_f = \Omega_{x_f}^T = \begin{bmatrix} 0 \\ 0 \\ 0 \\ \nu_x \\ \nu_y \\ \nu_z \end{bmatrix}. \tag{4.104}$$

After integrating $\dot{m}$ subject to the final condition the following solution is obtained

$$\dot{m} = (SB - A^T)m = -A^T m \tag{4.105}$$

$$m = \begin{bmatrix} 0 \\ 0 \\ 0 \\ \nu_x \\ \nu_y \\ \nu_z \end{bmatrix}. \tag{4.106}$$

The next solution that must be obtained is n and the terminal conditions for n are

$$n_f = \dot{e}_f = e_{t_f} + e_{x_f} f_f = \begin{bmatrix} u_f - u_T \\ v_f - v_T \\ w_f - w_T \\ -\tan\chi_f a_{x_f} + a_{y_f} \end{bmatrix}. \tag{4.107}$$

Now enforcing the final conditions on n and integrating $\dot{n}$ the solution is

$$\dot{n} = R^T B m \tag{4.108}$$

$$n = \begin{bmatrix} -\frac{1}{2}\nu_x(t_f - t)^2 + u_f - u_T \\ -\frac{1}{2}\nu_y(t_f - t)^2 + v_f - v_T \\ -\frac{1}{2}\nu_z(t_f - t)^2 + w_f - w_T \\ (\nu_x \tan\chi_f - \nu_y)t_{go} - \tan\chi_f a_{x_f} + a_{y_f} \end{bmatrix}. \tag{4.109}$$

The final differential equation that must be solved is $\dot{\alpha}$ and final condition for α is

$$\alpha_f = \dot{\Omega}_f = \Omega_{t_f} + \Omega_{x_f}\dot{x}_f = \nu_x a_{x_f} + \nu_y a_{y_f} + \nu_z(a_{z_f} + g). \tag{4.110}$$

Finally the resulting solution of α is

$$\alpha = -(\nu_x^2 + \nu_y^2 + \nu_z^2)(t_f - t) + \nu_x a_{x_f} + \nu_y a_{y_f} + \nu_z(a_{z_f} + g). \tag{4.111}$$

Using the solutions of S, R, m, Q, n, and α the matrices V and U can be formed

$$V = \begin{bmatrix} Q & n \\ n^T & \alpha \end{bmatrix} \tag{4.112}$$

$$U = \begin{bmatrix} R & m \end{bmatrix}. \tag{4.113}$$

4.4 Three Dimensional Moving Target with a Constraint on both the Terminal Flight Path Angle and the Terminal Heading Angle

In order to evaluate the sufficient conditions Eqns. 4.2 and 4.3 recall the Hamil -tonian and Bolza functions are

$$\begin{aligned} H &= \frac{1}{2}(a_x^2 + a_y^2 + a_z^2) + \lambda_x u + \lambda_y v + \lambda_z w + \lambda_u a_x + \lambda_v a_y \\ &\quad + \lambda_w(a_z + g) \end{aligned} \tag{4.114}$$

$$\begin{aligned} G &= \Gamma t_f + \nu_x[x_f - x_T - u_T(t_f - t)] + \nu_y[y_f - y_T - v_T(t_f - t)] \\ &\quad + \nu_z[z_f - z_T - w_T(t_f - t)] + \nu_4[w_f - u_f \tan\gamma_f] \\ &\quad + \nu_5[w_f \tan\chi_f - v_f \sin\gamma_f]. \end{aligned} \tag{4.115}$$

The terminal constraints for this scenario are defined to be

$$\boldsymbol{e} = \begin{bmatrix} x_f - x_T - u_T(t_f - t) \\ y_f - y_T - v_T(t_f - t) \\ z_f - z_T - w_T(t_f - t) \\ w_f - u_f \tan(\gamma_f) \\ w_f \tan\chi_f - v_f \sin\gamma_f \end{bmatrix} \tag{4.116}$$

and f is equal to $\dot{x}$ with the following form

$$f(x,u,t)^T = [\quad u \quad v \quad w \quad a_x \quad a_y \quad a_z + g \quad]^T. \tag{4.117}$$

The first and second partial derivatives of the Hamiltonian with respect to the control are

$$H_u = \begin{bmatrix} a_x + \lambda_u \\ a_y + \lambda_v \\ a_z + \lambda_w \end{bmatrix} \tag{4.118}$$

$$H_{uu} = \begin{bmatrix} 1 & 0 & 0 \\ 0 & 1 & 0 \\ 0 & 0 & 1 \end{bmatrix} \tag{4.119}$$

and also the partial derivative of the Hamiltonian with respect to u and then x yields

$$H_{ux} = 0_{3\times 6}. \tag{4.120}$$

H_{uu} is a constant identity matrix, which is greater than zero, and fulfills one of the second variation conditions for a minimum. The second partial derivative of the Hamiltonian with respect to x is

$$H_{xx} = 0_{6\times 6}. \tag{4.121}$$

The partial derivatives of f with respect to u and x are respectively

$$f_x = \begin{bmatrix} 0 & 0 & 0 & 1 & 0 & 0 \\ 0 & 0 & 0 & 0 & 1 & 0 \\ 0 & 0 & 0 & 0 & 0 & 1 \\ 0 & 0 & 0 & 0 & 0 & 0 \\ 0 & 0 & 0 & 0 & 0 & 0 \\ 0 & 0 & 0 & 0 & 0 & 0 \end{bmatrix} \tag{4.122}$$

$$f_u = \begin{bmatrix} 0 & 0 & 0 \\ 0 & 0 & 0 \\ 0 & 0 & 0 \\ 1 & 0 & 0 \\ 0 & 1 & 0 \\ 0 & 0 & 1 \end{bmatrix}. \tag{4.123}$$

Evaluating Eqns. 4.13-4.15 using f_x, f_u, H_{uu}, H_{ux}, and H_{xx} we get

$$A = f_x - f_u H_{uu}^{-1} H_{ux} = f_x = \begin{bmatrix} 0_{3\times3} & I_{3\times3} \\ 0_{3\times3} & 0_{3\times3} \end{bmatrix} \tag{4.124}$$

$$B = f_u H_{uu}^{-1} f_u^T = f_u f_u^T = \begin{bmatrix} 0_{3\times3} & 0_{3\times1} \\ 0_{3\times3} & I_{3\times3} \end{bmatrix} \tag{4.125}$$

$$C = H_{xx} - H_{xu} H_{uu}^{-1} H_{ux} = 0_{6\times6}. \tag{4.126}$$

Using the set of first order differential equations Eqns. 4.7-4.12 with the final conditions designated by Eqns. 4.16-4.21 the solutions S, R, Q, m, n, and α can be found. The solution S is obtained rather simply by integrating Eqn. 4.7 and enforcing the final condition

$$S_f = G_{x_f x_f} = 0_{6\times6} \tag{4.127}$$

such that the solution S is

$$S = 0_{6\times6} \tag{4.128}$$

The solution R is obtained by integrating Eqn. 3.8 and applying the final condition

$$R_f = e_{x_f}^T = \begin{bmatrix} 1 & 0 & 0 & 0 & 0 \\ 0 & 1 & 0 & 0 & 0 \\ 0 & 0 & 1 & 0 & 0 \\ 0 & 0 & 0 & -\tan\gamma_f & 0 \\ 0 & 0 & 0 & 0 & -\sin\gamma_f \\ 0 & 0 & 0 & 1 & \tan\chi_f \end{bmatrix} \tag{4.129}$$

such that the solution R is

$$R = \begin{bmatrix} 1 & 0 & 0 & 0 & 0 \\ 0 & 1 & 0 & 0 & 0 \\ 0 & 0 & 1 & 0 & 0 \\ t_f - t & 0 & 0 & -\tan\gamma_f & 0 \\ 0 & t_f - t & 0 & 0 & -\sin\gamma_f \\ 0 & 0 & t_f - t & 1 & \tan\chi_f \end{bmatrix}. \tag{4.130}$$

Integrating Eqn. (4.10) leads to the solution for Q by applying the final condition

$$Q_f = 0_{5\times 5}. \tag{4.131}$$

The solution Q is

$$Q_{(1-5,1-3)} = \begin{bmatrix} -\frac{1}{3}t_{go}^3 & 0 & 0 \\ 0 & -\frac{1}{3}t_{go}^3 & 0 \\ 0 & 0 & -\frac{1}{3}t_{go}^3 \\ \frac{1}{2}t_{go}^2\tan\gamma_f & 0 & -\frac{1}{2}t_{go}^2 \\ 0 & \frac{1}{2}t_{go}^2\sin\gamma_f & -\frac{1}{2}t_{go}^2\tan\chi_f \end{bmatrix}$$

$$Q_{(1-5,4-5)} = \begin{bmatrix} \frac{1}{2}t_{go}^2\tan\gamma_f & 0 \\ 0 & \frac{1}{2}t_{go}^2\sin\gamma_f \\ -\frac{1}{2}t_{go}^2 & -\frac{1}{2}t_{go}^2\tan\chi_f \\ -t_{go}(1+\tan^2\gamma_f) & -t_{go}\tan\chi_f \\ -t_{go}\tan\chi_f & -(\sin^2\gamma_f + \tan^2\chi_f)t_{go} \end{bmatrix} \tag{4.132}$$

where

$$t_{go} = t_f - t. \tag{4.133}$$

The next solution to be obtained is m which requires the terminal condition m_f

$$m_f = \Omega_{x_f}^T = \begin{bmatrix} 0 \\ 0 \\ 0 \\ \nu_x \\ \nu_y \\ \nu_z \end{bmatrix}. \tag{4.134}$$

After integrating $\dot{m}$ subject to the final condition the following solution is obtained

$$\dot{m} = (SB - A^T)m = -A^T m \tag{4.135}$$

$$m = \begin{bmatrix} 0 \\ 0 \\ 0 \\ \nu_x \\ \nu_y \\ \nu_z \end{bmatrix}. \tag{4.136}$$

The next solution that must be obtained is n and the terminal conditions for n are

$$n_f = \dot{e}_f = e_{t_f} + e_{x_f} f_f = \begin{bmatrix} u_f - u_T \\ v_f - v_T \\ w_f - w_T \\ -\tan\gamma_f a_{x_f} + a_{z_f} + g \\ -\sin\gamma_f a_{y_f} + \tan\chi_f (a_{z_f} + g) \end{bmatrix}. \tag{4.137}$$

Now enforcing the final conditions on n and integrating $\dot{n}$ the solution is

$$\dot{n} = R^T B m \tag{4.138}$$

$$n = \begin{bmatrix} -\frac{1}{2}\nu_x t_{go}^2 + u_f - u_T \\ -\frac{1}{2}\nu_y t_{go}^2 + v_f - v_T \\ -\frac{1}{2}\nu_z t_{go}^2 + w_f - w_T \\ (\nu_x \tan\gamma_f - \nu_z) t_{go} - a_{x_f} \tan\gamma_f + a_{z_f} + g \\ (\nu_y \sin\gamma_f - \nu_z \tan\chi_f) t_{go} - \sin\gamma_f a_{y_f} + \tan\chi_f (a_{z_f} + g) \end{bmatrix}. \tag{4.139}$$

The final differential equation that must be solved is $\dot{\alpha}$ and final condition for α is

$$\alpha_f = \dot{\Omega}_f = \Omega_{t_f} + \Omega_{x_f}\dot{x}_f = \nu_x a_{x_f} + \nu_y a_{y_f} + \nu_z (a_{z_f} + g). \tag{4.140}$$

Finally the resulting solution of α is

$$\alpha = -(\nu_x^2 + \nu_y^2 + \nu_z^2)(t_f - t) + \nu_x a_{x_f} + \nu_y a_{y_f} + \nu_z (a_{z_f} + g). \tag{4.141}$$

Using the solutions of S, R, m, Q, n, and α the matrices V and U can be formed

$$V = \begin{bmatrix} Q & n \\ n^T & \alpha \end{bmatrix} \tag{4.142}$$

$$U = \begin{bmatrix} R & m \end{bmatrix}. \tag{4.143}$$

Chapter 5

Results: Four Optimal Guidance Laws

5.1 Satisfaction of First Variation Necessary Conditions

Recall from Eqn. 2.29 the Hamiltonian must be constant at every instant in time and the transversality condition must be equal to zero for an optimal solution. Eqn. 2.29 is restated below as a reminder

$$H = \text{constant} = -G_{t_f}.$$

The transversality condition is the sum of the Hamiltonian and the partial derivative of the Bolza function with respect to the final time. Using Eqn. 2.29 it is possible to check whether the four guidance laws are indeed correct. Since Eqn. 2.29 is a necessary condition for a minimum it can be used to determine if the guidance laws meet this condition. A simulation was developed in Matlab© in order that given a set of initial conditions for the missile and the target, the Hamiltonian and transversality condition can be evaluated over time until the missile intercepts the target. Over this period of time the Hamiltonian, commanded accelerations, Bolza function, and transversality condition were computed. Each of the four guidance laws were evaluated. The initial state of the missile used in the simulation was chosen to

reflect a realistic scenario and is as follows

$$x = -50,000\,\text{ft} \tag{5.1}$$

$$y = 0\,\text{ft} \tag{5.2}$$

$$z = 50,000\,\text{ft} \tag{5.3}$$

$$u = 1100\,\frac{\text{ft}}{\text{sec}} \tag{5.4}$$

$$v = 0\,\frac{\text{ft}}{\text{sec}} \tag{5.5}$$

$$w = 0\,\frac{\text{ft}}{\text{sec}}. \tag{5.6}$$

The target initial state was chosen to exercise all six components of the target state (which include a three dimensional position with coordinates in all three axes, and a three dimensional velocity vector maneuving the target in all three axes). The target initial state, used to create all Hamiltonian and transversality condition results, is as follows

$$x_T = -5000\,\text{ft} \tag{5.7}$$

$$y_T = 3000\,\text{ft} \tag{5.8}$$

$$z_T = 500\,\text{ft} \tag{5.9}$$

$$u_T = -10\,\frac{\text{ft}}{\text{sec}} \tag{5.10}$$

$$v_T = -10\,\frac{\text{ft}}{\text{sec}} \tag{5.11}$$

$$w_T = 10\,\frac{\text{ft}}{\text{sec}}. \tag{5.12}$$

The results for the situation of a moving target with no terminal angle constraints are shown below. The Hamiltonian is shown in Figure 5.1 and is a constant value. A few seconds before interception the Hamiltonian displays a sharp curve towards zero and then seems to go quickly towards negative infinity. The reason for this behavior is that the guidance laws are based on the value of t_{go}. As the current time approaches the final time, t_{go} approaches zero, the equations calculating the accelerations of the missile divide by very small numbers which inevitably approach zero. Since the

equations that calculate acceleration must divide by t_{go} this sharp curve at the end of the Hamiltonian curve is expected. In practice, once t_{go} gets small (i.e. 0.1) it is best to stop calculating acceleration commands and simply compute the missile acceleration commands based upon the last value calculated for t_{go}. Also according to the previous analysis Eqn. 2.29, the transversality condition should maintain a constant value of zero during the interception. The transversality condition will maintain a constant value of zero over all time because the derivative of the Bolza function with respect to the final time, $-G_{t_f}$, mirrors the Hamiltonian's behavior as t_{go} approaches zero. This is shown in Figure 5.2. The same target initial state was used to perform a simulation using the guidance law that incorporates a constraint on the terminal flight path angle which in this scenario is negative eighty-five degrees. The Hamiltonian is shown in Figure 5.3. Again, the Hamiltonian behaves erratically as t_{go} moves close to zero. Also, the transversality condition maintains a constant value of zero as shown in Figure 5.4. The results for the constrained heading

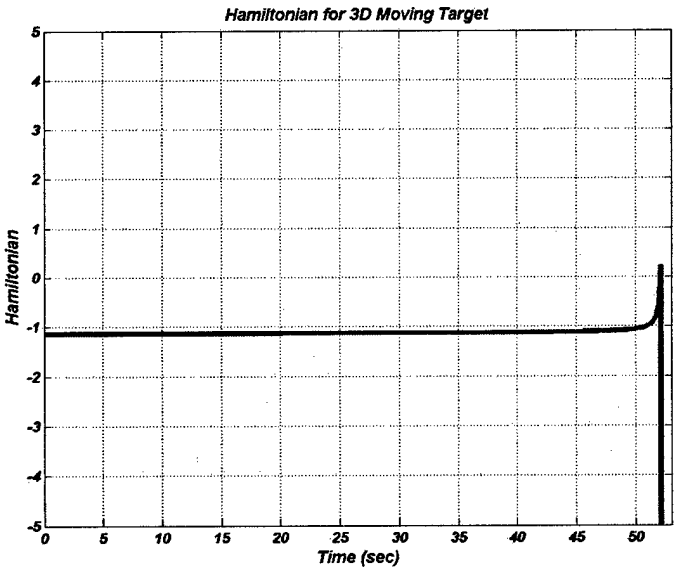

Figure 5.1: The Hamiltonian for a three dimensional moving target with no additional terminal angle constraints

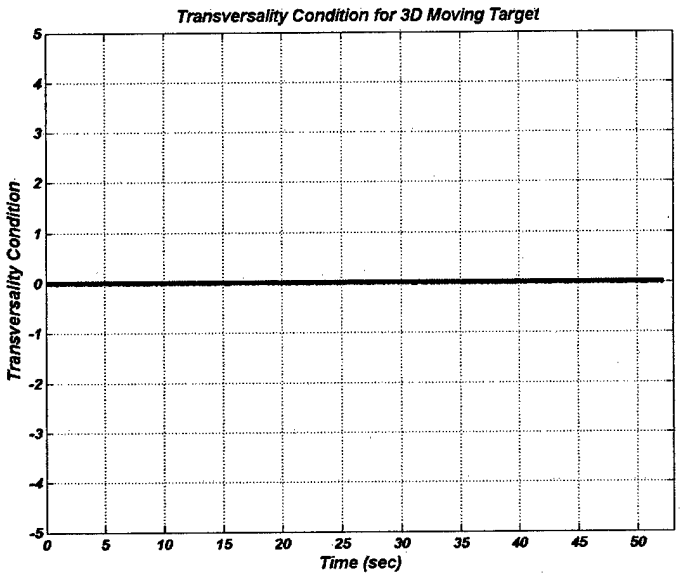

Figure 5.2: The transversality condition for a three dimensional moving target with no additional terminal angle constraints

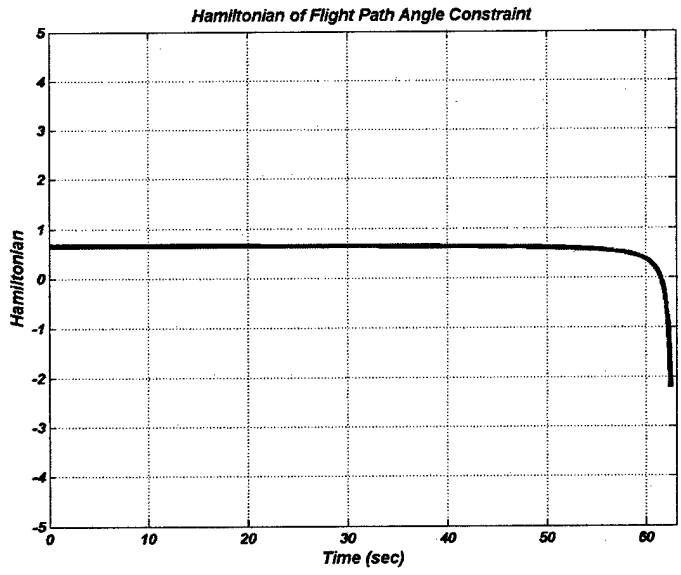

Figure 5.3: The Hamiltonian for a three dimensional moving target with a terminal flight path angle constraint of $-85°$

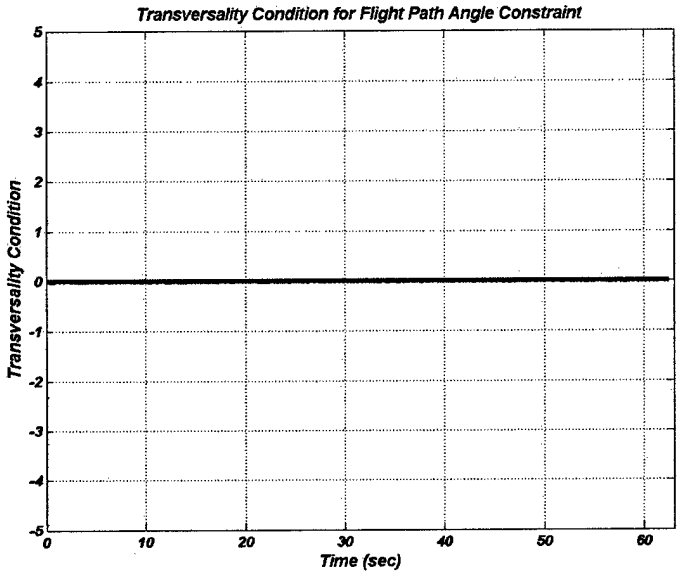

Figure 5.4: The transversality condition for a three dimensional moving target with a terminal flight path angle constraint of $-85°$

angle, which in this case is sixty degrees, are as follows. The constant Hamiltonian is shown in Figure 5.5. The transversality condition is shown in Figure 5.6. Finally the results for a constrained heading angle (sixty degrees) and a constrained flight path angle (negative eighty-five degrees) are as follows. The Hamiltonian maintains a constant value as shown in Figure 5.7. Last, but not least, the transversality condition maintains a constant zero as shown in Figure 5.8.

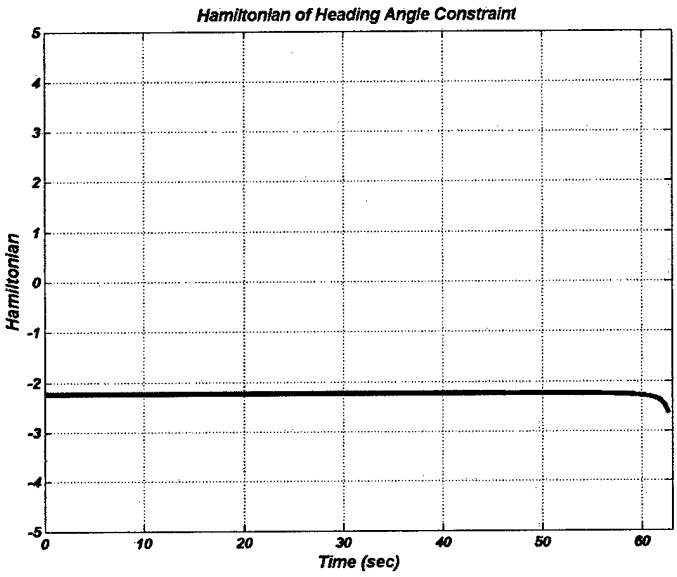

Figure 5.5: The Hamiltonian resulting for a three dimensional moving target with a terminal heading angle constraint of 60°

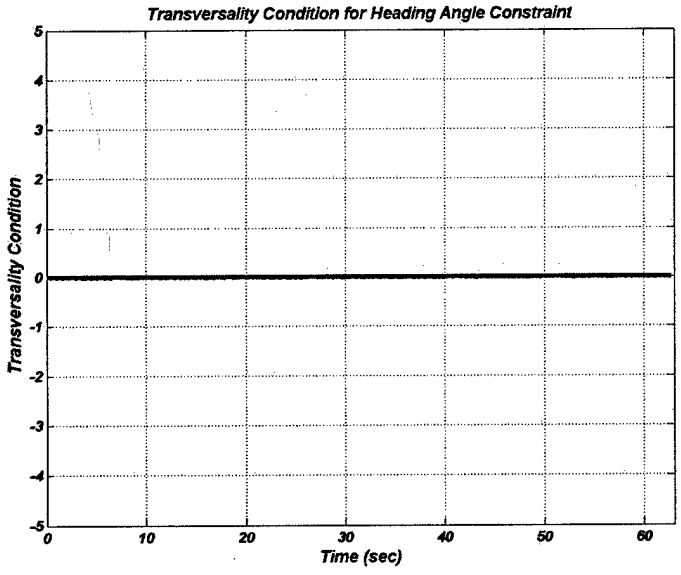

Figure 5.6: The transversality condition for a three dimensional moving target with a terminal heading angle constraint of 60°

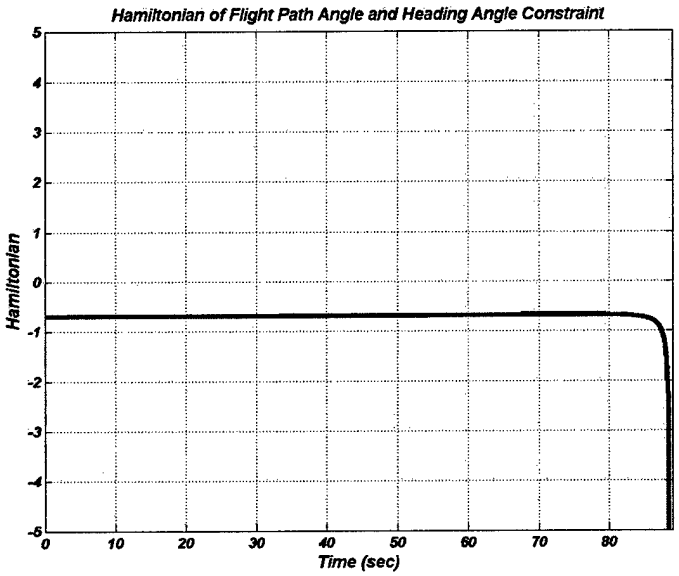

Figure 5.7: The Hamiltonian for a three dimensional moving target with terminal flight path angle of $-85°$ and terminal heading angle constraint of $60°$

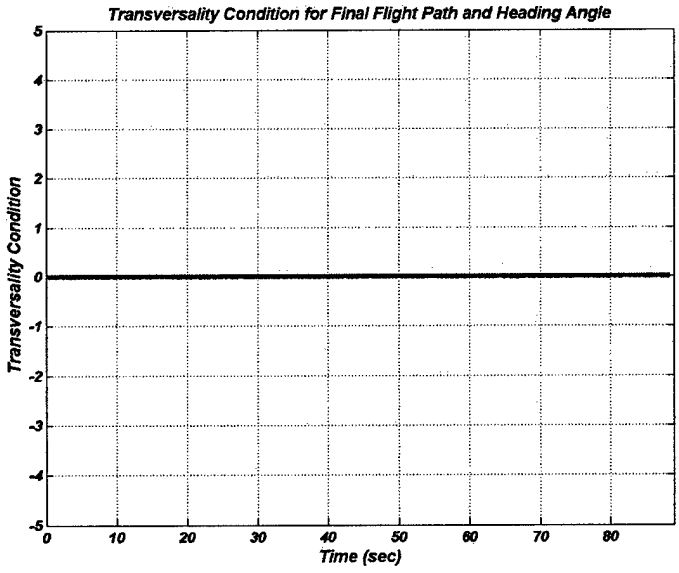

Figure 5.8: The transversality condition for a three dimensional moving target with terminal flight path angle of $-85°$ and terminal heading angle constraint of $60°$

5.2 Satisfaction of the Second Variation Conditions

Recall from the analysis of the second variation necessary conditions in Chapter 3 that the second variation necessary conditions were met for all four guidance laws. In order to ensure that the guidance laws were indeed the optimal solution it was necessary to ensure that the conditions in Eqn. 4.2 and 4.3 were satisfied (second variation sufficient conditions). The condition listed in Eqn. 4.2 $H_{uu} > 0$ was easily met in all four guidance laws because the resulting matrix of $\frac{\partial H}{\partial u \partial u}$ is in fact the identity matrix as shown in Eqns. 4.30, 4.59, 4.89, and 4.119. Recall that from the derivation in [10] that in order to test the condition on $\hat{S}$ represented by Eqn. 4.3 it was necessary to incorporate the value of S, R, m, Q, n, and α throughout the life of the simulation. Using these solutions it is possible to construct the matrices U and V throughout the simulation. In order to ensure that $\hat{S}$ is always finite throughout the life of the simulation two conditions must be satisfied. First of all the matrix U can never go to infinity. Second the determinant of the matrix V must never go to zero for $(t < t_f)$ thereby making it noninvertible. As long as these two conditions are met the second variation sufficient conditions are satisfied. All four guidance laws were tested given numerous different initial conditions and the guidance laws did indeed satisfy the second variation sufficient conditions. One of the tests conducted used the same missile and target initial conditions that were used to conduct the Hamiltonian and transversality condition tests and constrained the terminal flight path angle to negative eighty-five degrees and the terminal heading angle to sixty degrees. Figure 5.9 shows the determinant of the U matrix over the flight time of the missile. Clearly the determinant does not go to infinity for $(t < t_f)$ and therefore the matrix will never be infinity. Again, the sharp turn to negative infinity that occurs at the final time is due to the fact that the accelerations are calculated by dividing by t_{go}. As t_{go} approaches zero the guidance laws are essentially dividing by small numbers and finally zero. This behavior occurs in every test. Figure 5.10 shows the

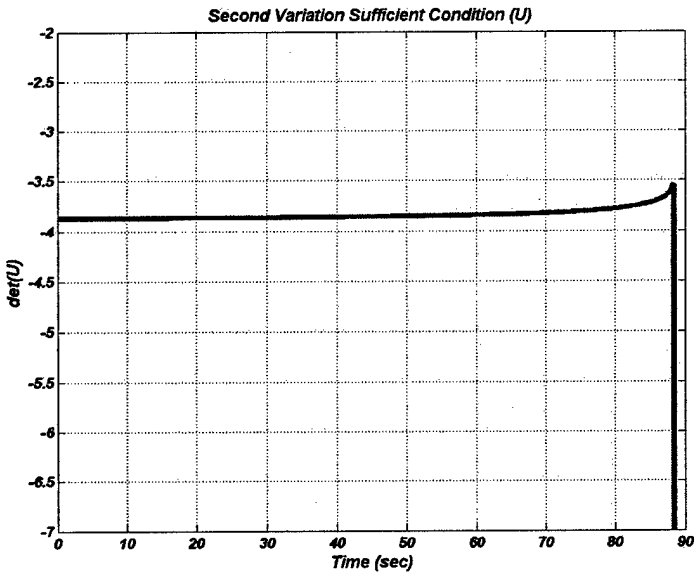

Figure 5.9: The determinant of the matrix U for a three dimensional moving target with a terminal flight path angle constraint of $-85°$ and terminal heading angle constraint of $60°$

determinant of V over the flight time of the missile. The figure shows the determinant of V exponentially approaching zero. Figure 5.11 shows the determinant of V in the final seconds of testing. In order to give a better perspective of the behavior of the determinant of V as t_{go} approaches zero the exact values of the determinant were also monitored in order to check for zero or extremely small values. The determinant of V approaches zero as time-to-target approaches zero. Table 5.1 displays the last four calculated time-to-targets and the four determinants of V associated with those times. Every determinant prior to these four determinants of V are farther from zero than the first determinant in the table. Again, this behavior can be attributed to the fact that the accelerations are calculated by dividing by time-to-target. As t_{go} approaches zero this behavior of the determinant is an expected result.

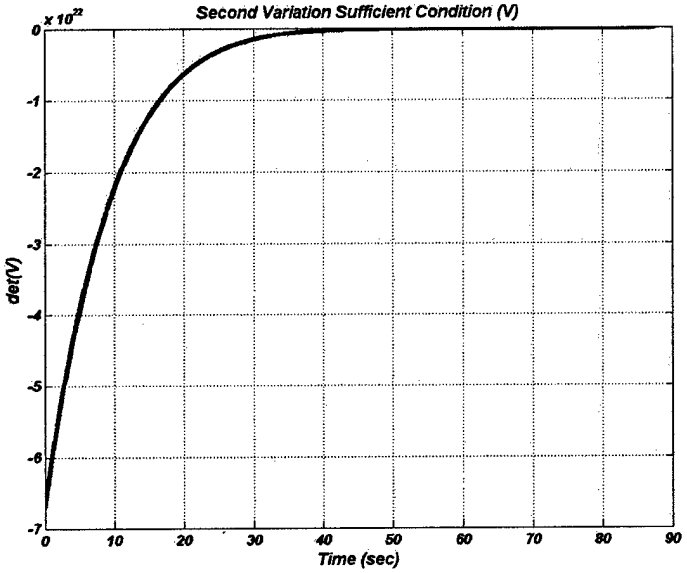

Figure 5.10: The determinant of the matrix V for a three dimensional moving target with a terminal flight path angle constraint of $-85°$ and terminal heading angle constraint of $60°$

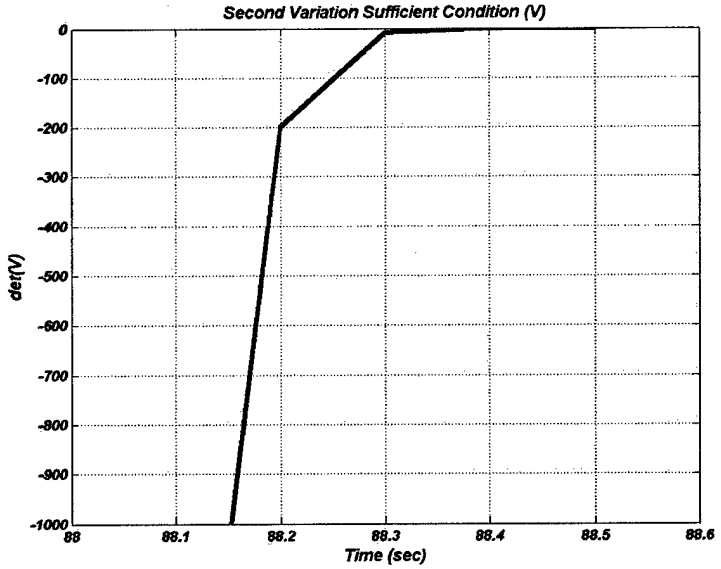

Figure 5.11: The determinant of the matrix V for a three dimensional moving target with a terminal flight path angle constraint of $-85°$ and terminal heading angle constraint of $60°$

t_{go} (sec)	0.30832	0.20832	0.10832	0.024966
det(V)	-199.24	-8.6523	-0.046224	-8.3761×10^{-8}

Table 5.1: Determinant of V vs. t_{go} for a three dimensional moving target with a terminal flight path angle constraint of $-85°$ and a terminal heading angle constraint of $60°$

5.3 Comparison with Results from DIDO

Another method that was used to verify the proposed guidance laws was to compare them with the results of a numerical optimization package. The DIDO/Tomlab optimization tool was developed at the Naval Postgraduate School and is used in this thesis to develop numerically optimal trajectories (and accelerations). This tool solves the same problem as the analytic guidance laws. It is possible to compare the numerical optimal solutions from DIDO to the accelerations calculated by the analytic guidance laws to see if they agree. The results from the analytic guidance laws were created using the same computer simulation and initial states that were used to determine if the Hamiltonian was constant and the transversality condition was zero. This simulation used the analytic guidance laws to generate the commanded accelerations at uniformly distributed points in time. Figure 5.12 shows the commanded accelerations produced by the analytic guidance law for a three dimensional moving target with no angle constraints. Figure 5.13 shows the numerically optimal commanded accelerations produced by DIDO. Using the trajectories calculated by DIDO and the Matlab© simulation it was possible to compare the commanded accelerations calculated by these two methods. Since DIDO doesn't uniformly distribute its data points over constant intervals in time and since the Matlab© simulation and the DIDO tool have a different total number of data points (at different points in time) it is necessary to use linear interpolation to generate points along both curves at the same points in time. Once these interpolations are performed it is possible to generate data calculating the difference in the commanded accelerations at each instant in time. A sizable portion of the magnitude of the calculated differences can be attributed to errors with the linear interpolation and different sampling points. This is true in all of the test cases using DIDO and the analytic guidance laws. Figure 5.14 displays the difference in the two commanded accelerations. The errors in the data, although the data was generated using a linear interpolation, are still relatively

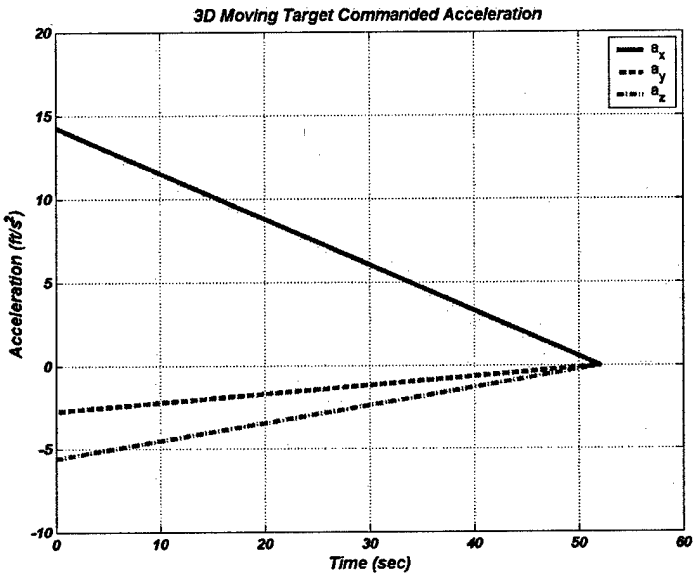

Figure 5.12: The commanded accelerations calculated by the analytic guidance law involving a three dimensional moving target with no angle constraints

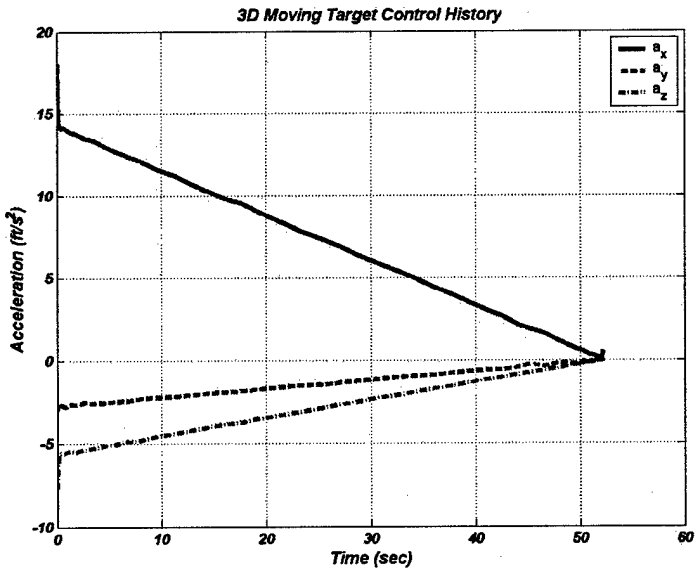

Figure 5.13: The commanded accelerations found by DIDO for a three dimensional moving target with no angle constraints

small and show the accuracy of the analytic three dimensional moving target guidance law compared with the numerically optimal results generated by DIDO. Additionally, DIDO found that the initial time to target should be 52.2117 seconds whereas the analytic guidance law found the initial time to target to be 52.2096 seconds. Figure 5.15 displays the time to target determined analytically by the proposed guidance law over the flight path time of the missile. Figure 5.16 shows the commanded acceleration numerical results generated by the proposed guidance law that considers a three dimensional moving target with a constraint on the terminal flight path angle. The constrained terminal flight path angle is negative eighty-five degrees. Figure 5.17 shows the numerically optimized accelerations found by DIDO for a three dimensional moving target with a constraint on the terminal flight path angle. These results match up extremely well with the results found by the analytic guidance law. As before, using a linear interpolation scheme the accelerations from DIDO were compared

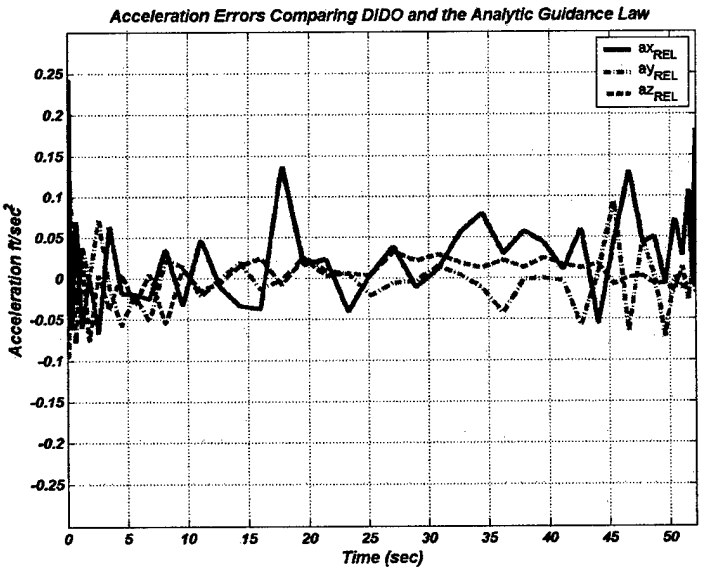

Figure 5.14: The difference of the commanded accelerations generated by DIDO and the analytic guidance law for the three-dimensional moving target guidance law with no angle constraints

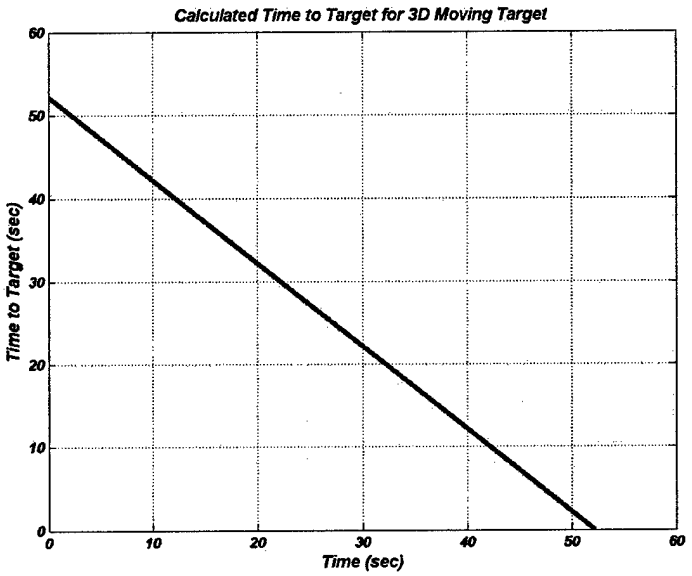

Figure 5.15: The time to target found analytically using the analytic guidance law for a three dimensional moving target with no angle constraints

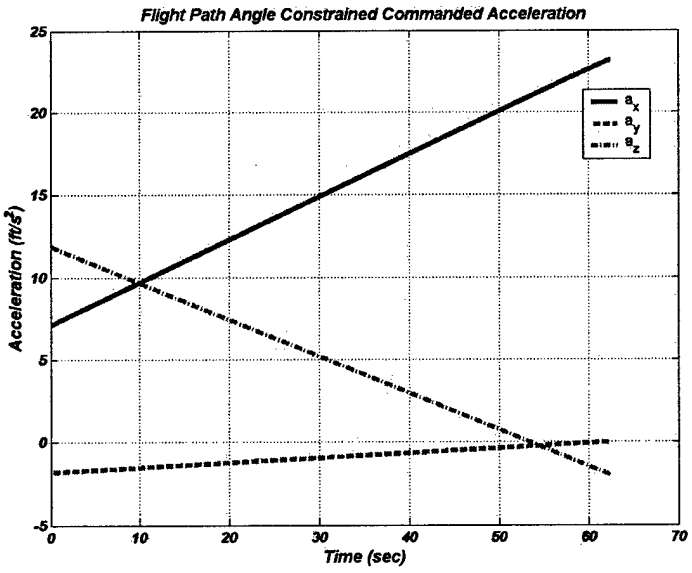

Figure 5.16: The commanded accelerations calculated by the analytic guidance law for a three dimensional moving target with a constraint on the terminal flight path angle of $-85°$

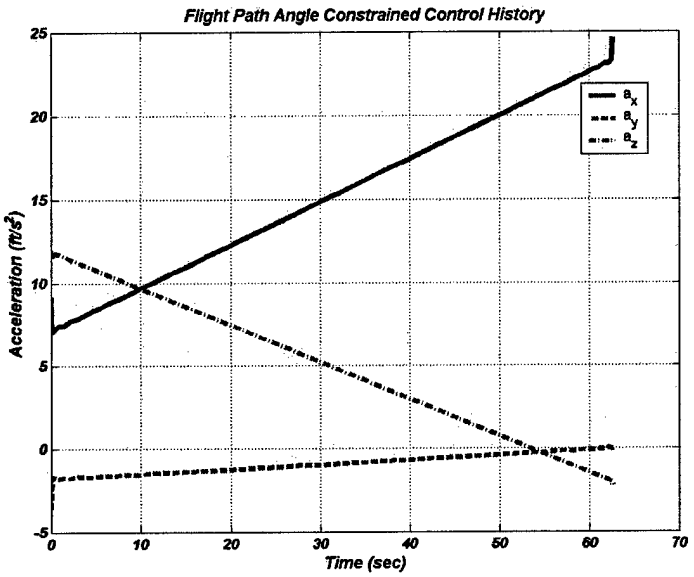

Figure 5.17: The comanded accelerations found numerically by DIDO for a three dimensional moving target with a constraint on the terminal flight path angle of $-85°$

with the commanded accelerations generated by the analytic guidance law and the results are shown in Figure 5.18. The difference between the two solutions, despite the interpolation and distribution of points, is still small and gives strong proof that the analytic guidance law is indeed optimal. The DIDO optimization tool also found the initial time to target to be 62.5970 seconds whereas the analytic guidance law found the intial time to target to be 62.5806 seconds. Figure 5.19 displays the time to target found analytically using the analytic guidance law. Figure 5.20 displays the commanded accelerations found by the proposed guidance law that considers a three dimensional moving target with an additional constraint on the terminal heading angle. The terminal heading angle that was used to generate these results was sixty degrees. Figure 5.21 displays the corresponding numerical results found by DIDO for a three dimensional moving target with a constraint on the terminal heading angle. The results found by the analytic guidance law and the DIDO optimization tool are

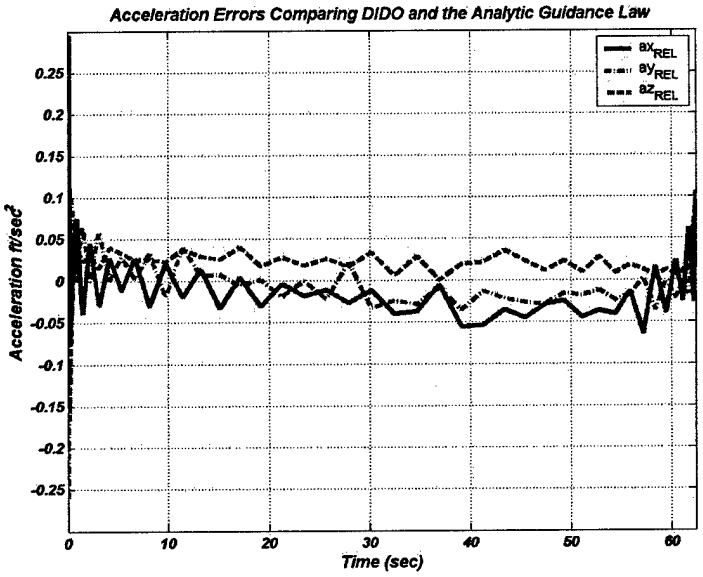

Figure 5.18: The difference of the commanded accelerations generated by DIDO and the analytic guidance law for the three-dimensional moving target guidance law with a constraint on the terminal flight path angle of $-85°$

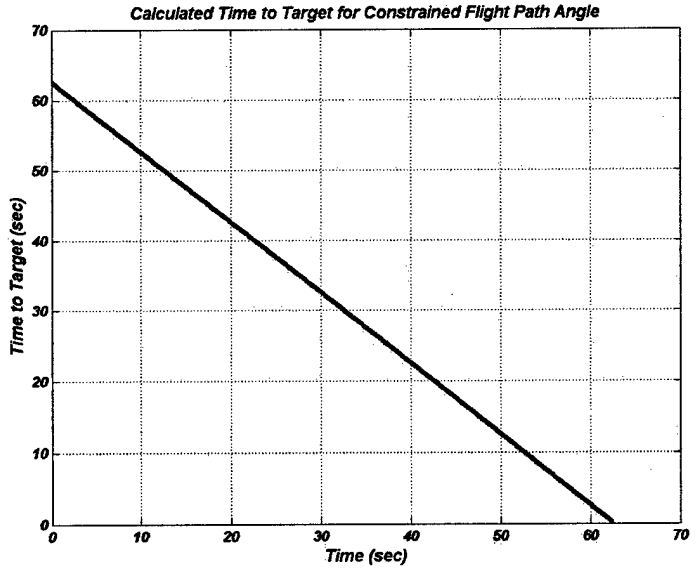

Figure 5.19: The time to target found analytically using the proposed guidance law for a three dimensional moving target with a constraint on the terminal flight path angle of $-85°$

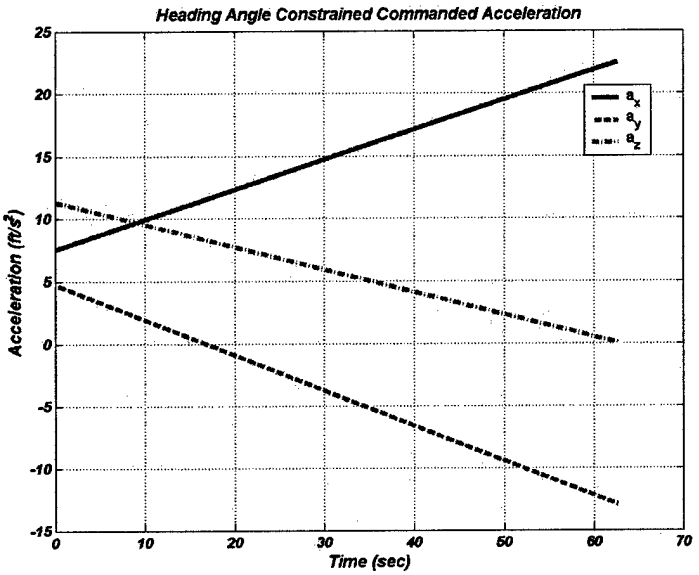

Figure 5.20: The commanded accelerations calculated by the analytic guidance law involving a three dimensional moving target with a constraint on the terminal heading angle of 60°

almost identical. A linear interpolation was used to create comparable points from the results generated by the DIDO optimal tool and the Matlab© simulation. These results are plotted in Figure 5.22. The calculated differences from the linear interpolation between the two generated results are small. DIDO found that the initial time to target should be 62.9680 seconds while the analytic guidance law gave a time of 62.9683 seconds. The time to target found analytically by the proposed guidance law is demonstrated in Figure 5.23 and the initial value matches the result found by DIDO. Finally, Figure 5.24 displays the commanded accelerations found by the analytic guidance law for a three dimensional moving target with a constraint on both the terminal flight path angle and the terminal heading angle. The terminal flight path angle enforced is negative eighty-five degrees and the terminal heading angle is sixty degrees. Figure 5.25 displays the control history found by DIDO for a three dimensional moving target with a constraint on both the terminal flight path angle

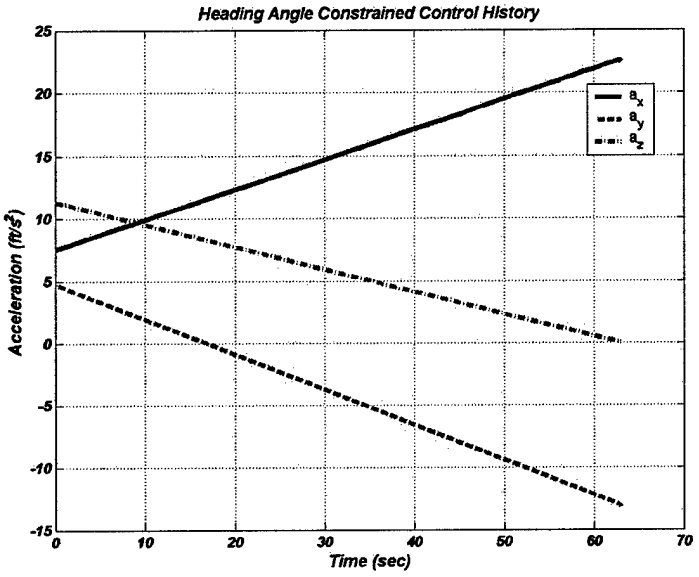

Figure 5.21: The commanded accelerations found numerically by DIDO for a three dimensional moving target with a constraint on the terminal heading angle of 60°

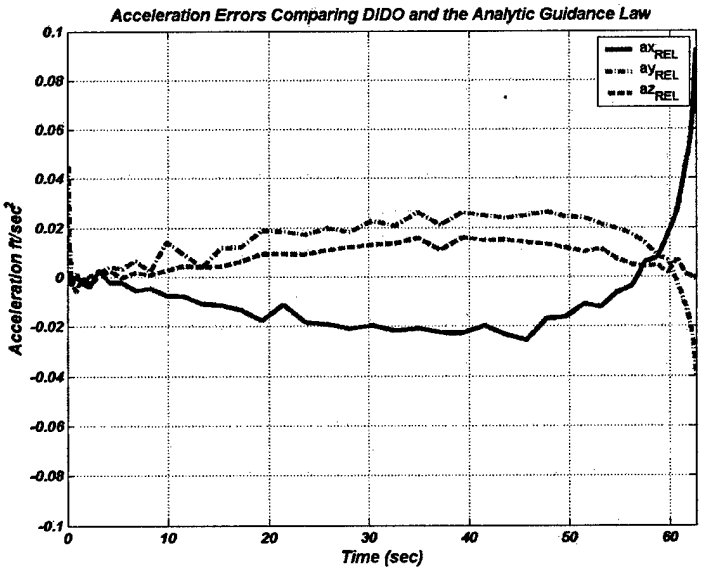

Figure 5.22: The difference of the commanded accelerations generated by DIDO and the analytic guidance law for a three dimensional moving target with a constraint on the terminal heading angle of 60°

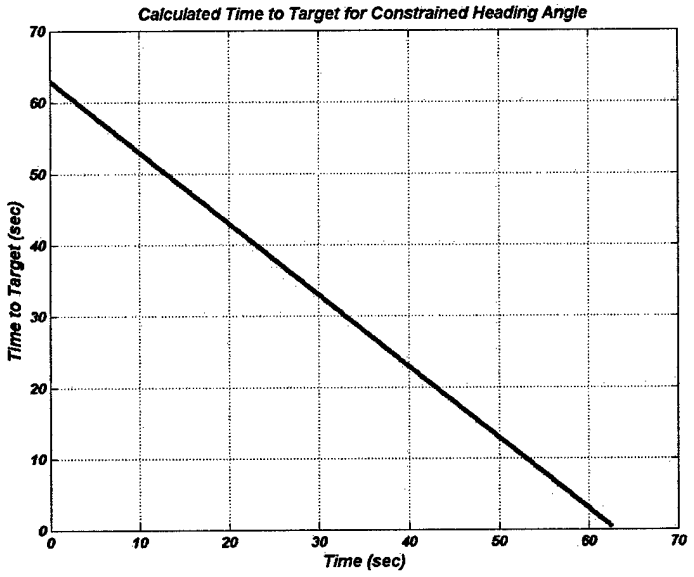

Figure 5.23: The time to target found analytically using the analytic guidance law for a three dimensional moving target with a constraint on the terminal heading angle of 60°

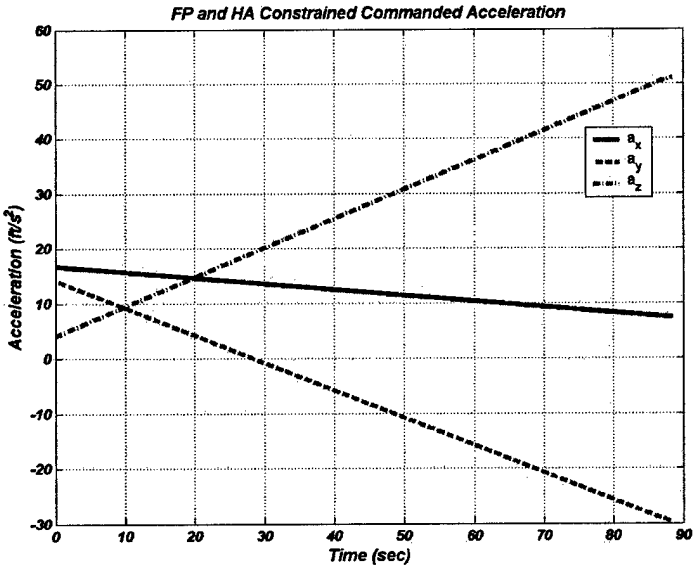

Figure 5.24: The commanded accelerations calculated by the analytic guidance law for a three dimensional moving target with a constraint on both the terminal flight path angle of $-85°$ and the terminal heading angle of 60°

and the terminal heading angle. Again, using linear interpolation comparable points were generated from the data created by the DIDO optimal tool and the Matlab© simulation which is using the proposed guidance law. Using these points it is possible to compare the difference between the numerically optimal points from DIDO and the commanded accelerations generated by the analytic guidance law. Figure 5.26 displays the differences in these two results. Also, Figure 5.27 displays the time to target found by the analytic guidance law. The initial time to target found by DIDO is 88.5154 seconds and the initial time to target found by the analytic guidance law is 88.5439 seconds. The analytic guidance law matches DIDO very well for this initial time to target.

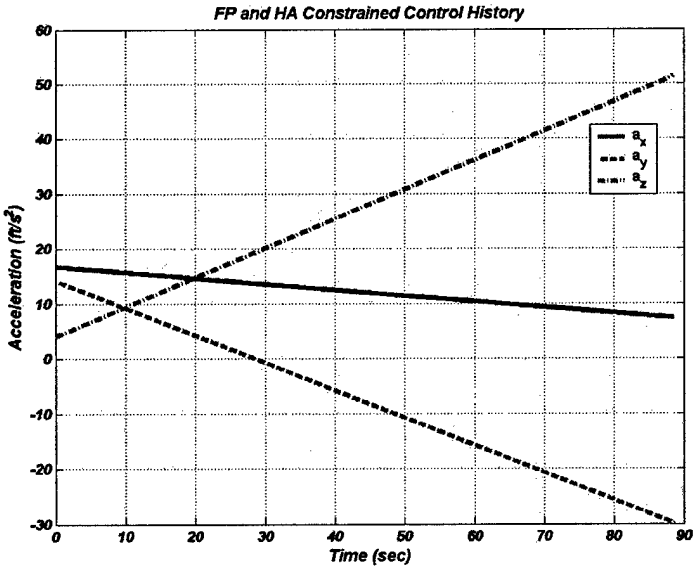

Figure 5.25: The commanded accelerations found by DIDO for a three dimensional moving target with a constraint on the terminal flight path angle of $-85°$ and the terminal heading angle of $60°$

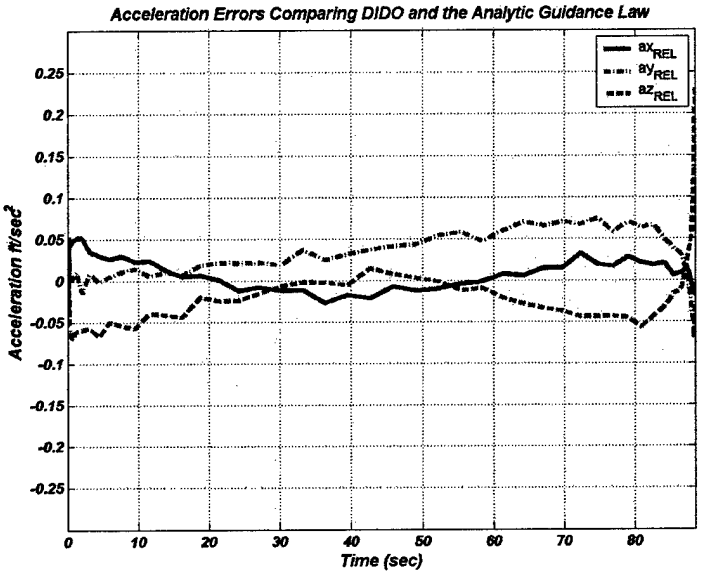

Figure 5.26: The difference of the commanded accelerations generated by DIDO and the analytic guidance law for a three dimensional moving target with a constraint on both the terminal flight path angle of $-85°$ and the terminal heading angle of $60°$

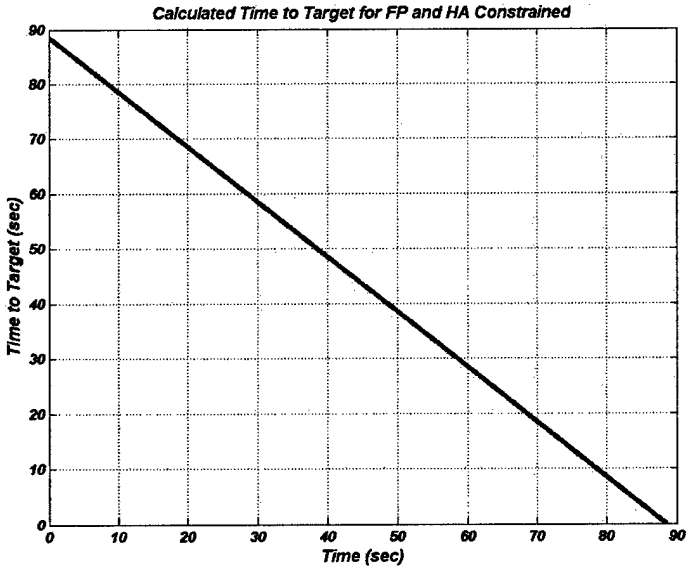

Figure 5.27: The time to target found by the analytic guidance law for a three dimensional moving target with a constraint on both the terminal flight path angle of $-85°$ and the terminal heading angle of $60°$

5.4 Evaluation of the Analytic Guidance Laws in a 6-DOF Simulation

In order to provide real world implementation using the analytic guidance laws, they were incorporated into a missile simulation in Simulink/Matlab© used by Draper Laboratory. The simulation mentioned earlier in the thesis is a three dimensional simulation; consequently errors due to drag effects, discrete time effects, bang-bang control, or an actual missile autopilot which commands the canards on the missile to achieve certain accelerations were not incorporated. The six degree of freedom simulation incorporates all of these neglected effects so that it provides a realistic environment for evaluation of the analytic guidance laws. The simulation and its structure as implemented in Simulink are illustrated in Figure 5.28. Using this simulation numerous tests were run to test the application and implementation of the

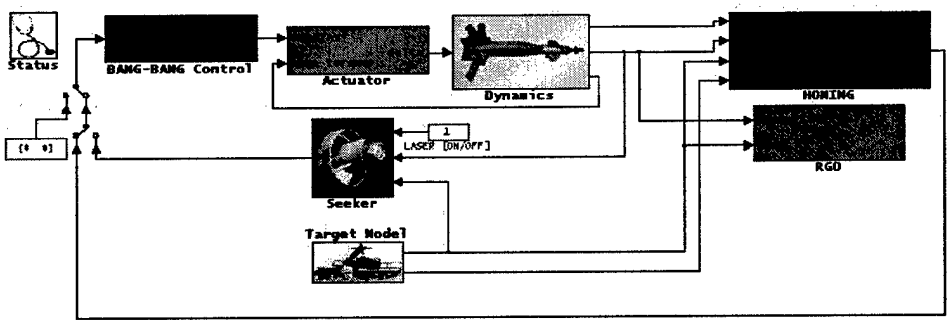

Figure 5.28: 6-DOF simulation environment

analytic guidance laws. The missile was given an initial condition as shown below.

$$x = -50,000\,\text{ft} \tag{5.13}$$

$$y = 0\,\text{ft} \tag{5.14}$$

$$z = 50,000\,\text{ft} \tag{5.15}$$

$$u = 1100\,\frac{\text{ft}}{\text{sec}} \tag{5.16}$$

$$v = 0\,\frac{\text{ft}}{\text{sec}} \tag{5.17}$$

$$w = 0\,\frac{\text{ft}}{\text{sec}}. \tag{5.18}$$

The target initial velocities were chosen to represent movement in all three directions and signify a vehicle moving at roughly top speed (roughly 60 to 70 mph). The target initial state, used to create all of the following results, is as follows

$$x_T = -5000\,\text{ft} \tag{5.19}$$

$$y_T = 0\,\text{ft} \tag{5.20}$$

$$z_T = 0\,\text{ft} \tag{5.21}$$

$$u_T = 88\,\frac{\text{ft}}{\text{sec}} \tag{5.22}$$

$$v_T = -10\,\frac{\text{ft}}{\text{sec}} \tag{5.23}$$

$$w_T = 10\,\frac{\text{ft}}{\text{sec}}. \tag{5.24}$$

Figure 5.29 shows the relative position between the missile and the target from the 6-DOF simulation using the guidance law for a three dimensional moving target with no angle constraints. Figure 5.30 shows the relative position between the missile and the target from a simulation using the guidance law for a three dimensional moving target with a constraint on the terminal flight path angle of $-70°$. Also, Figure 5.31 shows the flight path angle history. Clearly from Figure 5.31 it is possible to see that the missile satisfied the terminal flight path angle constraint. Figure 5.32 shows the relative position between the missile and the target using the guidance law for a three dimensional moving target with a constraint on the terminal heading angle of $30°$.

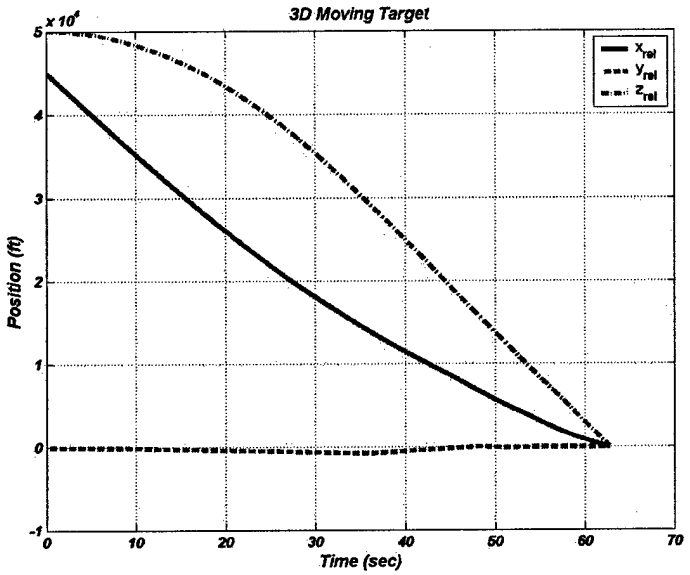

Figure 5.29: Relative position between the missile and the target for a three dimensional moving target with no angle constraints in the 6-DOF simulation

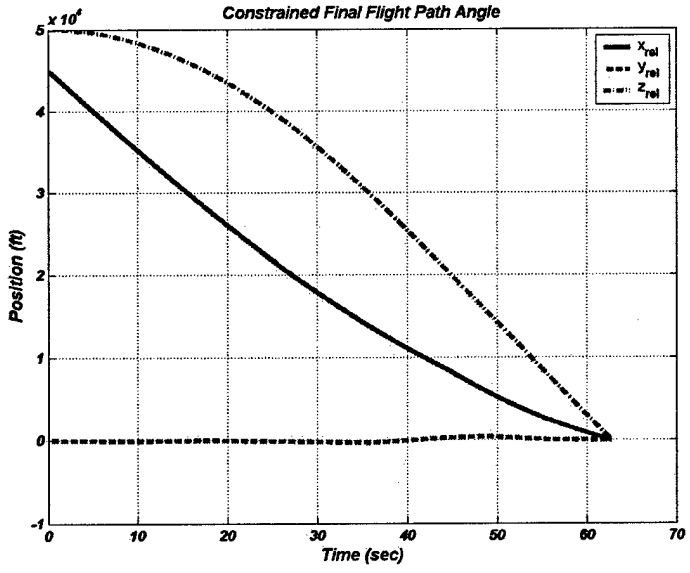

Figure 5.30: Relative position between the missile and the target for a three dimensional moving target with a constraint on the terminal flight path angle of $-70°$

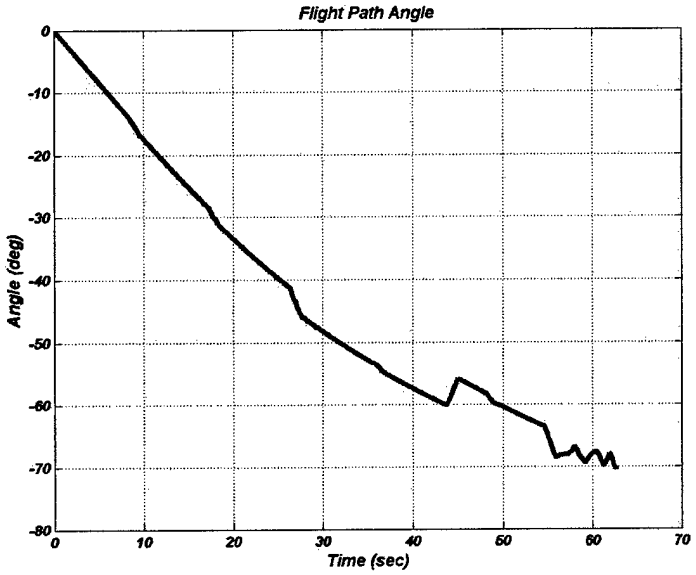

Figure 5.31: Flight path angle of the missile for a three dimensional moving target with a constraint on the terminal flight path angle of $-70°$

Also, Figure 5.33 shows the heading angle history. Although the missile is extremely close to achieving the commanded terminal heading angle it is noticeably off by a few degrees. This is due to the sluggish control capability of the missile.

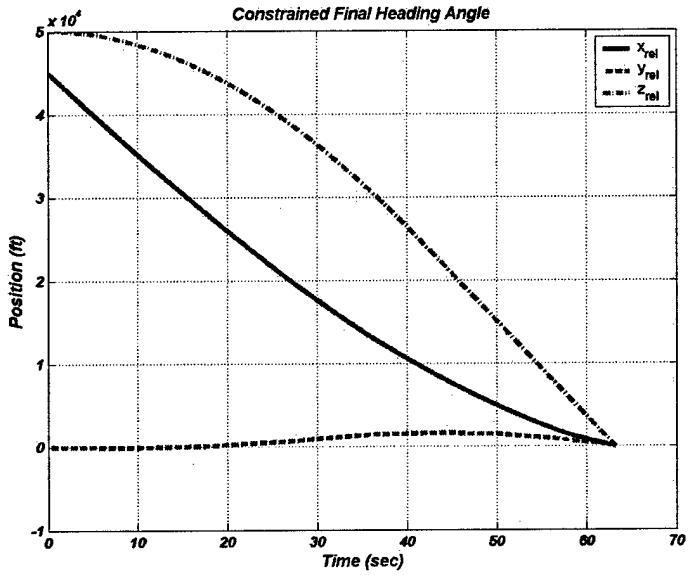

Figure 5.32: Relative position between the missile and the target for a three dimensional moving target with a constraint on the terminal heading angle of 30°

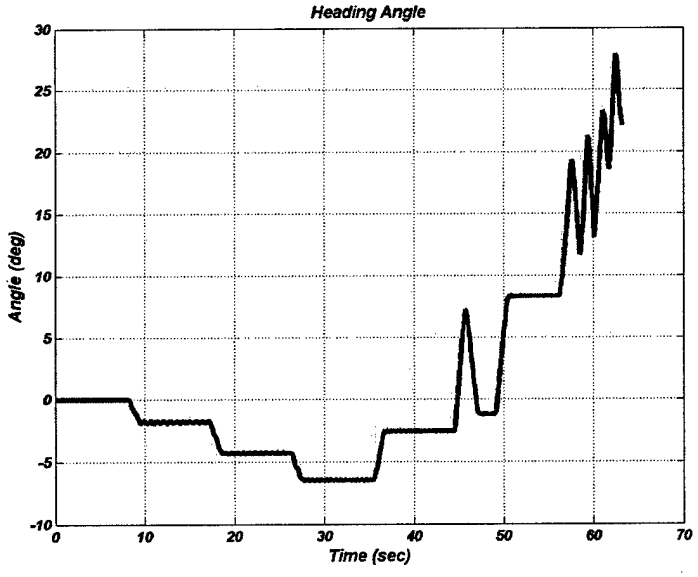

Figure 5.33: Heading angle of the missile for a three dimensional moving target with a constraint on the terminal heading angle of 30°

Finally, Figure 5.34 shows the relative position between the missile and the target using the guidance law for a three dimensional moving target with a constraint on both the terminal flight path angle of $-60°$ and a terminal heading angle of $5°$. Figure 5.35 demonstrates the flight path angle of the missile over the entire simulation. It is clear from Figure 5.35 that the missile achieves the terminal flight path angle constraint. Figure 5.36 demonstrates the heading angle of the missile over the entire simulation. The heading angle overshoots the five degree mark by roughly three degrees. As before, this can be attributed to the sluggish control capability of the missile.

5.5 Results from the Monte Carlo Analysis

The 6-DOF simulation was also used to evaluate the family of analytic guidance laws in a Monte Carlo fashion. The quantities that were varied were the initial position

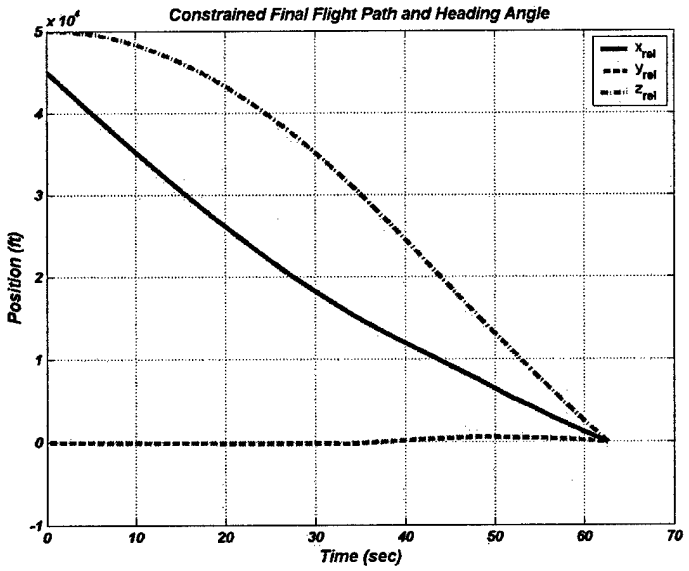

Figure 5.34: Relative position between the missile and the target for a three dimensional moving target with both a terminal flight path angle constraint of $-60°$ and a terminal heading angle constraint of $5°$

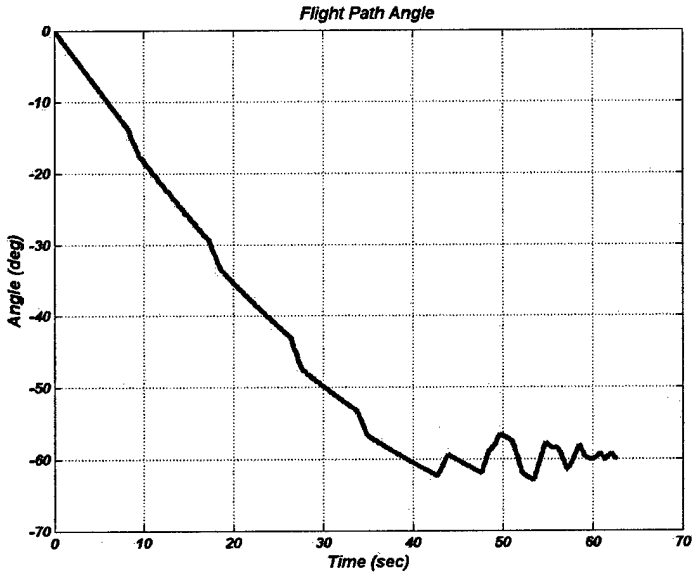

Figure 5.35: Flight path angle of the missile for a three dimensional moving target with a constraint on the terminal flight path angle of $-60°$ and the terminal heading angle of $5°$

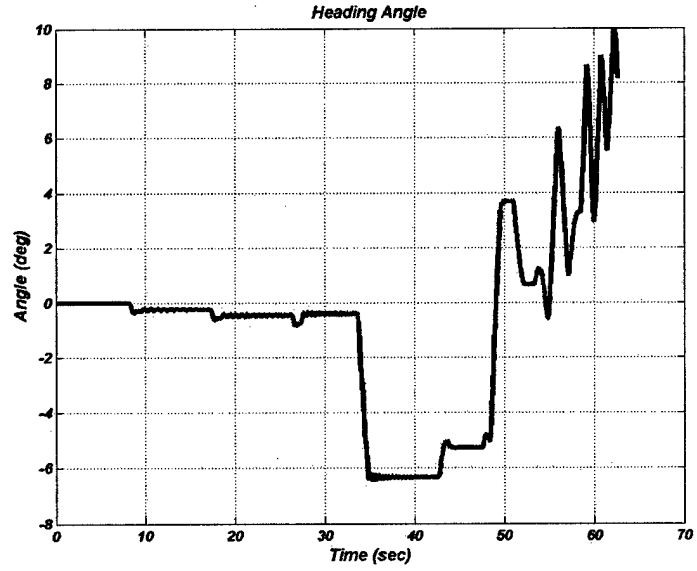

Figure 5.36: Heading angle of the missile for a three dimensional moving target with a constraint on the terminal flight path angle of $-60°$ and the terminal heading angle of $5°$

(altitude and range) and the initial roll rate. Using a standard deviation of 1000 ft, the initial position (altitude and range) was varied based on a Gaussian distribution with a mean of zero. Also, using a standard deviation of $30\frac{\text{deg}}{\text{sec}}$, the initial roll rate was varied based on a Gaussian distribution with a mean of zero. The eight drop points tested are shown in Table 5.2. Figure 5.37 shows the different drop points and their parameters.

Number	Release Angle	Speed (KTAS)	Alt (ft)	Range (ft)
1	-45	450	8,000	10,000
2	-45	450	12,000	7,500
3	-45	450	20,000	16,000
4	-45	450	20,000	10,000
5	0	450	8,000	22,000
6	0	450	12,000	18,500
7	0	450	20,000	23,500
8	0	450	20,000	29,000

Table 5.2: Monte Carlo Drop Points

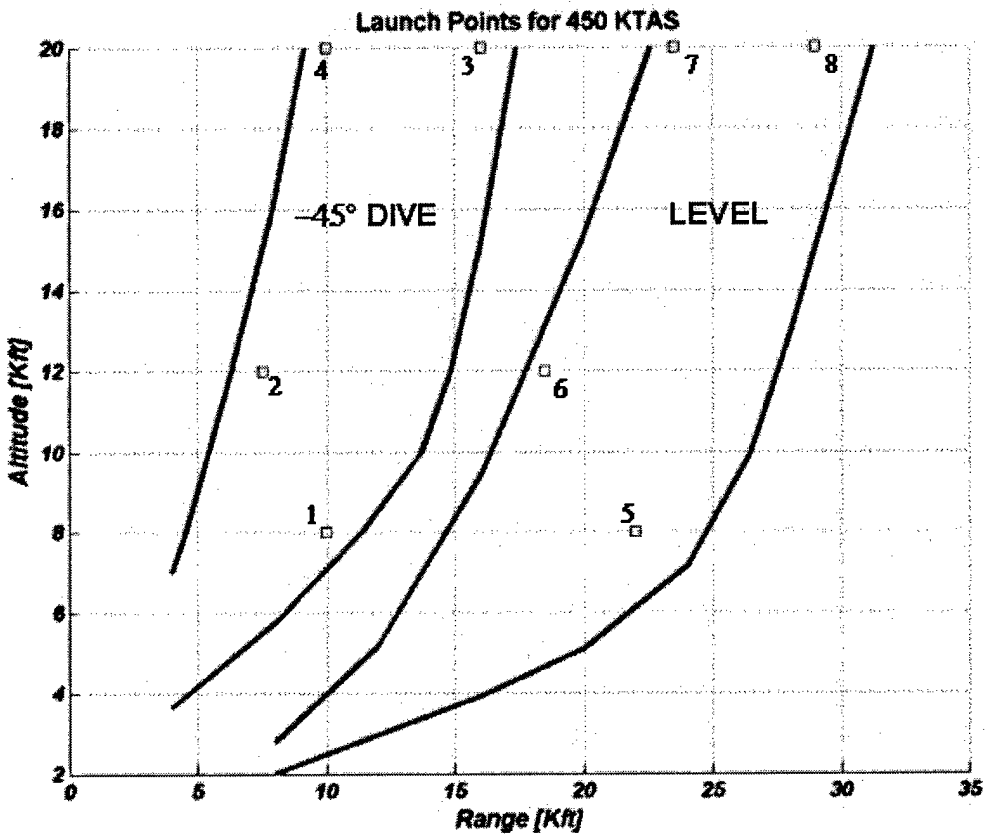

Figure 5.37: Eight drop points considered in Monte Carlo analysis

Tests were run using fifty samples for each guidance law from each of the eight drop points. Of the eight drop points, point four is typically the hardest on the guidance law. It is a high and short drop point and usually causes the vehicle the most trouble. The initial conditions for the target are as follows

$$x_T = 170\,\text{ft} \tag{5.25}$$

$$y_T = 0\,\text{ft} \tag{5.26}$$

$$z_T = 100\,\text{ft} \tag{5.27}$$

$$u_T = -10\,\frac{\text{ft}}{\text{sec}} \tag{5.28}$$

$$v_T = -10\,\frac{\text{ft}}{\text{sec}} \tag{5.29}$$

$$w_T = 10\,\frac{\text{ft}}{\text{sec}}. \tag{5.30}$$

The first results are from the Monte Carlo analysis testing the three dimensional moving target guidance law with no angle constraints. Figure 5.38 shows the resulting confidence interval for the drop points one through eight. Figure 5.39 shows the impact dispersions around the target for all eight drop points. Note the tight spread of points about the center of the circle. Although the plot shows an exact altitude, that is not necessarily the actual altitude of the target. Since the target is a moving target and fifty different initial conditions are being tested varied from eight different drop points the flight time of the missile is different in each case and therefore the altitude of the target is also different in each case. The target altitude varies from roughly three-hundered and twenty feet to approximately four-hundred and fifty feet depending on the type of guidance law used and the flight time of the missile. Because of the target motion (horizontal and vertical) the dispersions in the plot are due to the limitation of the plotting environment.

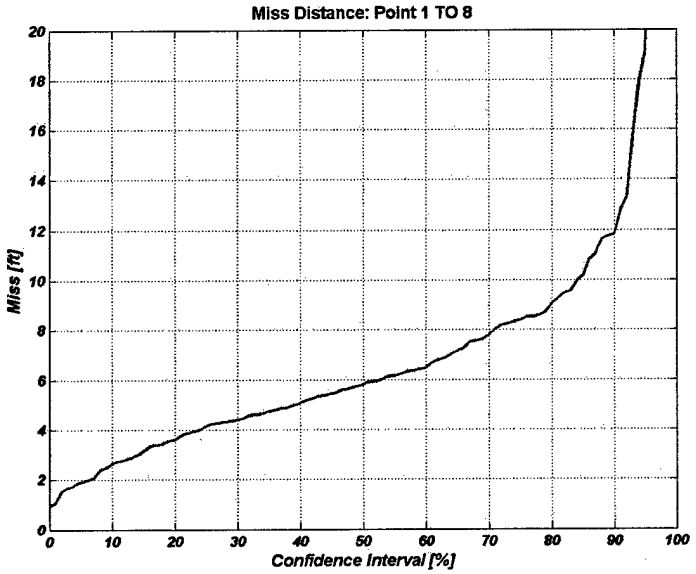

Figure 5.38: Confidence interval for miss distance from drop points one through eight for a three dimensional moving target with no angle constraints

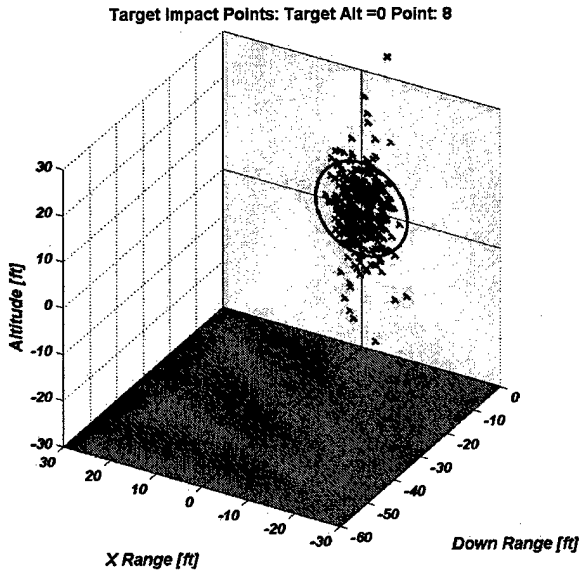

Figure 5.39: Target impact dispersions from drop points one through eight for a three dimensional moving target with no angle constraints

The next guidance law tested constrained the terminal flight path angle to an angle of negative sixty degrees. Again, the Monte Carlo tests were run from all eight drop points. Figure 5.40 shows the confidence interval for miss distance for drop points one through eight. Figure 5.41 shows the impact dispersions around the target for drop points one through eight. Finally, Figure 5.42 shows the confidence interval for the terminal flight path angle considering all eight drop points. It is possible to see from these results that the missile is meeting its terminal flight path angle constraint very well.

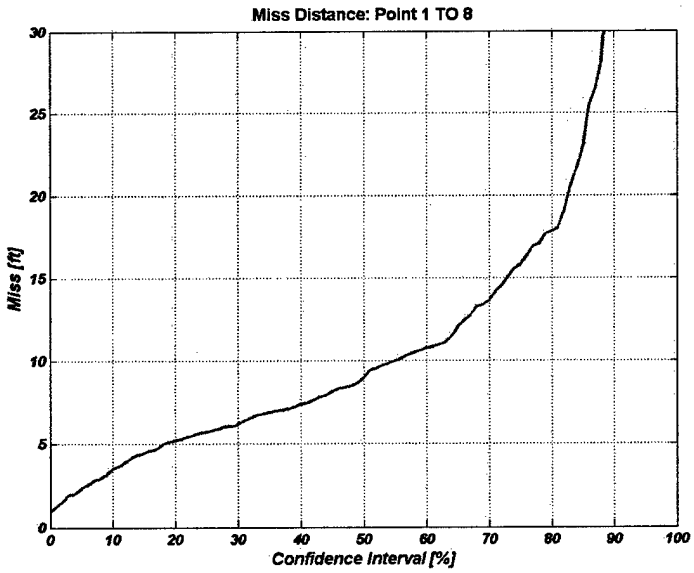

Figure 5.40: Confidence interval for miss distance from drop points one through eight for a three dimensional moving target with a terminal flight path angle constraint of $-60°$

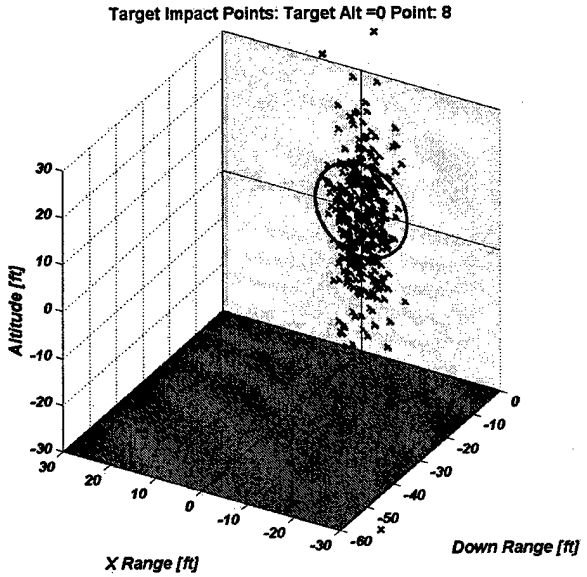

Figure 5.41: Target impact dispersions around the target from drop points one through eight for a three dimensional moving target with a terminal flight path angle constraint of $-60°$

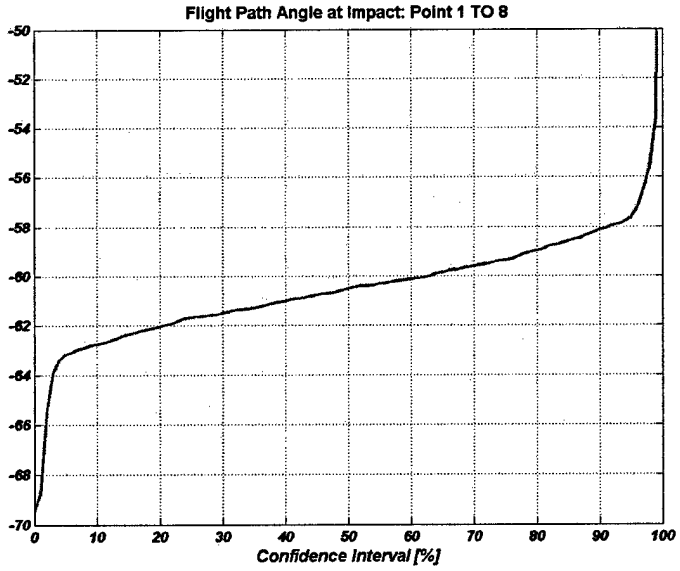

Figure 5.42: Confidence interval for terminal flight path angle from drop points one through eight for a three dimensional moving target with a terminal flight path angle constraint of $-60°$

The next guidance law tested constrained the terminal heading angle to an angle of five degrees. Again, the Monte Carlo tests were run from all eight drop points. Figure 5.43 shows the confidence interval for miss distance from drop points one through eight. Figure 5.44 shows the impact dispersions around the target considering all eight drop points. Also, Figure 5.45 shows the confidence interval for the terminal heading angle for all eight drop points. Although the missile is rather sluggish, it still does a good job of meeting its terminal heading angle constraint.

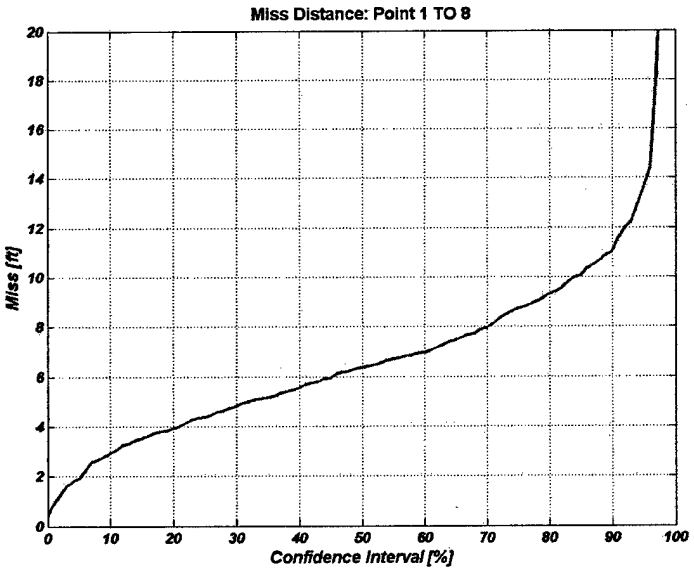

Figure 5.43: Confidence interval for miss distance from drop points one through eight for a three dimensional moving target with a terminal heading angle constraint of 5°

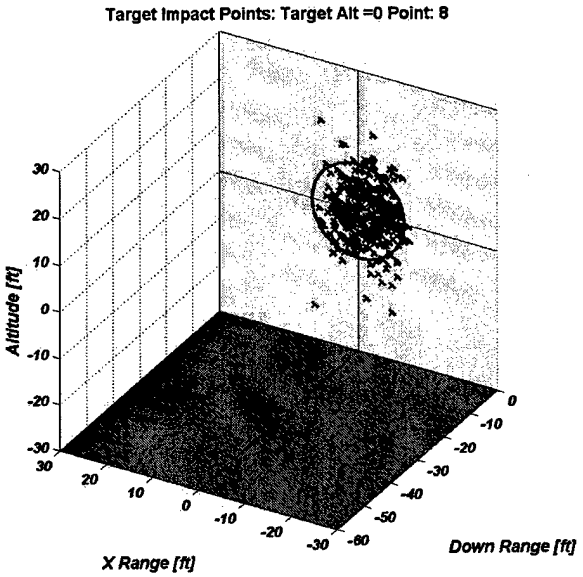

Figure 5.44: Target impact dispersions from drop points one through eight for a three dimensional moving target with a terminal heading angle constraint of 5°

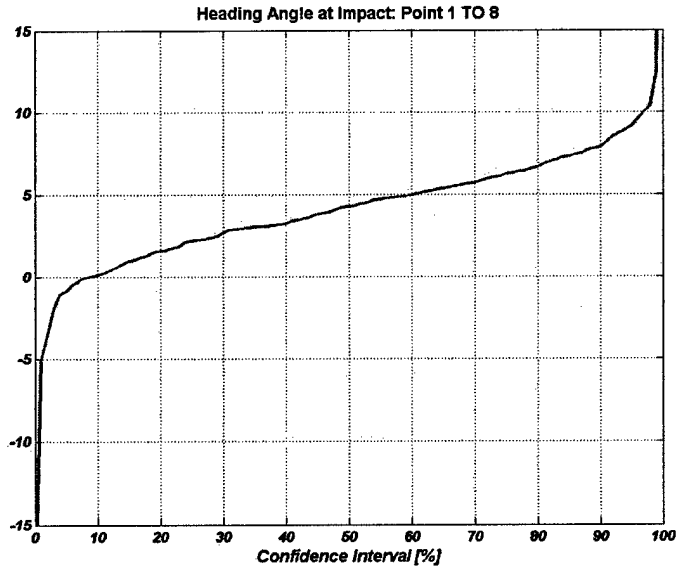

Figure 5.45: Confidence interval for terminal heading angle from drop points one through eight for a three dimensional moving target with a terminal heading angle constraint of 5°

The final guidance law tested constrained the terminal flight path angle to an angle of negative sixty degrees and the terminal heading angle to an angle of five degrees. Again, the Monte Carlo tests were run from all eight drop points. Figure 5.46 shows the confidence interval for miss distance for all eight drop points. Figure 5.47 shows the impact dispersions around the target from all eight drop points. Figure 5.48 shows the confidence interval for the terminal flight path angle at each drop point considering all eight drop points. It is possible to see from these results that the missile is meeting its terminal flight path angle constraint very well. Finally, Figure 5.49 shows the confidence interval for the terminal heading angle considering all eight drop points. As expected, the missile has trouble meeting its heading angle constraint.

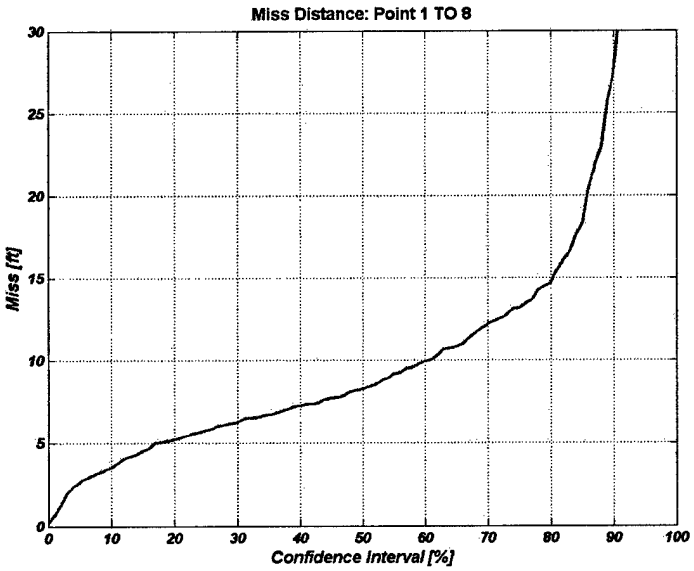

Figure 5.46: Confidence interval for miss distance from drop points one through eight for a three dimensional moving target with a terminal flight path angle constraint of $-60°$ and a terminal heading angle constraint of $5°$

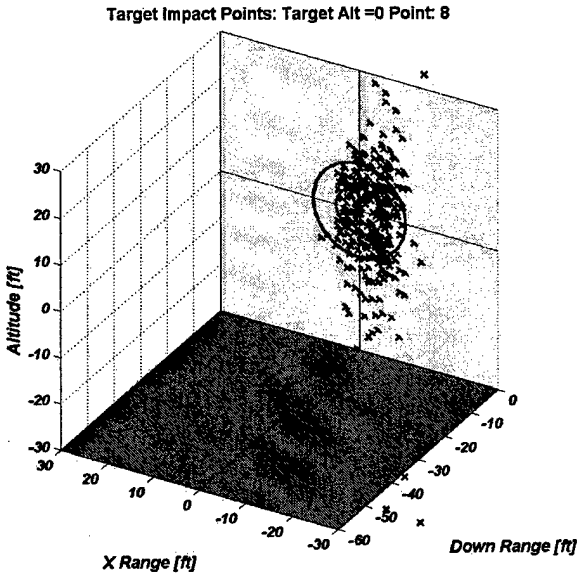

Figure 5.47: Target impact dispersions around the target from drop points one through eight for a three dimensional moving target with a terminal flight path angle constraint of $-60°$ and a terminal heading angle constraint of $5°$

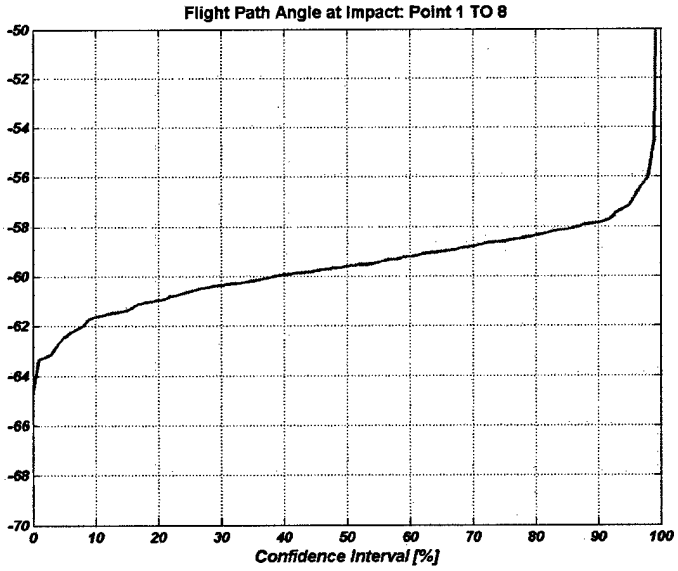

Figure 5.48: Confidence interval for terminal flight path angle from drop points one through eight for a three dimensional moving target with a terminal flight path angle constraint of $-60°$ and a terminal heading angle constraint of $5°$

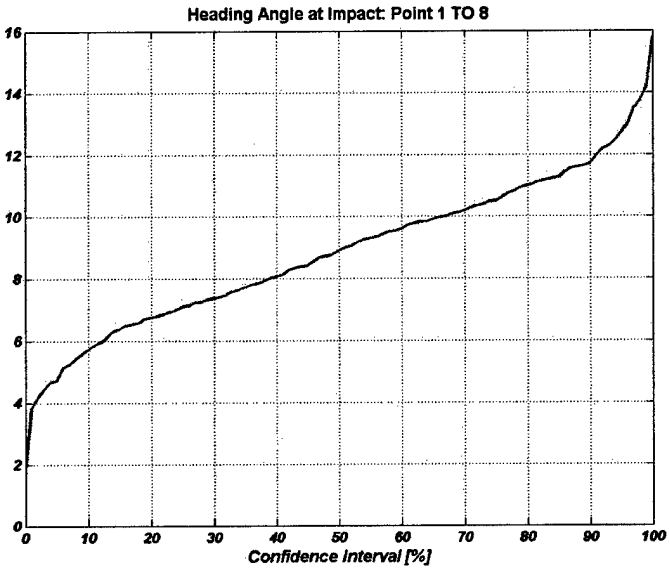

Figure 5.49: Confidence interval for terminal heading angle from drop points one through eight for a three dimensional moving target with a terminal flight path angle constraint of $-60°$ and a terminal heading angle constraint of $5°$

Chapter 6

Conclusion

In this thesis a family of optimal control guidance laws were presented. These optimal control guidance laws minimize the commanded acceleration or could be used to minimize the total flight time of the missile depending on the desire of the user. It was shown using the first and second variation necessary conditions along with the second variation sufficient conditions that the family of guidance laws were minima. All four guidance laws were implemented in a six degree of freedom missile simulation to evaluate their performance. Monte Carlo analysis with this simulation was used to develop statistical properties of the missile's capability to meet target, flight path angle, and heading angle constraints.

In Chapter 2, the first variation necessary conditions were used to derive the four guidance laws. The four guidance laws were: (1) three dimensional moving targets with no angle constraints; (2) three dimensional moving targets with a terminal flight path angle constraint; (3) three dimensional moving targets with a terminal heading angle constraint; and (4) three dimensional moving targets with both a terminal flight path angle constraint and a terminal heading angle constraint. The transversality condition placed on the Hamiltonian was also strengthened by testing the total derivative of the Hamiltonian. Since the total derivative of the Hamiltonian of each guidance law was zero, this set up a framework to later test whether or not each guidance law had been derived correctly.

Chapter 3 demonstrated that the family of guidance laws satisfied the second variation necessary conditions for a minimum. This proved that the guidance laws were not maximums. It was still possible that the guidance laws could be minima

or saddle points and therefore it was necessary to proceed to the second variation sufficient conditions.

Chapter 4 established the optimality of the family of guidance laws by applying the second variation sufficient conditions. Using these conditions it was possible to determine that the family of analytic guidance laws were in fact minima.

Chapter 5 validated the derived guidance laws by testing the Hamiltonian of each guidance law to ensure that it remained constant. The Hamiltonian is constant due to the fact that the total derivative of the Hamiltonian is equal to zero from the first variation necessary conditions obtained in Chapter 2. Next the optimality of the analytic guidance laws were established by applying the second variation sufficient conditions. Based on the second variation sufficient conditions, the analytic guidance laws are minima. A particular test case was presented using a three dimensional moving target guidance law constraining the terminal flight path angle and the terminal heading angle and it was shown that the second variation sufficient conditions were satisfied. Next the commanded accelerations found by the analytic guidance laws were compared with the commanded accelerations found by the DIDO optimization tool. This comparison further validated the optimality of the analytic guidance laws along with the fact that the initial time-to-target found by DIDO matched the initial time-to-target solved analytically by the guidance laws. The analytic guidance laws were then implemented in a six degree of freedom missile simulation in order to test their performance using various initial conditions. These tests proved highly successful and led to a more in depth analysis of the capabilities of the missile using the analytic guidance laws and Monte Carlo analysis. Monte Carlo tests were run on each guidance law varying the initial position and velocity of the missile along with the initial roll rate and delivered impressive results.

The analytic guidance laws described in this thesis have several benefits to today's guidance technology. First of all the effects of gravity are considered in all four of the analytic guidance laws and as a result of minimizing commanded acceleration

they reduce actuator usage. Another benefit of the analytic guidance laws is that the time-to-target is solved analytically at every instance in time. The time to target is an integral part of the analytic guidance laws.

The most important benefit of the analytic guidance laws is that they minimize the commanded accelerations or total flight time depending on the desire of the user. By minimizing the commanded accelerations it is possible to achieve maximum velocity which comes as a result of reducing the amount of drag. These new guidance laws also give the missile the capability to strike a target with a specified flight path angle or heading angle or both. With the freedom that these new guidance laws provide with respect to constraining the terminal flight path angle, heading angle, or both it will give the system the increased capability that is necessary to make precision strikes in civilian surroudings.

In conclusion, the fact that the new guidance laws include the effect of gravity, allow for four different types of terminal constraints, solve the time to target analytically so that it is known at every instant in time, and are proven to be optimal solutions demonstrates their superior performance and capability compared to what is currently available in air-to-surface missile technology.

Bibliography

[1] Anosov, D. V., et al. "On the Mathematical Work of L. S. Pontryagin." *Current Problems of Mathematics, Differential Equations, Mathematical Analysis, and Their Applications.* Providence: American Mathematical Society, 1986.

[2] Bryson, A. E., and Ho, Y-C. *Applied Optimal Control.* New York: Hemisphere Publishing Corp., 1975.

[3] Ben-Asher, J. Z., and Yaesh, I. *Advances in Missile Guidance Theory.* Vol. 180. Reston: American Institute of Aeronautics and Astronautics, Inc., 1998.

[4] Blakelock, J. H. *Automatic Control of Aircraft and Missiles.* 2nd Ed. New York: John Wiley & Sons, Inc. 1991.

[5] D'Souza, C. N. "The Optimal Control Problem." Draper Laboratories Lecture Series. Feb. 2003.

[6] D'Souza, C. N. "An Introduction to Trajectory Optimization Using Pseudospectral Methods." Draper Laboratories Lecture Series. Feb. 2003.

[7] Escobal, P. R. *Methods of Orbit Determination.* New York: John Wiley & Sons, 1965.

[8] FLIGHT International 22nd April 1971.

[9] Garnell, P., and East, D. J. *Guidance Weapon Control Systems.* Oxford: Pergamon Press, 1977.

[10] Hull, D. G. *Optimal Control Theory for Applications.* New York: Springer-Verlag, 2003.

[11] Goodstein, R. "Guidance Law Applicability for Missile Closing." *AGARD Lecture Series No. 52: Guidance and Control of Tactical Missiles.* London: Technical Editing and Reproduction Ltd Harford House, 1972.

[12] Miele, A. *An Engineering Approach to Optimal Control,* Class Notes, Rice University, 2003.

[13] Miele, A. *Theory of Optimum Aerodynamic Shapes.* New York: Academic Press, 1965.

[14] Miele, A., and Salvetti, A. *Applied Mathematics in Aerospace Science and Engineering.* New York: Plenum Press, 1994.

[15] Murtaugh, S. A., and Criel, H. E. "Fundamentals of proportional navigation". *IEEE Spectrum.* Dec. 1996.

[16] Nesline, F. W., and Zarchan, P. "A New Look at Classical Versus Modern Homing Guidance," *Journal of Guidance and Control,* Vol. 4, Jan.-Feb. 1981, pp.78-85.

[17] Pontryagin, L. S., et al. *The Mathematical Theory of Optimal Processes.* New York: Interscience Publishers, 1962.

[18] Press, W. H., Teukolsky, S. A., etc. *Numerical Recipes in FORTRAN: The Art of Scientific Computing.* 2d ed. New York: Press Syndicate of the University of Cambridge, 1992.

[19] Ross, I. M., and Fahroo, F. "DIDO 2003a." 31 Aug. 2002. CD-ROM. Charles Stark Draper Laboratory. 2003.

[20] Sobol', I. M., *A primer for the Monte Carlo method.* Boca Raton: CRC Press, 1994.

[21] Zarchan, P. *Tactical and Strategic Missile Guidance.* 2nd Ed. Vol. 157. Washington DC: American Institute of Aeronautics and Astronautics, 1994.